Copyright Warning & Restrictions

The copyright law of the United States (Title 17, United States Code) governs the making of photocopies or other reproductions of copyrighted material.

Under certain conditions specified in the law, libraries and archives are authorized to furnish a photocopy or other reproduction. One of these specified conditions is that the photocopy or reproduction is not to be "used for any purpose other than private study, scholarship, or research." If a, user makes a request for, or later uses, a photocopy or reproduction for purposes in excess of "fair use" that user may be liable for copyright infringement,

This institution reserves the right to refuse to accept a copying order if, in its judgment, fulfillment of the order would involve violation of copyright law.

Please Note: The author retains the copyright while the New Jersey Institute of Technology reserves the right to distribute this thesis or dissertation

Printing note: If you do not wish to print this page, then select "Pages from: first page # to: last page #" on the print dialog screen

GOTTFRIED, ARTHUR HERMAN

THEORY AND DESIGN OF CYCLOTRON-WAVE TRAVELING-WAVE AMPLIFIERS

New Jersey Institute of Techology D.ENG.SC. 1979

THEORY AND DESIGN OF
CYCLOTRON-WAVE TRAVELING-WAVE AMPLIFIERS

BY

ARTHUR H. GOTTFRIED

A DISSERTATION

PRESENTED IN PARTIAL FULFILLMENT OF

THE REQUIREMENTS FOR THE DEGREE

OF

DOCTOR OF ENGINEERING SCIENCE IN ELECTRICAL ENGINEERING

AT

NEW JERSEY INSTITUTE OF TECHNOLOGY

Newark, New Jersey
1979

ABSTRACT

A theory and design procedure for traveling-wave tubes using cyclotron-wave interactions is developed. An analysis is presented of the energy exchange mechanism and the axial beam velocity spread induced by the r.f. interactions. The analysis of the energy spread in a realistic model of the beam with nonzero size and nonzero space-charge density shows that higher maximum efficiencies at higher power is attainable (with collector depression) in cyclotron-wave amplifiers than in synchronous-wave amplifiers.

A one-watt, and a ten-watt cyclotron-wave amplifier at 3 GHz, utilizing bifilar helix circuits, scaled from a 2 kW, 5 GHz design, were constructed. A computer was used to design a pitch taper for the circuit of the ten-watt tube to maintain synchronism between beam and circuit waves so as to enable the extraction of more energy from the beam.

In general, test results verify the theory, and indicate the possibility of attaining efficiencies of the order of 70% in a 2 kW, 5 GHz cyclotron-wave amplifier. Because of the relatively low interaction impedance available for transverse-wave interactions, it is estimated that gains of the order of 1 dB/inch are possible.

APPROVAL OF DISSERTATION

THEORY AND DESIGN OF

CYCLOTRON-WAVE TRAVELING-WAVE AMPLIFIERS

BY

ARTHUR H. GOTTFRIED

DEPARTMENT OF ELECTRICAL ENGINEERING

NEW JERSEY INSTITUTE OF TECHNOLOGY

BY

FACULTY COMMITTEE

APPROVED: _____ CHAIRMAN

_____

_____

_____

_____

NEWARK, NEW JERSEY

OCTOBER 1979

ACKNOWLEDGEMENTS

The author acknowledges support of this project by the Microwave Power Tubes Team of Electronics Technology and Devices Laboratory, ERADCOM, Fort Monmouth, N.J. He also is indebted to Mr. John Tancredi for help with the computer analyses; Mr. Gunther Wurthmann for assistance with the experiments; Mrs. Genevieve Toohey for the typing of the dissertation; my dissertation advisor, Dr. Gerald Whitman for his help in preparing the dissertation; and my wife, Isabelle, for her patience and encouragement.

TABLE OF CONTENTS

TABLE OF CONTENTS (cont'd)

TABLE OF CONTENTS (cont'd)

TABLE OF CONTENTS (cont'd)

TABLE OF CONTENTS (cont'd)

LIST OF FIGURES

LIST OF FIGURES (cont'd)

LIST OF FIGURES (cont'd)

LIST OF TABLES

CHAPTER I

INTRODUCTION

Extended interaction of circuit waves with electron beam waves are utilized in traveling-wave tubes and klystrons to amplify signals in the frequency range 1 - 100 GHz. Improvement in the efficiency of conversion of d.c. power to r.f. power in these devices not only increases the power handling capability, but also decreases the size and power required for the prime power supplies and ancillary equipment such as modulators, and decreases cooling requirements needed to dissipate unconverted d.c. power. For example, if the efficiency is doubled, the power required from the power supply for the same r.f. output power is halved. Thus, for tubes with r.f. power outputs in the kilowatt range, considerable prime power is saved.

Most of the work to date on efficiency improvement has been done on traveling-wave tubes (TWT's) which use longitudinal space charge waves in the electron beam.[5] Efficiencies of the order of 50% have been attained by utilizing combinations of:

(1) Velocity taper of the circuit to maintain synchronism between circuit wave and the slow space-charge beam wave. (The beam slows down in d.c. velocity as r.f. energy is extracted by the circuit.)

(2) D.C. velocity jumps of the beam (accomplished by d.c. voltage jumps of the circuit) to maintain synchronism of the beam and circuit waves.

(3) Depressed voltage collectors to recoup unused d.c. energy in the beam.

However, it does not appear that significantly higher efficiencies can be attained in space charge wave tubes with these approaches. The amount of r.f. interaction and the amount of collector voltage depression that can be utilized is limited by the axial velocity spread of the beam electrons caused by r.f. velocity modulation.

Crossed-field amplifiers (in which the electron beam is focused by crossed d.c. electric and magnetic fields which assists in maintaining synchronism) have been constructed with efficiencies of the order of 60%, but these amplifiers are limited to frequencies at and below C-band (5000 GHz).

Siegman[7], in his original classic paper, has shown the possibility of utilizing filamentary electron-beam waves with d.c. transverse velocity and/or position modulation in TWT amplifiers. A property of transverse waves is that, to first order, the beam is free of axial and transverse r.f. velocity modulation. This leads to the expectation that very high efficiencies should be attainable in power tubes employing transverse waves, utilizing collector depression.

A new type of TWT utilizing transverse-waves[1] has been investigated for obtaining high efficiency. This transverse-wave TWT utilizes the interaction of the negative synchronous beam wave with a polarized circuit wave. The depressed collector efficiency for this type of interaction is given by[1]

$$\eta_{dep} = \frac{1}{1 + \frac{2b}{a_L}} \tag{1.1}$$

where η_{dep} = depressed collector efficiency

b = electron beam radius

a_L = final deflection of the center of the beam off axis of the tube. (It should be noted that the output power is proportional to a_L^2.)

From formula (1.1), it can be seen that as the beam becomes a filamentary one, i.e, $b \ll a_L$, the depressed collector efficiency approaches 100%. To obtain high efficiencies, the beam radius must be small. This limits the beam current and the power output, so that kilowatts of power are difficult to obtain.

It appears that this power limitation could be circumvented by utilizing another transverse beam wave mode, i.e., the slow cyclotron-wave. For this mode of operation, the depressed collector efficiency is given by[1]

$$\eta_{dep} = \frac{1}{1 + K_n \frac{\omega_c}{\omega} + \left(\frac{\omega+\omega_c}{\omega}\right)\left(\frac{\omega_R}{\omega_c}\right)\left(\frac{2b}{a_L}\right)} \tag{1.2}$$

where η_{dep}, b, and a_L are the same as in equation (1.1)

ω = angular operating frequency

ω_R = angular velocity of the beam about its center

ω_c = cyclotron frequency

$= \eta B_0$ = angular velocity of center of beam about the tube axis

$\eta = \frac{e}{m}$ = electron charge to mass ratio

B_o = longitudinal d.c. magnetic focusing field at the circuit

$K_n = B_{coll}/B_o$

B_{coll} = longitudinal d.c. magnetic field at the collector

Now,

(1.3) $$\omega_R = \frac{\omega_p^2}{2\omega_c}$$

where ω_p = plasma frequency of the beam (proportional to square root of beam charge density)

The minimum longitudinal d.c. magnetic field required to focus the beam (Brillouin field, B_B) is given by

(1.4) $$\omega_c^2 = 2\omega_p^2, \text{ or } \omega_c = \sqrt{2}\omega_p$$

$$\left(\text{where } B_B = \frac{\omega_c}{\eta}\right)$$

The factor ω_R/ω_c in (1.2) permits one to use a beam with a large radius to obtain high beam currents and thus high powers, and yet obtain high efficiency. As an example, suppose $b/a_L = 1$, i.e., the beam radius equals the final deflection of the beam center off the tube axis. From (1.1), the depressed collector efficiency for the synchronous wave mode is

$$\eta_{dep} = \frac{1}{1 + \frac{2b}{a_L}} = \frac{1}{1 + 2} = 33\%$$

In (1.2), if one uses twice the Brillouin field for focusing,

$$\omega_c = 2\ (\sqrt{2}\omega_p)$$

or $$\omega_p^2 = \frac{\omega_c^2}{8}$$

Then from (1.3)

$$\omega_R = \frac{\omega_p^2}{2\omega_c} = \frac{\omega_c^2}{8}\ (\frac{1}{2\omega_c}) = \frac{\omega_c}{16}$$

Also in (1.2), if one uses $K_n = 0.1$, $b = a_L$, and $\omega_c/\omega = 0.5$, equation (1.2) for the cyclotron wave mode then becomes

$$\eta_{dep} = \frac{1}{1 + (.1)\ (.5) + (1.5)\ (1/16)\ (2)}$$

$$= 80.8\%$$

This indicates a thick beam capable of generating high power might be used with the cyclotron mode, with higher efficiencies possible than with the synchronous mode.

The purpose of this dissertation is to investigate the utilization of the slow cyclotron beam wave mode in high power, high efficiency, depressed collector cyclotron-wave traveling-wave tubes. Design criteria and practical design limitations caused by beam size and space charge will be considered. The analytic results will be verified experimentally on actual tubes.

CHAPTER II

GENERAL PROPERTIES OF TRANSVERSE WAVES

2.1 Beam Waves

Siegman[7] has shown that a filamentary beam of electrons, drifting with constant velocity parallel to a uniform d.c. magnetic field, can support transverse wave propagation in the direction of electron travel in four distinct primary modes. These are the fast and slow cyclotron waves, and positive and negative synchronous waves. These modes constitute a complete, orthogonal set, appropriate combinations of which can describe any state of transverse modulation on the filamentary beam.

To assist in visualizing these waves, a snapshot of the beam pattern for the slow cyclotron and positive synchronous waves is shown in Figure 2-1 and for the fast cyclotron and negative synchronous waves in Figure 2-2. A center cylinder along the beam "rest" position has been inserted to make the pattern clearer. In Figure 2-1 the wave has a right-hand twist (right-hand polarization). (If the thumb of the right hand points in the $+z$ direction, the fingers curl in the direction of twist as one advances in the $+z$ direction.) In Figure 2-2, the wave has a left-hand polarization.

For the cyclotron waves, the individual electrons move to the right with velocity, u_0, and hence the pattern will have an axial component of velocity equal to u_0. However, the electrons also rotate clockwise at cyclotron angular velocity, ω_c, which gives an additional

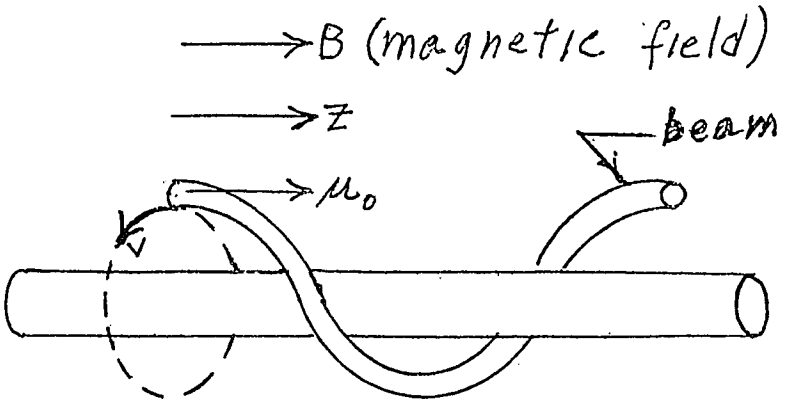

Figure 2-1 Snapshot of beam pattern for slow cyclotron and positive synchronous waves

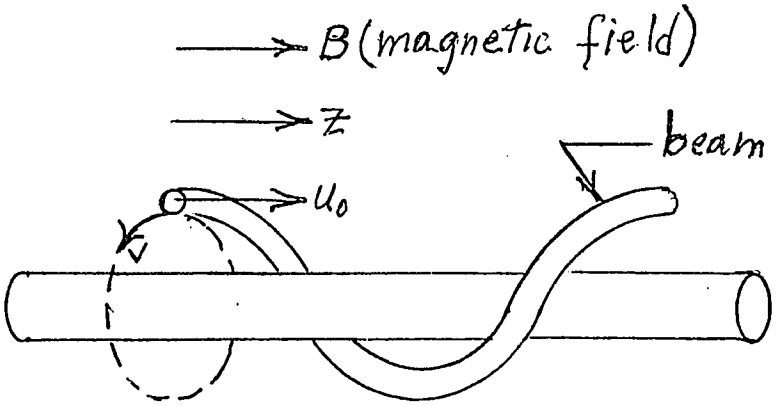

Figure 2-2 Snapshot of beam pattern for fast cyclotron and negative synchronous waves

backward component of velocity to the slow cyclotron wave pattern in Figure 2-1 and an additional forward component of velocity to the fast cyclotron wave pattern in Figure 2-2.

For the synchronous waves in Figures 2-1 and 2-2, the individual electrons have no transverse (rotational) velocity at all, and no rotations at ω_c are involved. These wave patterns move synchronous with the electron velocity, u_o.

If one sets up an X-Y plane at a given Z and views the intersection of the wave pattern with the plane in the negative Z-direction (so as to see a right-hand X-Y coordinate system in the plane), as the waves move to the right, the intersection rotates clockwise at signal frequency, ω, in Figure 2-1 and counterclockwise at signal frequency, ω, in Figure 2-2. For this reason, the right-hand polarization in Figure 2-1 is called negative polarization by some authors, and the left-hand polarization in Figure 2-2 is called positive polarization. (Louiselle[4] uses this convention. Siegman[7], on the other hand, uses the convention that right-hand polarization is positive, and left-hand polarization is negative.) To avoid confusion, the terms RH for right-hand, and LH for left-hand polarization will be used in this dissertation.

It can be noted that the electrons in the slow cyclotron wave (Figure 2-1) move faster than the phase velocity of the beam pattern wave, and move ahead relative to the beam pattern longitudinal motion, while the electrons in the fast cyclotron wave (Figure 2-2) move more

slowly than the phase velocity of the wave, and slip back relative to the beam pattern motion.

The important properties of transverse waves are: their phase velocities, polarizations, and parity. The parity is +1 for waves which carry positive kinetic power or a.c. energy, and -1 for those which carry negative kinetic power or a.c. energy. Positive kinetic power refers to the fact that the beam wave absorbs energy from the fields of a circuit wave so that the average energy of the electrons is increased. Positive kinetic power is the excess power over the initial power in the electrons that is absorbed by the beam from the circuit wave in setting up the beam wave. In this case, on average, electrons are trapped in accelerating longitudinal r.f. electric fields of the circuit wave. Negative kinetic power refers to the fact that the beam wave gives up energy to a circuit wave so that the average energy of the electrons is decreased. Negative kinetic power is the deficient power under the initial power in the electrons that is given up by the beam to the circuit wave in setting up the beam wave. In this case, electrons are trapped in decelerating longitudinal r.f. electric fields of the circuit wave.

When waves of opposite parity interact, the negative parity wave continually gives up energy to the positive parity one. This is called active interaction. When waves of like parity interact, energy oscillates back and forth between the two waves. This is called passive interaction. A circuit wave which carries power in

the forward direction has positive parity, while one which carries power in the negative direction has negative parity.

To make a forward traveling circuit wave grow so as to obtain amplification, negative kinetic power beam waves must interact with the circuit wave to increase the energy in the circuit wave. The properties of transverse waves are summarized in Table 2.1. The group velocity of all four waves is equal to the electron velocity, u_0. The mode amplitudes (A_1, A_2, A_3 and $A4$) are normalized so that the squares of their absolute values equal the kinetic power in the wave. The parities determine whether the kinetic power is positive or negative.

The slow cyclotron and the negative synchronous waves have negative parity and can be used to amplify a circuit wave. The slow cyclotron mode involves only transverse position and d.c. transverse velocity modulation of the beam, while the negative synchronous mode involves only transverse position. To first order, a beam with one of these modes is free of axial r.f. velocity modulation, so that high efficiency should be attainable by recouping unused d.c. energy of the electrons by collector depression. When the collector voltage is depressed below that of the circuit, the electrons are decelerated and energy is pumped back into the power supply. For comparison, it should be noted that longitudinal-wave devices, such as ordinary traveling-wave tubes and klystrons, depend on first-order longitudinal r.f. velocity modulation to bunch the beam electrons into space-charge waves. This inevitably results in a high degree of longitudinal

TABLE 2.1 PROPERTIES OF TRANSVERSE BEAM WAVES

Name	Symbol for Mode Amplitude	Phase Velocity	Propagation Constant	Polarization	Parity
Fast Cyclotron	A_1	$u_o/(1 - \omega_c/\omega)$	$\beta_e - \beta_c$	LH	+1
Slow Cyclotron	A_2	$u_o/(1 + \omega_c/\omega)$	$\beta_e + \beta_c$	RH	-1
Negative Synchronous	A_3	u_o	β_e	LH	-1
Positive Synchronous	A_4	u_o	β_e	RH	+1

where $\beta_e \equiv \omega/u_o$, $\beta_c \equiv \omega_c/u_o$

$$u_o = \sqrt{2|e|V_o/m}, \quad \omega_c = |e|B_o/m$$

B_o, the axial d.c. magnetic field is in the positive Z-direction.

velocity modulation of the electrons in the spent beam, preventing efficient collector depression.

The dispersion characteristics of the transverse beam waves is shown in the Brillouin (ω-β) diagram in Figure 2-3. The signal radian frequency, ω, is plotted as a function of the propagation constant, β. The fast cyclotron wave line extends into the second quadrant because the phase velocity is negative, or anti-parallel to the reference direction. This occurs because the fast cyclotron wave reverses its polarization from left-hand in the first quadrant to right-hand in the second quadrant. In Figure 2-3, the upper line corresponds to the fast cyclotron wave, and the lower line to the slow cyclotron wave. Both synchronous waves can be represented by a single straight line through the origin, although this line is really two coincident lines.

Typical ω-β curves for the two space-charge longitudinal waves are also depicted in Figure 2-3. The departure of these curves from the synchronous-wave line is a measure of the reduced plasma frequency, and therefore depends on space-charge density. In the limits of zero space-charge density, the space-charge wave curves would coincide with the synchronous-wave line. For space-charge densities as normally encountered in traveling-wave tubes, the space-charge wave curves depart only a little from the synchronous-wave line in a symmetrical fashion. For very high space charge densities, the physical limits on space charge waves are such that the space-charge wave curves can

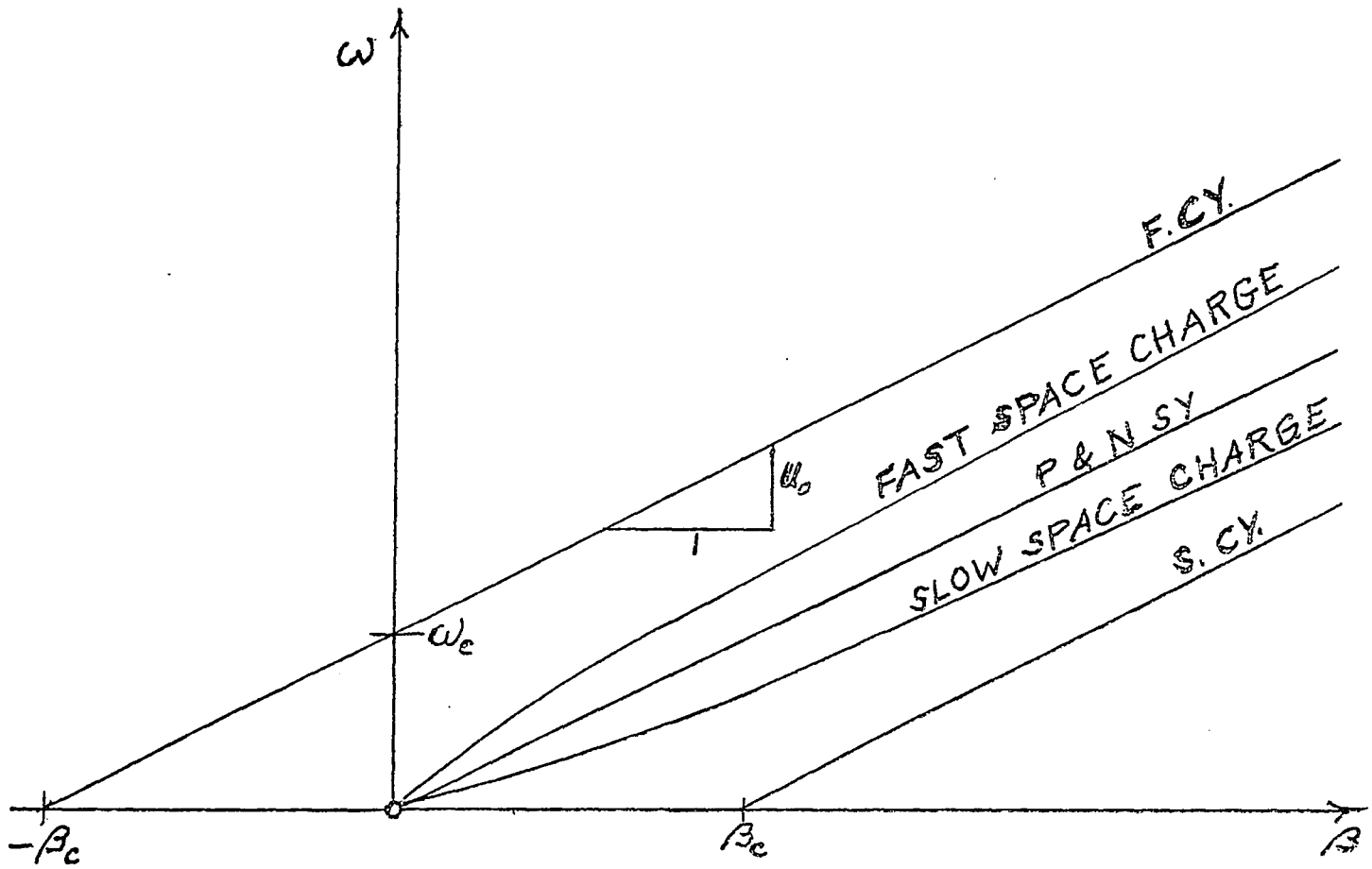

Figure 2-3 (ω-β) diagram with space-charge waves added

never escape from the first quadrant, their phase velocities are always positive. It should be noted that the space-charge waves, which involve longitudinal modulation only, are unpolarized.

The group and phase velocities in the Brillouin diagram of Figure 2-3 are given by:

(2.1) Phase velocity: $v_p = \frac{\omega}{\beta}$

(2.2) Group velocity: $v_g = \frac{d\omega}{d\beta}$

The group velocity corresponds to the direction of power flow. In the first quadrant, the phase velocity is positive and in the same direction as the group velocity. In the second quadrant, the phase velocity is negative and in the opposite direction to the group velocity. The synchronous waves always have positive phase velocity as does the slow cyclotron wave, while the fast cyclotron wave can have either positive or negative phase velocity depending on whether ω is greater than or less than the cyclotron frequency, ω_c. The group velocity of all the transverse wavesis constant, equal to the electron velocity, u_o. Hence, the slopes of the lines in Figure 2-3 is u_o.

The equations for the phase velocities and propagation constants of the transverse waves in Figure 2-3 are given below.

Synchronous Waves

Since u_o is the slope,

$$\omega = u_o$$

$$\text{or } \beta = \omega/u_o$$

By definition,

$$v_p = \frac{\omega}{\beta} = u_o$$

Define

$$\omega/u_o = \beta_e$$

Then

(2.3) $v_p = \frac{\omega}{\beta}$

(2.4) with $\beta = \beta_e$

Slow Cyclotron Wave

Since the slow cyclotron wave line is shifted down by ω_c from the synchronous wave line,

$$\omega = \beta u_o - \omega_c$$

$$\text{or } \beta = \frac{\omega + \omega_c}{u_o}$$

Define

$$\frac{\omega_c}{u_o} = \beta_c$$

Then

(2.5) $v_p = \frac{\omega}{\beta}$

(2.6) with $\beta = \frac{\omega + \omega_c}{u_o} = \beta_e + \beta_c$

Fast Cyclotron Wave

Since the fast cyclotron wave line is shifted by ω_c from the synchronous wave line,

$$\omega = \beta u_o + \omega_c$$

$$\text{or } \beta = \frac{\omega - \omega_c}{u_o}$$

Then

(2.7) $v_p = \frac{\omega}{\beta}$

(2.8) with $\beta = \frac{\omega - \omega_c}{u_o} = \beta_e - \beta_c$

The above values of β for each of the waves has already been listed in Table 2.1.

2.2 Circuit Waves

To obtain interaction between a circuit wave and a beam wave, the phase velocities must be nearly equal. To accomplish this, circuits are utilized which slow down the circuit wave.

A snapshot of a typical electric field pattern of a circuit wave that can interact with the longitudinal beam space charge wave modes along the axis of the tube is shown in Figure 2-4b. The variation of the longitudinal field, E_z, with radius, r, is shown in Figure 2-4a.

For a sheath helix[5] (a thin conducting cylinder which conducts only in a helical direction), the longitudinal field varies as

$E_z \sim \{I_o(\gamma r)\} \sin \beta z$

where I_o is modified Bessel function

γ = radial propagation constant

r = radial distance

β = longitudinal propagation constant = $2\pi/\lambda$

λ = wavelength in the guide

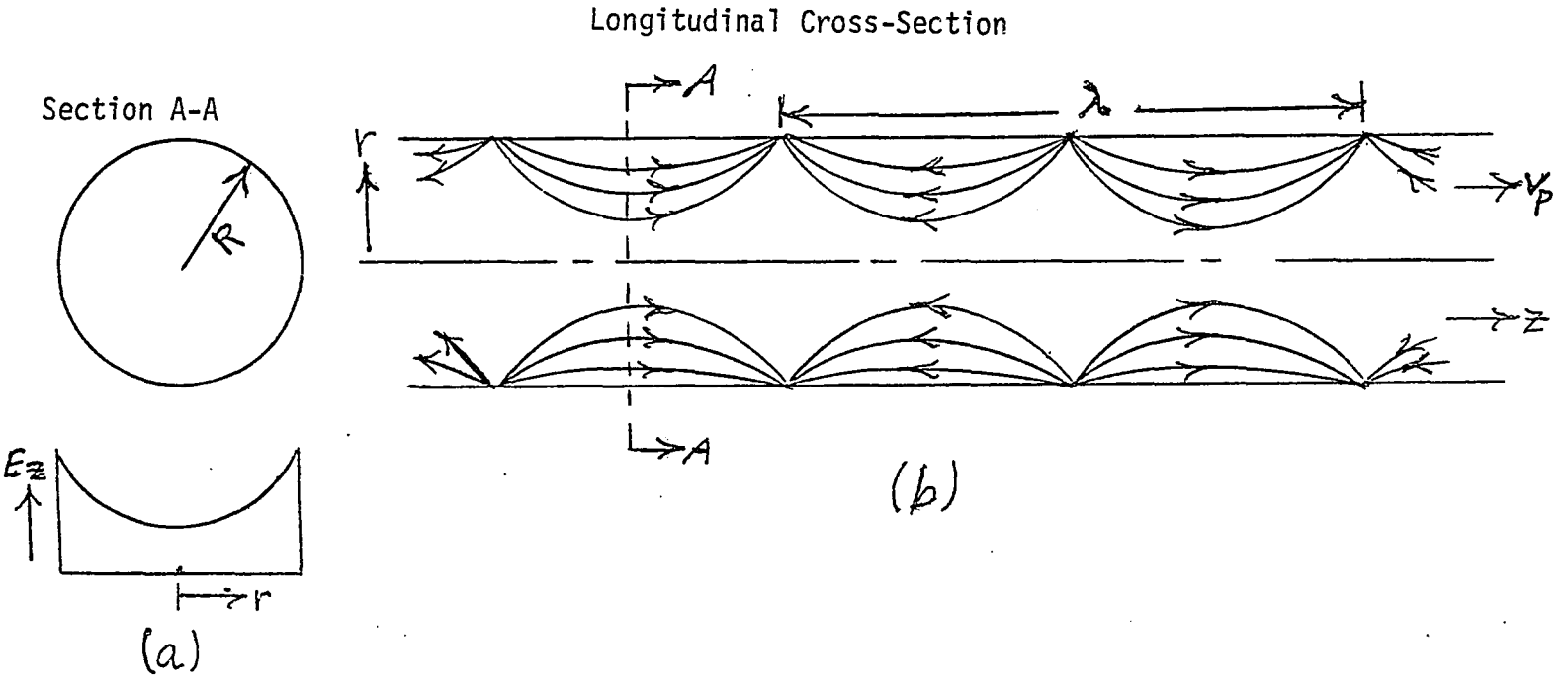

Figure 2-4 Electric field pattern of a longitudinal circuit-wave mode

The fields do not vary in the θ-direction. (This corresponds to the n = 0 mode to be discussed later.) The longitudinal fields along the axis set up the space charge waves causing space charge density and velocity modulation of the beam on the axis.

A snapshop of a typical electric field pattern of a circuit transverse wave that can interact with a beam transverse wave is shown in Figure 2-5b. The transverse field at section A-A is shown in Figure 2-5a. The longitudinal field on axis is zero because the fields from diametrically opposite sides of the circuit cancel on axis. The variation of the longitudinal electric field with radius, r, close to the axis, is linear as shown in Figure 2-5c. The longitudinal field close to the axis varies as

$$E_z \sim r \sin \beta z$$

where r = radial distance

β = longitudinal propagation constant $= \frac{2\pi}{\lambda}$

The fields have one periodic variation in the θ-direction. (This corresponds to the n = ±1 modes to be discussed later.)

If the wave has linear polarization (no twist), it can be decomposed into the sum of equal amplitude left-and right-polarized waves. Siegman[7] has shown that a linearly polarized circuit wave will not excite the beam transverse synchronous waves.

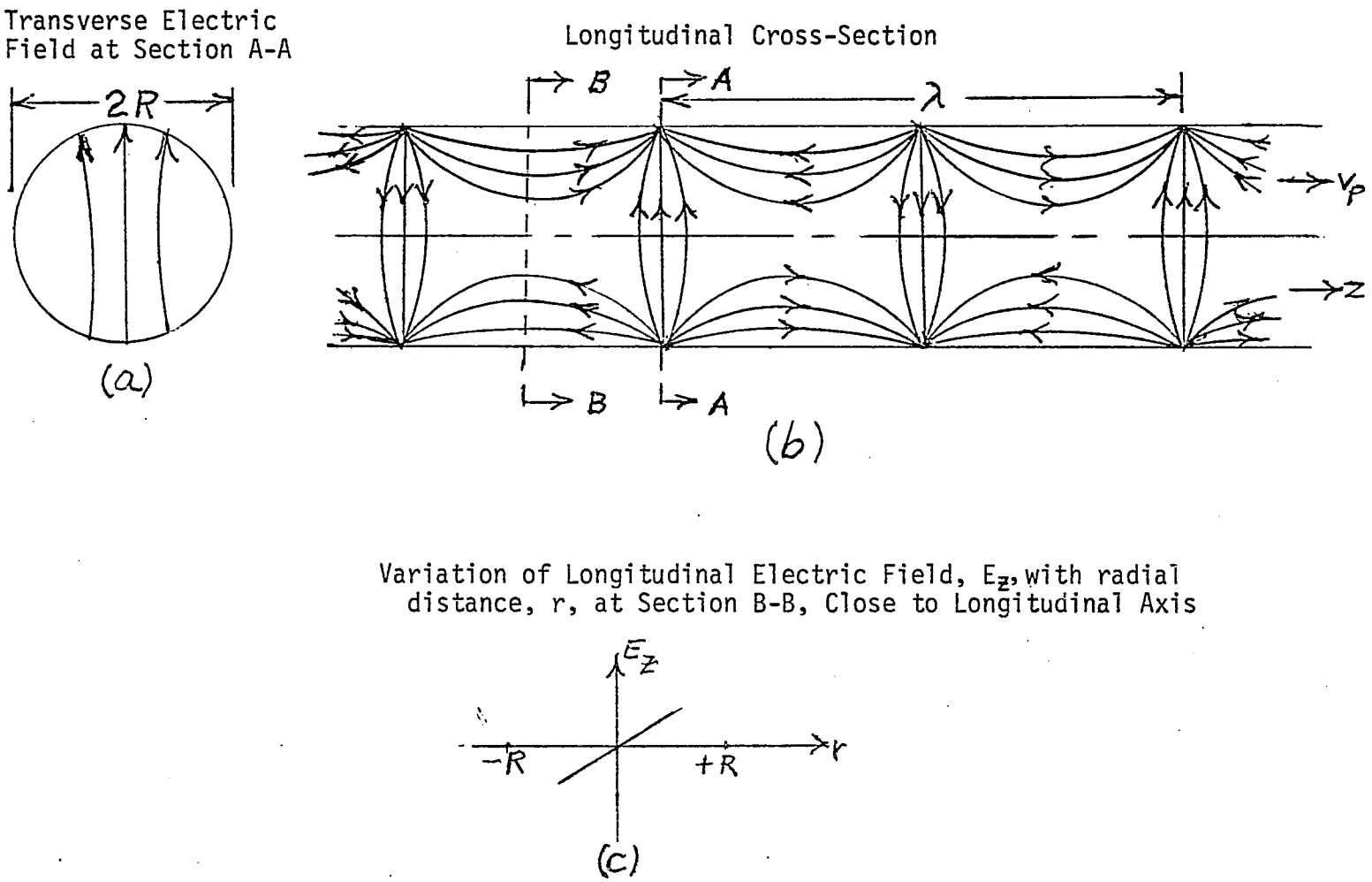

Figure 2-5 Electric Field Pattern of a Transverse Circuit-Wave Mode

CHAPTER III

BACKGROUND THEORY

3.1 Maxwell's Equations[2, 3]

Maxwell's equations, which describe all macroscopic electromagnetic phenomena are given by:

$$(3.1)\quad \nabla \times \overline{E} = \frac{-\partial \overline{B}}{\partial t}$$

$$(3.2)\quad \nabla \times \overline{H} = \frac{\partial \overline{D}}{\partial t} + \overline{J}$$

with auxiliary relations

$$(3.3)\quad \nabla \cdot \overline{D} = \rho$$

$$(3.4)\quad \nabla \cdot \overline{B} = 0$$

$$(3.5)\quad \overline{B} = \mu \overline{H}$$

$$(3.6)\quad \overline{D} = \varepsilon \overline{E}$$

where

$\overline{J}$ is the vector current density in amperes/(meter)^2

$\overline{E}$ is the electric field vector in volts/meter

$\overline{H}$ is the magnetic field vector in amperes/meter

$\overline{D}$ is the electric flux density vector in coulombs/(meter)^2

$\overline{B}$ is the magnetic flux density vector in webers/(meter)^2

ρ is the charge density in coulombs/(meter)^2

ε is the dielectric constant of the medium in farads/meter

μ is the permeability of the medium in henries/meter

3.2 The Wave Equation

In cylindrical coordinates in a nonconducting region where the current density, J, and the charge density, ρ, equal zero, and where variations with time and z are given by $e^{j\omega t-\gamma z}$, Maxwell's equations (3.1), (3.2), (3.5) and (3.6) are

$$(3.7)\quad \nabla \times \overline{E} = -j\omega\mu\overline{H}$$

$$(3.8)\quad \frac{\partial E_z}{r\partial\phi} + \gamma E\phi = -j\omega\mu H_r$$

$$(3.9)\quad -\gamma E_r - \frac{\partial E_z}{\partial r} = -j\omega\mu H_\phi$$

$$(3.10)\quad \frac{1}{r}\left(\frac{\partial(rE\phi)}{\partial r} - \frac{\partial Er}{\partial\phi}\right) = -j\omega\mu H_z$$

$$(3.11)\quad \nabla \times \overline{H} = j\omega\epsilon\overline{E}$$

$$(3.12)\quad \frac{\partial H_z}{r\partial\phi} + \gamma H\phi = j\omega\epsilon E_r$$

$$(3.13)\quad -\gamma H_r - \frac{\partial H_z}{\partial r} = j\omega\epsilon E\phi$$

$$(3.14)\quad \frac{1}{r}\left(\frac{\partial(rH\phi)}{\partial r} - \frac{\partial Hr}{\partial\phi}\right) = j\omega\epsilon E_z$$

These equations can be combined to give

$$(3.15)\quad h^2H_r = \frac{j\omega\epsilon}{r}\frac{\partial E_z}{\partial\phi} - \gamma\frac{\partial H_z}{\partial r}$$

$$(3.16)\quad h^2H\phi = -j\omega\epsilon\frac{\partial E_z}{\partial r} - \frac{\gamma}{r}\frac{\partial H_z}{\partial\phi}$$

$$(3.17)\quad h^2E_r = -\gamma\frac{\partial E_z}{\partial r} - j\frac{\omega\mu}{r}\frac{\partial H_z}{\partial\phi}$$

$$(3.18)\quad h^2E_\phi = -\frac{\gamma}{r}\frac{\partial E_z}{\partial\phi} + j\omega\mu\frac{\partial H_z}{\partial r}$$

$$(3.19)\quad h^2 = \gamma^2 + K^2;\ K^2 = \omega^2\mu\epsilon$$

In equations (3.15) - (3.18), all the fields are expressed in terms of E_z and H_z. It is only necessary to determine E_z and H_z in order to solve for all of the field components.

E_z and H_z satisfy the so-called wave equation, which can be derived as follows.

Taking the curl of (3.7)

$$\nabla \times \nabla \times \overline{E} = -j\omega\mu\nabla \times \overline{H}$$

Substitute (3.11)

$$\nabla \times \nabla \times \overline{E} = \omega^2\mu\varepsilon\overline{E}$$

$$= K^2\overline{E} \quad \text{where } K^2 = \omega^2\mu\varepsilon \tag{3.20}$$

Now, from a vector identity,

$$\nabla \times \nabla \times \overline{E} = \nabla(\nabla\cdot\overline{E}) - \nabla^2\overline{E}$$

But $\nabla\cdot\overline{E} = 0$, since $\rho=o$ in equation (3.3)

Hence,

$$\nabla \times \nabla \times \overline{E} = -\nabla^2\overline{E} \tag{3.21}$$

Substituting (3.21) into (3.20), the wave equation is

$$\nabla^2\overline{E} = -K^2\overline{E} \tag{3.22}$$

In cylindrical coordinates, (3.22) becomes

$$(3.23)\quad \hat{r}\left(\nabla^2 E_r - \frac{2}{r^2}\frac{\partial E\phi}{\partial \phi} - \frac{E_r}{r^2}\right) + \hat{\phi}\left(\nabla^2 E_\phi + \frac{2}{r^2}\frac{\partial E_r}{\partial \phi} - \frac{E\theta}{r^2}\right) + \hat{z}\left(\nabla^2 E_z\right) = -K^2(\hat{r}E_r + \hat{\phi}E_\phi + \hat{z}E_z)$$

where $\hat{r}$, $\hat{\phi}$, and $\hat{z}$ are unit vectors of the coordinate system.

Equating the z-components of both sides of (3.23),

$$(3.24)\quad \nabla^2 E_z = -K^2 E_z$$

Equation (3.24) shows that E_z satisfies the wave equation (3.22).

In cylindrical coordinates, (3.24) becomes

$$(3.25)\quad \frac{\partial^2 E_z}{\partial r^2} + \frac{1}{r}\frac{\partial E_z}{\partial r} + \frac{1}{r^2}\frac{\partial^2 E_z}{\partial \phi^2} + \frac{\partial^2 E_z}{\partial z^2} = -K^2 E_z$$

Since $E_z \sim e^{j\omega t - \gamma z}$, the last term of the left side of (3.25) is

$$\frac{\partial^2 E_z}{\partial z^2} = \gamma^2 E_z$$

Equation (3.25) becomes

$$(3.26)\quad \boxed{\frac{\partial^2 E_z}{\partial r^2} + \frac{1}{r}\frac{\partial E_z}{\partial r} + \frac{1}{r^2}\frac{\partial^2 E_z}{\partial \phi^2} = -h^2 E_z}$$

where again $h^2 = \gamma^2 + K^2$

In a similar manner, starting with equation (3.11) leads to

(3.27) $\nabla^2 H_z = - K^2 H_z$

Equation (3.27) shows that H_z also satisfies the wave equation (3.22)

Using an identical procedure as above, starting with equation (3.11) gives

(3.28) $$\boxed{\frac{\partial^2 H_z}{\partial r^2} + \frac{1}{r}\frac{\partial H_z}{\partial r} + \frac{1}{r^2}\frac{\partial^2 H_z}{\partial \phi^2} = - h^2 H_z}$$

E_z and H_z are determined from equations (3.26) and (3.28). The other field components are determined from equations (3.15) - (3.19).

3.3 Solutions to the Wave Equation

Let A represent either E_z or H_z. A is assumed to vary with time and the coordinate z as $\exp(j\omega t - \gamma z)$. The differential equation in r and ϕ is (Equation (3.26) or (3.28)).

(3.29) $$\frac{\partial^2 A}{\partial r^2} + \frac{1}{r}\frac{\partial A}{\partial r} + \frac{1}{r^2}\frac{\partial^2 A}{\partial \phi^2} = - h^2 A$$

(3.30) where $h^2 = \gamma^2 + K^2$

Assume a product solution

(3.31) $A = R(r) \cdot \Phi(\phi)$

where R(r) is a function r only

and $\Phi(\phi)$ is a function of ϕ only

Substituting (3.31) into (3.29) gives

$$\Phi \frac{d^2R}{dr^2} + \frac{\Phi}{r} \frac{dR}{dr} + \frac{R}{r^2} \frac{d^2\Phi}{d\phi^2} + h^2\Phi R = 0$$

Multiply by $\frac{r^2}{\Phi R}$

$$(3.32) \quad \frac{r^2}{R} \frac{d^2R}{dr^2} + \frac{r}{R} \frac{dR}{dr} + r^2h^2 = - \frac{1}{\Phi} \frac{d^2\Phi}{d\phi^2}$$

The left side of (3.32) is a function of r only, while the right side is a function of ϕ only. The only way these independent functions can be equal is for them to be equal to a constant. Setting the right side of (3.32) equal to a constant, say n^2,

$$(3.33) \quad \frac{d^2\Phi}{d\phi^2} + n^2\Phi = 0$$

The solution of (3.33) can be expressed as,

$$(3.34) \quad \boxed{\Phi = A_n \cos n\phi + B_n \sin n\phi}$$

where A_n and B_n are constants determined by the boundary conditions.

Since the fields at every point in space must be univalued, n must be an integer.

Setting the left side of (3.32) equal to n^2, and multiplying by $\frac{R}{r^2}$

$$\frac{d^2R}{dr^2} + \frac{1}{r} \frac{dR}{dr} + (h^2 - \frac{n^2}{r^2})R = 0$$

Dividing by h^2,

$$(3.35) \qquad \boxed{\frac{d^2R}{d(rh)^2} + \frac{1}{rh}\frac{dR}{d(rh)} + \left(1 - \frac{n^2}{(rh)^2}\right) R = 0}$$

This is a standard form of the Bessel equation of order n in terms of (rh), the solution of which can be expressed as

$$(3.36) \qquad \boxed{R = C_n J_n (rh) + D_n N_n (rh)}$$

where J_n is Bessel function of first kind of order n

N_n is Bessel function of second kind of order n

C_n and D_n are constants determined by the boundary conditions

n is any positive or negative integer

Substituting (3.34) and (3.36) into (3.31), the solution for A is

$$(3.37) \qquad A = (A_n \cos n\phi + B_n \sin n\phi)(C_n J_n(rh) + D_n N_n(rh)$$

The fields E_z or H_z can be express in the form

$$(3.38) \qquad \boxed{E_z \text{ or } H_z = (A_n \cos n\phi + B_n \sin n\phi)(C_n J_n (rh) + D_n N_n (rh)) \cdot e^{j\omega t - \gamma z}}$$

In general $\gamma = \alpha + j\beta$. If propagation occurs in a lossless waveguide, the wave does not grow or decay, so that $\alpha = 0$ and γ is purely imaginary, i.e., $\gamma = j\beta$. Hence $\gamma^2 < 0$. It will be recalled that

$$h^2 = \gamma^2 + K^2, \text{ where } K^2 = \omega^2\mu\varepsilon > 0$$

If $|\gamma^2| < K^2$ with $\gamma^2 < 0$, then $h^2 > 0$, so that h is purely real. The phase velocity in the guide will be

$$v_p = \frac{\omega}{\beta}$$

Since $\beta < K$, $v_p > C$ (a fast wave)

If $|\gamma^2| > K^2$ with $\gamma^2 < 0$, then $h^2 < 0$, so that h is purely imaginary. In this case, since $\beta > K$, $v_p < C$ (a slow wave). The Bessel functions in (3.36) will then have imaginary arguments. Equation (3.36) can then be put into another form.

In the Bessel equation (3.35), let $h = j\gamma_r$, where γ_r is real. Equation (3.35) is then transformed to

$$\frac{d^2R}{d(\gamma_r r)^2} + \frac{1}{\gamma_r r}\frac{dR}{d(\gamma_r r)} - \left(1 + \frac{n^2}{(\gamma_r r)^2}\right) R = 0 \tag{3.39}$$

This is the modified Bessel equation of order n, the solution of which can be express as .

$$R = C_n I_n(\gamma_r r) + D_n K_n(\gamma_r r) \tag{3.40}$$

where I_n is modified Bessel function of the first kind of order n

K_n is modified Bessel function of the second kind of order n

C_n and D_n are again constants determined by the boundary conditions

n is any positive or negative integer

For slow waves (where $v_p < C$) in a lossless medium, fields E_z or H_z can be expressed in the form

$$E_z \text{ or } H_z = (A_n \cos n\phi + B_n \sin n\phi)(C_n I_n(\gamma_r r) + D_n K_n(\gamma_r r)) \cdot e^{j(\omega t - \beta z)} \tag{3.41}$$

Equation (3.41) can be written in the form

$$E_z \text{ or } H_z = (C_n I_n(\gamma_r r) + D_n K_n(\gamma_r r))\, e^{jn\phi} \cdot e^{j(\omega t - \beta z)} \tag{3.42}$$

where the constants C_n and D_n can be complex and can contain the initial phase of $e^{jn\phi}$ and where n is any positive or negative integer.

In (3.42), since,

$$h^2 = \gamma^2 + K^2$$

where $h = j\gamma_r$

$$\gamma = j\beta$$

$$K = \omega\sqrt{u\varepsilon}$$

Then,

(3.43) $$\gamma_r^2 = \beta^2 - K^2$$

(3.44) $$\gamma_r = + (\beta^2 - K^2)^{\frac{1}{2}}$$

The arguments of the I_n and K_n functions in (3.42) are real and positive.

3.4 Floquet's Theorem and Space Harmonics[10]

Floquet's Theorem is a basis for a study of periodic transmission systems, and may be stated as follows:

> "For a given mode of propagation at a given steady-state frequency, the fields at one cross-section differ from those one period away only by a complex constant."

The theorem is true whether the structure contains loss or not so long as it is periodic. The proof of the theorem lies in the fact that when the structure having infinite length is displaced along its axis by one period it cannot be distinguished from its original self.

Let the electric or magnetic field be

$$E = \hat{E}\ (x, y, z)\ e^{-\gamma z}\ e^{j\omega t}$$

where $\hat{E}\ (x, y, z)$ is an amplitude factor periodic in z with period L

γ = complex propagation constant

$= \alpha + j\beta$

$$e^{-\gamma z} = e^{-(\alpha+j\beta)z} = e^{-\alpha z}\ e^{-j\beta z}$$

Start at z_1, call the field here E_1, move to $z_2 = z_1 + L$ and call the field here E_2; then

$$E_1 = \hat{E}\ (x, y, z_1)\ e^{-\gamma z_1}\ e^{j\omega t}$$

$$E_2 = \hat{E}\ (x, y, z_1 + L)\ e^{-\gamma(z_1 + L)}\ e^{j\omega t}$$

but

$$\hat{E}\ (x, y, z_1) = \hat{E}\ (x, y, z_1 + L)$$

Therefore

$$E_2 = E_1\ e^{-\gamma L}$$

so that Floquet's theorem is satisfied.

The field $\hat{E}\ (x, y, z)\ e^{-\gamma z}$ can be expanded in a Fourier series of the form

$$\hat{E}\ (x, y, z)\ e^{-\gamma z} = \sum_{\text{All } n} E_n\ (x, y)\ e^{-j(2\pi n/L)z}\ e^{-\gamma z} \tag{3.45}$$

To find $E_n\ (x, y)$ multiply by $e^{j(2\pi m/L) + \gamma z}$:

$$\hat{E}\ (x, y, z)\ e^{j(2\pi m/L)z} = \sum_{\text{All } n} E_n\ (x,y)\ e^{j(2\pi m/L)z\ -j(2\pi n/L)z}$$

Integrate both sides from z_1 to $z_1 + L$.

$$\int_{z_1}^{z_1 + L} \hat{E}\ (x, y, z) \cdot e^{j(2\pi m/L)z}\ dz = \sum_{\substack{\text{All} \\ n}} \int_{z_1}^{z_1 + L} E_n(x,y) e^{j(2\pi/L)(m-n)z} dz$$

$$= 0,\ m = n$$

$$= E_n\ (x, y)L,\ m = n$$

Hence,

$$E_n(x,y) = \frac{1}{L} \int_{z1}^{z1+L} \{\hat{E}(x,y,z)e^{-\gamma z}\}\, e^{\{\gamma + j(2\pi n/L)\}z} dz$$

This expression is used to calculate the amplitude of individual space harmonics.

The nth term on the right of equation (3.45) is called the nth space harmonic, or Hartree harmonic. It has a propagation constant

$$\gamma + j\,\frac{2\pi n}{L} \tag{3.46}$$

If there are no losses in the system, it turns out that γ is either purely real or purley imaginary. For propagation, γ is imaginary, so that

$$\gamma = j\beta o$$

Define

$$j\beta_n = j\beta_o + j\,\frac{2\pi n}{L}$$

or

$$\beta_n = \beta_o + \frac{2\pi n}{L} \tag{3.47}$$

where β_n is called the phase constant for the nth space harmonic.

In analyzing specific structures the problem is to find β_o, E_n, H_n (H_n is the magnetic field) as functions of ω so as to satisfy the required boundary conditions.

3.5 The Sheath Helix[10]

A concept[5] known as the "sheath helix" yields solutions to Maxwell's equations which show many of the properties of an actual helix. The sheath helix is a circular cylindrical surface conducting in only the "helical" direction. A sheath helix is shown in Figure 3-1, and a developed right-hand sheath helix is shown in Figure 3-2. A sheath helix is perfectly conducting in a direction making an angle ψ with the plane perpendicular to the axis. Its conductivity is zero in a direction normal to the direction of conduction. The sheath model is found to be a good approximation to an actual helix. Since slow waves ($v_p<c$) rather than fast waves are expected, the fields are written in terms of modified Bessel functions.

Inside the sheath helix, the modified Bessel functions must be of the first kind, I_n, because the fields must be finite at $r = o$. Outside the sheath helix, the modified Bessel functions must be of the second kind, K_n, because the fields must approach zero as $r \to \infty$. The superscript i will be used for fields inside the sheath and the superscript o will be used for fields outside. Thus, utilizing the appropriate variation for the E_z and H_z fields in equation (3.42), and utilizing equations (3.15) to (3.18) and the fact that $h = j\gamma_r$, the field components are (with time variation, $e^{j\omega t}$, understood).

Inside the sheath, $a>r>o$,

$$E_z^i = A_n^i I_n(\gamma_r r)e^{-j\beta z} e^{jn\phi} \tag{3.48}$$

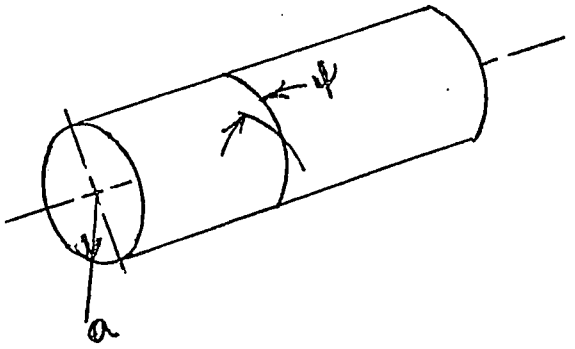

Figure 3-1 Sheath Model Helix

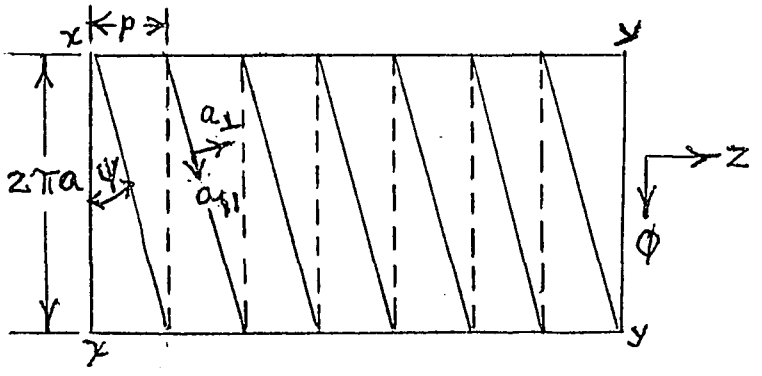

Figure 3-2 The outside of a developed right-hand sheath helix. The surface conducts only in the direction of the unit vector $a_{\parallel}$. When rolled back into a right-circular cylindrical surface the points x and y coincide.

(3.49) $$H_z{}^i = B_n{}^i \, I_n(\gamma_r r) \, e^{-j\beta z} \, e^{jn\phi}$$

(3.50) $$E_r{}^i = \{\frac{j\beta}{\gamma_r} A_n{}^i \, I_n'(\gamma_r r) - \frac{n\omega u}{\gamma_r{}^2 r} B_n{}^i \, I_n(\gamma_r r)\} e^{-j\beta z} \, e^{jn\phi}$$

(3.51) $$E_\phi{}^i = \{\frac{-n\beta}{\gamma_r{}^2 r} A_n{}^i \, I_n(\gamma_r r) - \frac{j\omega u}{\gamma_r} B_n{}^i \, I_n'(\gamma_r r)\} e^{-j\beta z} \, e^{jn\phi}$$

(3.52) $$H_r{}^i = \{\frac{n\omega\varepsilon}{\gamma_r{}^2 r} A_n{}^i \, I_n(\gamma_r r) + \frac{j\beta}{\gamma} B_n{}^i \, I_n'(\gamma_r r)\} e^{-j\beta z} \, e^{jn\phi}$$

(3.53) $$H_\phi{}^i = \{\frac{j\omega\varepsilon}{\gamma_r} A_n{}^i \, I_n'(\gamma_r r) - \frac{n\beta}{\gamma_r{}^2 r} B_n{}^i \, I_n(\gamma_r r)\} e^{-j\beta z} \, e^{jn\phi}$$

Outside the sheath, $\infty > r > a$

(3.54) $$E_z{}^o = A_n{}^o \, K_n(\gamma_r r) \, e^{-j\beta z} \, e^{jn\phi}$$

(3.55) $$H_z{}^o = B_n{}^o \, K_n(\gamma_r r) \, e^{-j\beta z} \, e^{-jn\phi}$$

(3.56) $$E_r{}^o = \{\frac{j\beta}{\gamma_r} A_n{}^o \, K_n'(\gamma_r r) - \frac{n\omega u}{\gamma_r{}^2 r} B_n{}^o \, K_n(\gamma_r r)\} e^{-j\beta z} \, e^{jn\phi}$$

(3.57) $$E_\phi{}^o = \{\frac{-n\beta}{\gamma_r{}^2 r} A_n{}^o \, K_n(\gamma_r r) - \frac{j\omega u}{\gamma_r} B_n{}^o \, K_n'(\gamma_r r)\} e^{-j\beta z} \, e^{jn\phi}$$

(3.58) $$H_r{}^o = \{\frac{n\omega\varepsilon}{\gamma_r{}^2 r} A_n{}^o \, K_n(\gamma_r r) + \frac{j\beta}{\gamma_r} B_n{}^o \, K_n'(\gamma_r r)\} e^{-j\beta z} \, e^{jn\phi}$$

(3.59) $$H_\phi{}^o = \{\frac{j\omega\varepsilon}{\gamma_r} A_n{}^o \, K_n'(\gamma_r r) - \frac{n\beta}{\gamma_r{}^2 r} B_n{}^o \, K_n(\gamma_r r)\} e^{-j\beta z} \, e^{jn\phi}$$

with

(3.60) $$\gamma_r{}^2 = \beta^2 - K^2$$ (Same as equation (3.43))

In (3.50) - (3.53) and (3.56) - (3.59), the derivatives I_n' and K_n' are with respect to the argument $(\gamma_r r)$.

In Figure 3-2, the skew boundary conditions at $r = a$ are:

(3.61) $$E_{||}^{i} = 0$$

(3.62) $$E_{||}^{o} = 0$$

(3.63) $$E_{\perp}^{i} = E_{\perp}^{o}$$

(3.64) $$H_{||}^{i} = H_{||}^{o}$$

where subscripts || and $\perp$ mean parallel and perpendicular, respectively, to the direction of conduction.

Referring to Figure (3-2), the boundary conditions (3.61) - (3.64) can be written as

(3.65) $$E_z^i \sin\psi + E\phi^i \cos\psi = 0$$

(3.66) $$E_z^o \sin\psi + E\phi^o \cos\psi = 0$$

(3.67) $$E_z^i \cos\psi - E^i\phi \sin\psi = E_z^o \cos\psi - E\phi^o \sin\psi$$

(3.68) $$H_z^i \sin\psi + H\phi^i \cos\psi = H_z^o \sin\psi + H\phi^o \cos\psi$$

Inserting equations (3.48) - (3.59) into (3.65) - (3.68), the following determinantal equation is obtained:

$$\frac{I_n'(\gamma_r a)\, K_n'(\gamma_r a)}{I_n(\gamma_r a)\, K_n(\gamma_r a)} = -\frac{(\gamma_r^2 a^2 - n\beta a \cot\psi)^2}{K^2 a^2 \gamma_r^2 a^2 \cot^2\psi} \tag{3.69}$$

The solution of (3.69), together with (3.60), gives values of the propagation constant, β, of propagating waves that can exist with the given boundary conditions.

Examination of (3.69) shows that a right-hand helix is not different from a left-hand helix. Changing from the right-hand helix in Figure 3-2 to a left-hand helix is equivalent to changing the sign of the pitch angle, ψ, in equations (3.65) - (3.68). In equation (3.69), if we change the sign of ψ and hence the sign of cot ψ, the solution of (3.69) for β is the same as for the right-hand helix if the sign of n is changed. This is so because n occurs only together with cot ψ and the I_n's and K_n's are even functions of n. Hence, for every solution of the right-hand helix of the form $f_n(r)\, e^{-j\beta z}\, e^{jn\phi}$, there exists a solution of the form $f_{-n}(r)\, e^{-j\beta z}\, e^{-jn\phi}$ with the same β for the left-hand helix. Physically, this should be so, because the solutions for β should not depend on the direction of twist of the helix.

For n = 0, the determinantal equation (3.69) becomes

$$-\frac{Io'(\gamma_r a)Ko'(\gamma_r a)}{\gamma_r^2 a^2 Io(\gamma_r a)Ko(\gamma_r a)} = \frac{1}{K^2 a^2 \cot^2\psi} \tag{3.70}$$

This can be solved by assuming values of $\gamma_r a$ and solving for ka cot ψ. Then Ka can be plotted as a function of $\beta a/\cot \psi$ utilizing (3.60).

For n other than zero, a good approximation to the left side of equation (3.69) is[10]

$$\frac{I_n'(\gamma_r a)\, K_n'(\gamma_r a)}{I_n(\gamma_r a)\, K_n(\gamma_r a)} = -\frac{n^2 + \gamma_r^2 a^2}{\gamma_r^2 a^2} \tag{3.71}$$

Using (3.71) in (3.69)

$$\frac{n^2 + \gamma_r^2 a^2}{\gamma_r^2 a^2} = \frac{(\gamma_r^2 a^2 - n\, \beta a \cot \psi)^2}{K^2 a^2 \gamma_r^2 a^2 \cot^2 \psi} \tag{3.72}$$

or,

$$\gamma_r^2 a^2 \{(\gamma_r^2 a^2 - n\, \beta a \cot \psi)^2 - (n^2 + \gamma_r^2 a^2) K^2 a^2 \cot^2 \psi\} = 0 \tag{3.73}$$

Two solutions of (3.73) are found by setting each of the two factors equal to zero. The first is

$$\gamma_r^2 a^2 = 0 \tag{3.74}$$

Utilizing (3.60), Equation (3.74) yields

$$\beta a = \pm Ka \tag{3.75}$$

In the second factor, it is desirable to make the approximations $\gamma_r^2 a^2 \simeq \beta^2 a^2$ for slow waves, and $\gamma_r^2 a^2 >> n^2$ for small n. Using these approximations, the second factor in (3.73) results in

$$(\beta^2 a^2 - n\,\beta\, a \cot\psi)^2 = \beta^2 a^2 K^2 a^2 \cot^2\psi \tag{3.76}$$

or,

$$\frac{\beta a}{\cot\psi} = \pm Ka + n \tag{3.77}$$

All of the approximate solutions, together with the solutions for n = 0, are shown in Figure 3-3 as dashed lines. The exact solutions, calculated from (3.69) are shown as solid lines. No exact solutions exist in the shaded region. The shaded region is forbidden. This region exists because the magnitude of the n'th phase constant, $\beta = \beta_n$, must always be greater than the magnitude of the free-space constant, K, for the slow wave solutions as seen from equation (3.60), where γ_r (= γ_{rn} for the n'th mode) is real and γ_r^2 is positive. Modification of the approximate solutions is required only for $(\gamma_r a)$ near zero and in and near the forbidden region. In Figure 3-3, $K = \omega/c$, so that Figure 3-3 is proportional to an ω-β plot for the modes in which the phase velocity is $v_p = \frac{\omega}{\beta}$, and the group velocity is $v_g = \frac{d\omega}{d\beta}$ which is proportional to the slopes of the curves.

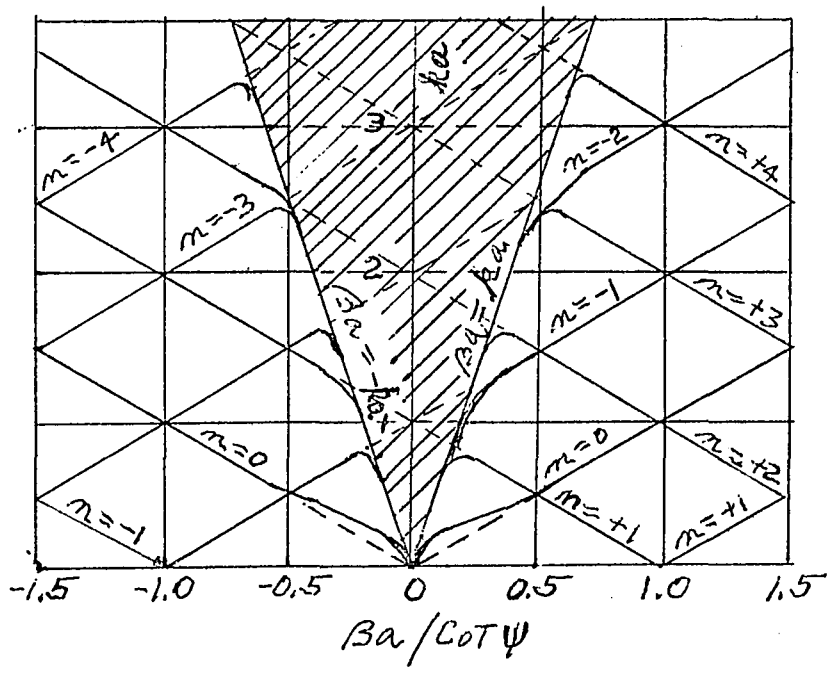

Figure 3-3 A plot of the approximate and the exact solutions to the determinantal equation for the sheath helix. Cot ψ has been taken as 5. (From Watkins, with corrected labeling for n.)

3.6 The Tape Helix[6,8,10]

3.6.1 The Model. A more representative model of the wire helix is the tape helix shown in Figure 3-4. The diameter is 2a and $\cot \psi = 2\pi a/p$ where p is the pitch. (Also see Figure 3-2.) The tape is of width δ and of zero thickness, and considered to be perfectly conducting in all directions.

Referring to section 3.4, Floquet's theorem shows that when the helix is moved a distance p in the z-direction it coincides with itself. Thus, the z-dependence of the n'th field space harmonic must be of the form

$$e^{-j\beta_n z} = e^{-j\beta_o z} e^{j(\frac{2\pi n}{p})z}$$

Also, if the helix is moved a distance less than p and then rotated in ϕ through an appropriate angle, it again coincides with itself. Consider the general form of the total field, E_z, which consists of the summation of all the space harmonic components, having the foregoing z-dependence:

$$E_z^{o,i} = e^{-j\beta_o z} \sum_{m,n} A_{m,n}^{o,i} \frac{I_m}{K_m} (\gamma_{rn} r) e^{-jm\phi} e^{-j(\frac{2\pi n}{p})z} \tag{3.78}$$

where the cylindrical co-ordinates r, ϕ, and z are used. Superscripts i and o denote quantities inside the helix and outside the helix, respectively. The modified Bessel functions, I_m and K_m, are for inside and outside quantities, respectively. m and n may be any positive or negative integers.

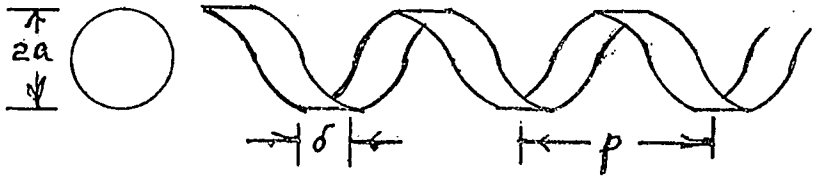

Figure 3-4(a) Tape Helix

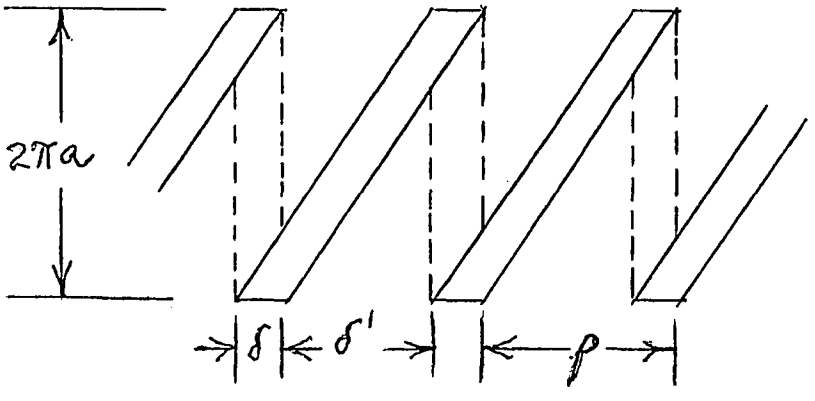

Figure 3-4(b) Developed Helix

Let

$$z = z' + z$$

$$\phi = \phi' + 2\pi z/p$$

where $\frac{2\pi z}{p}$ is the angle through which the helix must be rotated to make it coincide with itself. When these substitutions are made in equation (3.78),

$$E_z^{o,i} = \sum_{m,n} E_{zm,n}^{o,i} = e^{-j\beta_o z}\, e^{-j\beta_o z'}.$$

$$(3.79) \qquad \cdot \sum_{m,n} A_{m,n}^{o,i}\, \frac{I_m}{K_m}(\gamma_{rn} r) e^{-j(m+n)(\frac{2\pi z}{p})} e^{-jm\phi'} e^{-jn(\frac{2\pi z'}{p})}$$

Now, according to Floquet's theorem, the solution as a function of ϕ' and z' must be of the same form as it is as a function of ϕ and z. This must be true for all z, not only for $z = p$. To ensure this, it is necessary to take $m = -n$ and for $m \neq -n$ to make $A_{m,n}^{o,i} = 0$. Thus, noting that $I_n(x) = I_{-n}(x)$ and $K_n(x) = K_{-n}(x)$,

$$(3.80) \qquad E_z^{o,i} = \sum_n E_{zn}^{o,i} = e^{-j\beta_o z} \sum_n A_n^{o,i}\, \frac{I_n}{K_n}(\gamma_{rn} r) e^{-jn(\frac{2\pi z}{p} - \phi)}$$

$$(3.81) \qquad H_z^{o,i} = \sum_n H_z^{o,i} = e^{-j\beta_o z} \sum_n B_n^{o,i} \frac{I_n}{K_n}(\gamma_{rn} r) e^{-jn(\frac{2\pi z}{p} - \phi)}$$

The field components in (3.80) and (3.81) are bounded at $r = o$ by the I_n function and for $r \to \infty$ by the K_n function as long as γ_{rn} is real. It is seen from (3.80) and (3.81) that the fields of the nth component vary angularly as $e^{jn\phi}$ and propagate in the axial direction with a phase constant, β_n, given by

$$\beta_n = \beta_o + n \frac{2\pi}{p} \tag{3.82}$$

where n is any positive or negative integer. This should be so because of the periodicity of the helix. All of these Fourier components are solutions of the wave equation. A summation of them tied together so as to satisfy boundary conditions at the tape forms a mode of propagation. In (3.82), if β_n and β_o are functions of ω, the group velocity of the n'th component is $\frac{1}{d\beta_n/d\omega} = \frac{1}{d\beta_o/d\omega}$, independent of n. Thus, all of the components of a common mode must have a common group velocity, but different phase velocities, and some of them may have oppositely directed group and phase velocities. It should be noted that in the case of the tape helix, the space harmonics are components of a common mode, where all of the components must exist together with the proper complex amplitudes to satisfy the boundary conditions. In the case of the sheath helix, however, each space harmonic is an individual mode which can individually satisfy the boundary conditions.

The boundary conditions for the tape helix at r = a are as follows:

(a) The tangential electric field is continuous for all ϕ and z.

(b) The discontinuity in tangential magnetic field is equal to the total surface current density.

$$E^{i}_{z,\phi} = E^{o}_{z,\phi} \tag{3.83}$$

$$J_{\phi} = H^{i}_{z} - H^{o}_{z} \tag{3.84}$$

$$J_{z} = H^{o}_{\phi} - H^{i}_{\phi} \tag{3.85}$$

where $J_{\phi,z}$ are the surface current densities in the ϕ and z directions. (The units for $J_{\phi,z}$ is amperes/meter.)

J_{ϕ} and J_{z} can be expressed as the sum of Fourier components as follows:

$$J_{\phi} = e^{-j\beta_o z} \sum_{n} j_{\phi n} e^{-jn(\frac{2\pi z}{p} - \phi)} \tag{3.86}$$

$$J_{z} = e^{-j\beta_o z} \sum_{n} j_{zn} e^{-jn(\frac{2\pi z}{p} - \phi)} \tag{3.87}$$

where $j_{\phi n}$ and j_{zn} are the complex Fourier amplitudes of the current densities associated with the n'th space harmonic.

3.6.2 Forbidden Regions for the Single Tape Helix. For the n'th space harmonic, equation (3.60) becomes

$$\gamma_{rn}^2 = \beta_n^2 - K^2 \tag{3.88}$$

Here, γ_{rn} is real and positive for the assumed slow wave solutions where phase velocity is less than the velocity of light in the medium. This is the reason modified Bessel functions are used in equations (3.80) and (3.81). Thus, since γ_{rn}^2 is positive,

$$|\beta n| > |K| \tag{3.89}$$

For n = o,

(3.90) $$|\beta_o| > |K|$$

Equation (3.82) is

(3.91) $$\beta_n = \beta_o + n\frac{2\pi}{p}$$

Referring to Figure 3-4,

(3.92) $$\cot \psi = \frac{2\pi a}{p}$$

From (3.91) and (3.92)

$$\beta_n a = \beta_o a + n \cot \psi$$

or,

(3.93) $$\frac{\beta_n a}{\cot \psi} = \frac{\beta_o a}{\cot \psi} + n$$

As a consequence of (3.90) and (3.93), the periodic forbidden region diagram of Figure 3-5 is obtained, assuming that all of the space harmonics are required to satisfy the boundary conditions. An explanation for the periodicity in Figure 3-5 is as follows.

Consider the case n = o and a point, A. At point A, $\beta_n a/\cot \psi = \beta_o a/\cot \psi < Ka/\cot \psi$, so point A does not satisfy (3.90) and thus point A is in a forbidden region. If all the space harmonics are required to satisfy the boundary conditions, by virtue of (3.93) there will be β_n's at points B, C, D, etc., for all the n's not equal to zero, corresponding to point A. Thus, if a solution β_n exists at

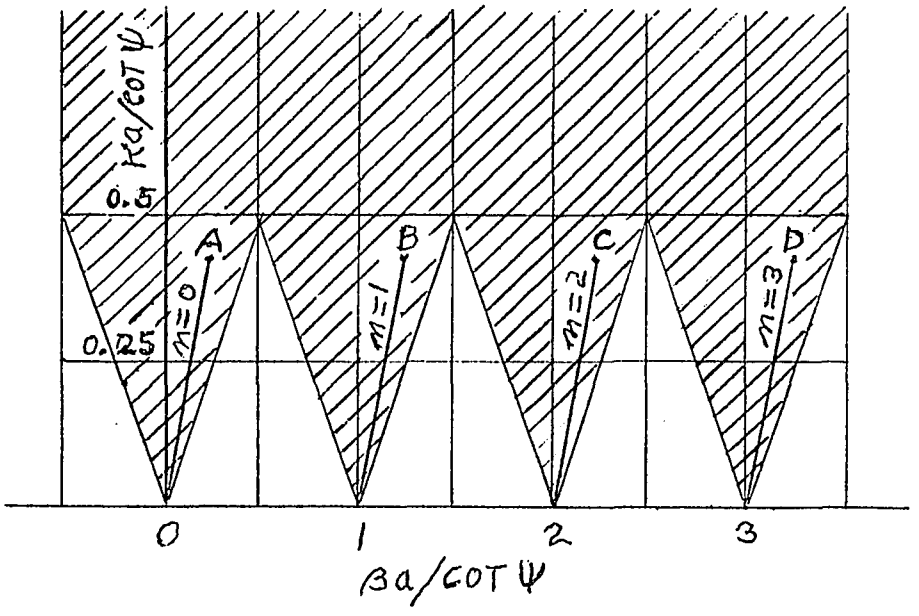

Figure 3-5 Forbidden regions (shaded) for single tape helix.

B, C, D, etc., a solution would exist at A which is forbidden. Hence B, C, D, etc., are in forbidden regions. Thus, the forbidden region is periodic in nature. Note that for the sheath helix, the forbidden region shown in Figure 3-3 is not periodic. This is so because all the space harmonics individually can satisfy the boundary conditions and a summation of the space harmonics is not necessary to satisfy the boundary conditions. Thus, points B, C, D, etc., can satisfy inequality (3.89) and need not exist in a forbidden region, because the existence of point A in a forbidden region is not forced.

3.6.3 Forbidden Regions for the Bifilar Helix (Twisted Transmission Line). The bifilar helix is wound with two wires (two tapes) with equal spacing between successive wires. The forbidden-region diagram will be different from that of the single wire (single tape) helix because some of the space harmonics have zero amplitude, depending on how the wires are excited.

If the two wires are fed with currents of equal amplitude and phase (++, or unbalanced feed), only even space harmonic components exist, as shown below.

The form of the fields is similar to that given by equation (3.78) for the single tape helix, except that the z-dependence of the field is modified. For the unbalanced feed (++), the boundary conditions at the tapes dictate that an even number of π radians exists between the tapes that are spaced a distance p/2, where p = pitch of each tape. Thus, the z- and ϕ-dependence of the fields is

$$E_{zn} \sim e^{-jm\phi}\, e^{-j\left(\frac{2n\pi}{p/2}\right)z}$$

Similar to the method in section 3.6.1, let

(3.94) $$z = z' + z$$

(3.95) $$\phi = \phi' + \frac{2\pi z}{p}$$

Here, the coordinate angle, ϕ, along each tape changes 2π radians in the pitch distance, p, like that for the single tape helix. The general form of the field is

(3.96) $$E_z^{o,i} = e^{-j\beta_o z} \sum_{m,n} A_{m,n}^{o,i} \frac{I_m}{K_m} (\gamma_{rn} r) e^{-jm\phi}\, e^{-j\left(\frac{2n\pi}{p/2}\right)z}$$

Substituting (3.94) and (3.95) into (3.96),

$$E_z^{o,i} = e^{-j\beta_o z}\, e^{-j\beta_o z'} \sum_{m,n} A_{m,n}^{o,i} \frac{I_m}{K_m} (\gamma_r r) \cdot$$

$$\cdot e^{-jm\left(\phi' + \frac{2\pi z}{p}\right)} e^{-j\left(\frac{2n\pi}{p/2}\right)(z + z')}$$

$$= e^{-j\beta_o z}\, e^{-j\beta_o z'} \sum_{m,n} A_{m,n}^{o,i} \frac{I_m}{K_m} (\gamma_r r) \cdot$$

$$\cdot e^{-j(m+2n)\frac{2\pi z}{p}}\, e^{-jm\phi'}\, e^{-j\left(\frac{2n\pi}{p/2}\right)z'}$$

As in section 3.6.2, according to Floquet's theorem, the solution as a function of ϕ' and z' must be of the same form as it as a function of ϕ and z. Thus, we must have $m = -2n$, and for $m \neq -2n$, $A_{m,n}^{o,i} = 0$.

The form of the fields for the ++ feed is then

$$(3.97) \qquad E_z^{o,i} = e^{-j\beta_o z} \sum_{n \text{ even}} A_n^{o,i} \frac{I_n}{K_n} (\gamma_{rn} r)\, e^{-jn(\frac{2\pi z}{p} - \phi)}$$

where n is any even integer.

Similarly, if the two wires are fed with currents of equal amplitude but opposite in phase (+-, or balanced feed), only odd space harmonic components exist. In this case, the boundary conditions at the tapes dictate that an odd number of π radians exists between tapes that are spaced a distance p/2. This is to allow for the reversal of current from tape to tape. Thus, the z and ϕ-dependence of the fields is

$$E_{zn} \sim e^{-jm\phi}\, e^{-j\frac{(2n-1)\pi}{p/2} z}$$

The general form of the fields is

$$(3.98) \qquad E_z^{o,i} = e^{-j\beta_o z} \sum_{m,n} A_{m,n}^{o,i} \frac{I_m}{K_m} (\gamma_{rn} r) e^{-jm\phi} e^{-j\frac{(2m-1)\pi}{p/2} z}$$

Similar to the method for unbalanced feed, substitution of (3.94) and (3.95) into (3.98) yields

$$E_z^{o,i} = e^{-j\beta_o z}\, e^{-j\beta_o z'} \sum A_{m,n}^{o,i} \frac{I_m}{K_m} (\gamma_{rn} r)\, e^{-j(2n-1+m)\frac{2\pi z}{p}} \cdot$$

$$\cdot e^{-j(2n-1)\frac{2\pi z'}{p}}\, e^{-jn\phi'}$$

Thus, we must have $m = -(2n-1)$.

The form of the fields for the +- feed is then

$$(3.99) \qquad E_z^{o,i} = e^{-j\beta_o z} \sum_{n \text{ odd}} A_n^{o,i} \frac{I_n}{K_n}(\gamma_{rn} r)\, e^{-jn(\frac{2\pi z}{p} - \phi)}$$

where n is any odd integer.

In summary, for unbalanced (++) feed for a bifilar helix, only even space harmonics exist, while for balanced (+-) feed, only odd space harmonics exist. This is verified later when the fields are solved utilizing appropriate boundary conditions.

The forbidden-region diagram for the bifilar helix is shown in Figure 3-6. The explanation for Figure 3-6 is similar to that for Figure 3-5 for the single tape helix and is as follows.

In Figure 3-6, take the case where only even space harmonics exist. Consider the case n = 0 with the point A on the n = 0 space harmonic line. At point A, $\beta_o a/\cot\psi < {}^{K}a/\cot\psi$, so point A does not satisfy inequality (3.90) and thus point A is in a forbidden region. If only the even space harmonics are required to satisfy the boundary conditions, by virtue of equation (3.93) there will be β_n's at points B, C, etc., for all even n's not equal to zero, corresponding to point A. Thus, if a solution β_n exists at B, C, etc., a solution also exist at A which is forbidden. Hence, B, C, etc., are in forbidden regions. Thus the shaded regions are forbidden.

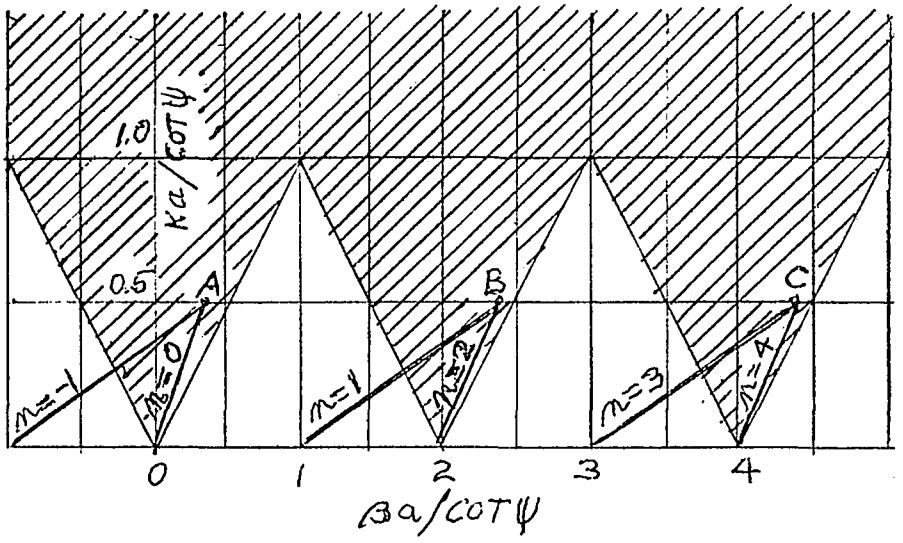

Figure 3-6 Forbidden Regions (shaded) for the Bifilar Helix.

Similarly, take the case where only odd space harmonics exist. Consider the case n = -1, with point A in a forbidden region on the extended n = -1 space harmonic line. Similar to the reasoning above, there will be β_n's at points B, C, etc., for all odd n's not equal to n = -1, corresponding to point A. Thus the same shaded regions are forbidden when only odd n's or only even n's exist.

Incidentally, the V-shaped forbidden regions are characteristic of all open structures[10], i.e., structures having one or more transverse dimensions going to infinity.

3.6.4 The Determinantal Equation for the Tape Helix[8,10]. The determinantal equation for the tape helix is obtained by applying the boundary conditions (3.83), (3.84) and (3.85) to the solution of the wave equation. For the n'th space harmonic, E_{zn} and H_{zn}, equations (3.80) and (3.81) become

$$E_{zn}^{o,i} = A_n^{o,i} \frac{I_n}{K_n} (\gamma_{rn} r)\, e^{-j\beta_n z}\, e^{jn\phi} \tag{3.100}$$

$$H_{zn}^{o,i} = B_n^{o,i} \frac{I_n}{K_n} (\gamma_{rn} r)\, e^{-j\beta_n z}\, e^{jn\phi} \tag{3.101}$$

where $\beta_n = \beta_o + n \frac{2\pi}{p}$

$$\gamma_{rn}^2 = \beta_n^2 - K^2$$

$$K^2 = \omega^2 u\varepsilon$$

The components $E_{rn}^{o,i}$, $E_{\phi n}^{o,i}$, and $H_{rn}^{o,i}$, and $H_{\phi n}^{o,i}$ are related to $E_{zn}^{o,i}$ and $H_{zn}^{o,i}$ by means of equations (3.50) through (3.53) and (3.56) through (3.59), with the subscript n added to the field quantities on the left side of the equations and to β and γ_r wherever they appear.

By utilizing the appropriate field quantities in the boundary condition equations (3.83) to (3.85), an infinite-by-infinite set of simultaneous equations involving the space harmonic currents and fields is obtained. From this set, the exact determinantal equation can be determined for solving for the unknown propagation constant, β_o. The solution will be simplified by utilizing good approximations to the exact equation. The following procedure is used.

(a) A reasonable current distribution in the tape is assumed.

(b) $E_{||}$, the total electric field in the direction of the tape as a function of ϕ and z at $r = a$, is calculated in terms of the assumed current distribution.

(c) $E_{||}$ is set equal to zero along the center line of the tape. This satisfies the boundary condition of E with a good approximation for narrow tapes.

It is assumed that the current in the tape flows only in the tape direction, that it does not vary in phase or amplitude over the width of the tape in the z-direction, and that the total current in the tape varies as $e^{-j\beta_o z}$ in the z-direction, where z is longitudinal distance along the centerline of the tape. The assumed approximate

amplitude variation across the tape is shown in Figure 3-7(b), while the actual current distribution is shown in Figure 3-7(a). Tien[9] has shown that the approximate distribution for narrow tapes gives solutions which differ very little from those utilizing the actual distribution, so that the constant current distribution in Figure 3-7(b) is a good approximation. Figure 3-7(c) indicates a picture of the current in the tape with the approximate distribution shown in Figure 3-7(b). The equi-phase fronts of J_{11} in Figure 3-7(c) are parallel to the z-axis.

The current, J_{11}, in the tape may be written

$$J_{11} = |J_{11}|e^{-j\beta_o z} \tag{3.102}$$

where z is distance along the centerline of the tape in the z-direction.

$|J_{11}|$ can be expanded into Fourier components,

$$|J_{11}| = \sum_n j_{11_n} e^{-jn(2\pi z/p - \phi)} \tag{3.103}$$

Thus, J_{11} becomes

$$J_{11} = \sum_n j_{11_n} e^{-j\beta_o z} e^{-jn(\frac{2\pi z}{p} - \phi)} \tag{3.104}$$

The ϕ and z-components of the current are given by

$$J_\phi = J_{11}.\cos\psi \tag{3.105}$$

$$J_z = J_{11} \sin\psi \tag{3.106}$$

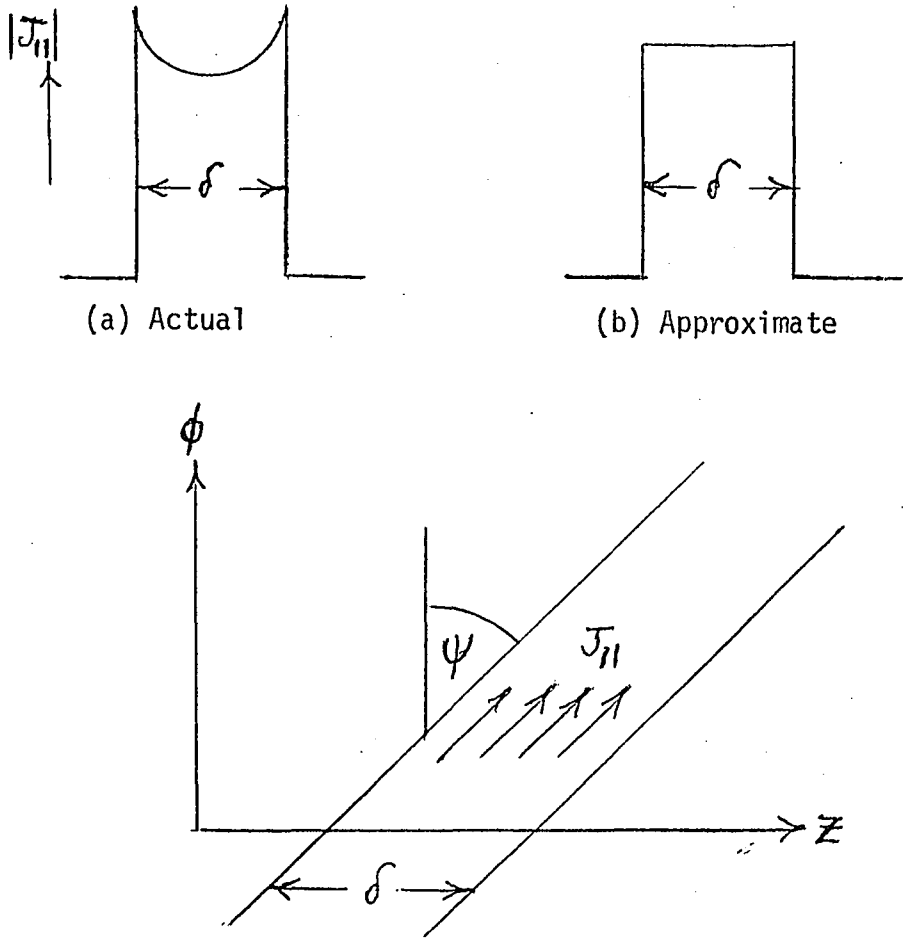

(a) Actual

(b) Approximate

(c) Picture of Approximate Distribution on Tape

Figure 3-7 Actual and Approximate Current Distribution on the Tape.

The amplitude coefficients, $j_{\parallel n}$, of the Fourier components are obtained below.

For the single helix

The current distribution on the tape for this case is shown in Figure 3-8(a).

$$J_{\parallel} = \Sigma j_{\parallel n} e^{-jn\frac{2\pi z}{p}}$$

where n = order of harmonic

p = helix pitch

δ = thickness of tape

$$j_{\parallel n}p = \int_{o}^{\frac{\delta}{2}} Je^{jn\frac{2\pi z}{p}} dz$$

$$+ \int_{p-\frac{\delta}{2}}^{p} Je^{jn\frac{2\pi z}{p}} dz$$

From which,

$$j_{\parallel n} = \frac{J\delta}{p} \frac{\sin(\frac{n\pi\delta}{p})}{\frac{n\pi\delta}{p}} \tag{3.107}$$

For the bifilar helix with balanced (+-) feed

The current distribution on the tape for this case is shown in Figure 3-8(b).

$$J_{\parallel} = \Sigma j_{\parallel n} e^{-jn\frac{2\pi z}{p}}$$

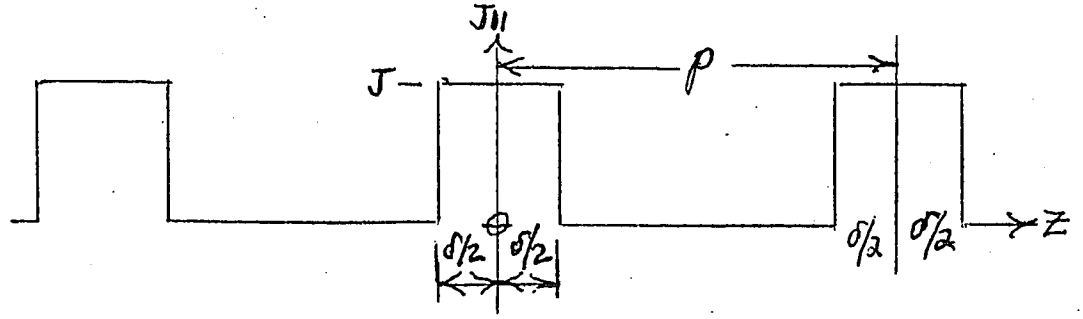

(a) Current Distribution for Single Helical Tape

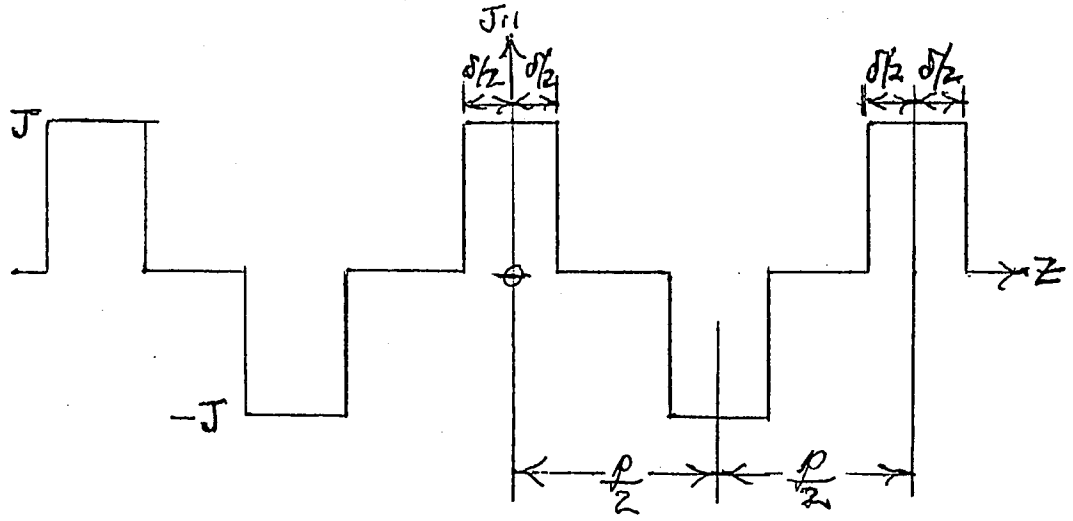

(b) Current Distribution for Bifilar Helical Tape with Balanced (+-) Feed

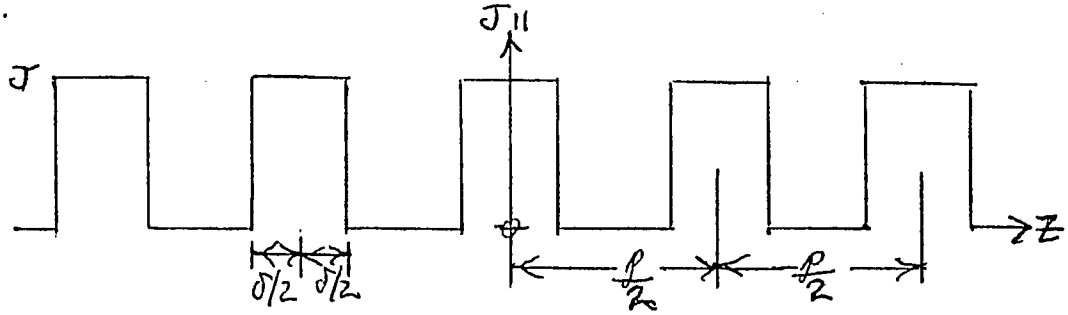

(c) Current Distribution for Bifilar Helical Tape with Unbalanced (++) Feed

Figure 3-8 Current Distributions for Single and Bifilar Tapes.

$$j_{\parallel n}p = \int_{-\frac{p}{2}}^{-\frac{p}{2}+\frac{\delta}{2}} -Je^{jn\frac{2\pi z}{p}}\,dz$$

$$+ \int_{-\frac{\delta}{2}}^{\frac{\delta}{2}} Je^{jn\frac{2\pi z}{p}}\,dz$$

$$+ \int_{\frac{p}{2}-\frac{\delta}{2}}^{\frac{p}{2}} -Je^{jn\frac{2\pi z}{p}}\,dz$$

From which,

$$(3.108) \qquad j_{\parallel n} = \frac{2J\delta}{p} \frac{\sin\frac{(n\pi\delta)}{p}}{\frac{n\pi\delta}{p}}$$

n only odd

$$j_{\parallel n} = 0 \text{ for } n \text{ even}$$

For the bifilar helix with unbalanced (++) feed

The current distribution on the tape for this case is shown in Figure-3-8(c).

$$J_{\parallel} = \Sigma j_{\parallel n}\, e^{-j\frac{n2\pi z}{p}}$$

$$j_{\parallel n}p = \int_{-\frac{p}{2}}^{-\frac{p}{2}+\frac{\delta}{2}} Je^{jn\frac{2\pi z}{p}}\,dz$$

$$+ \int_{-\frac{\delta}{2}}^{\frac{\delta}{2}} Je^{jn\frac{2\pi z}{p}}\,dz$$

$$+ \int_{\frac{p}{2} - \frac{\delta}{2}}^{\frac{p}{2}} J e^{jn\frac{2\pi z}{p}} \, dz$$

From which,

$$(3.109) \qquad J_{\parallel n} = \frac{2J\delta}{p} \frac{\sin \frac{n\pi\delta}{p}}{\frac{n\pi\delta}{p}} \qquad n \text{ only even}$$

$$J_{\parallel n} = 0 \text{ for } n \text{ odd}$$

Equations (3.108) and (3.109) verify section 3.6.3 in which it is shown that only odd or only even n exist for balanced or unbalanced feed, respectively.

The ϕ- and z-components of $j_{\parallel n}$ can be written

$$(3.110) \qquad j_{\phi n} = j_{\parallel n} \cos \psi$$

$$(3.111) \qquad j_{zn} = j_{\parallel n} \sin \psi$$

For the single and bifilar helices, in general, let

$$(3.112) \qquad j_{\parallel n} = C \frac{\sin \frac{n\pi\delta}{p}}{\frac{n\pi\delta}{p}}$$

where C = a constant

Utilizing boundary equations (3.83), (3.84) and (3.85) at r = a, equations (3.104), (3.105), (3.106), (3.110) and (3.111), together

with equations (3.48), (3.49), (3.51), (3.53), (3.54), (3.55), (3.57) and (3.59) results in four independent equations for solving for the unknown coefficients A_n^i, A_n^o, B_n^i, B_n^o in terms of $j_{\parallel n}$. Also utilizing

(3.113) $$(\gamma_{rn}a)^2 = (\beta_n a)^2 - (Ka)^2 \quad \text{(same as equation (3.88))}$$

(3.114) $$\frac{\beta_n a}{\cot \psi} = \frac{\beta_o a}{\cot \psi} + n \quad \text{(same as equation (3.93))}$$

(3.115) $$E_{\parallel n} = E_{zn} \sin \psi + E_{\phi n} \cos \psi$$

the following equation is obtained for $E_{\parallel n}|r = a$:

(3.116) $$E_{\parallel n}|r = a = j\frac{e^{-\beta_o z} \sin^2\psi}{\omega\epsilon a} e^{-jn(\frac{2\pi z}{p} - \phi)}$$

$$\left\{\left[(\gamma_{rn}a)^2 - 2n\beta_n a\cot \psi + n^2\beta_n{}^2a^2 \frac{\cot^2 \psi}{\gamma_{rn}{}^2a^2}\right] I_n(\gamma_{rn}a)K_n(\gamma_{rn}a)\right.$$

$$\left. + K^2a^2\cot^2 \psi\, I_n'(\gamma_{rn}a)\, K_n'(\gamma_{rn}a)\right\} j_{\parallel n}$$

and since $E_{\parallel}|r = a = \sum_n E_{\parallel n}|r = a$

(3.117) $$E_{\parallel}|r = a = j\frac{e^{-j\beta_o z} \sin^2 \psi}{\omega\epsilon a} \sum_n e^{-jn(\frac{2\pi z}{p} - \phi)}$$

$$\left\{\left[(\gamma_{rn}a)^2 - 2n\beta_n a\cot \psi + n^2\beta_n{}^2a^2 \frac{\cot^2 \psi}{\gamma_{rn}{}^2a^2}\right] I_n(\gamma_{rn}a)K_n(\gamma_{rn}a)\right.$$

$$\left. + K^2a^2\cot^2 \psi\, I_n'(\gamma_{rn}a)\, K_n'(\gamma_{rn}a)\right\} j_{\parallel n}$$

Equation (3.117) is to be set equal to zero along the center line of the tape, i.e., for $\phi = \frac{2\pi z}{p}$.

Using equation (3.112),

$$(3.118)\quad 0 = j\frac{e^{-j\beta_o z}\, C\sin^2\psi}{\omega\varepsilon a} \sum_n \left\{ \left[(\gamma_{rn}a)^2 - 2n\beta_n a\cot\psi + n^2\beta_n{}^2a^2\, \frac{\cot^2\psi}{\gamma_{rn}{}^2a^2} \right] \right.$$

$$\left. I_n(\gamma_{rn}a)K_n(\gamma_{rn}a) + K^2a^2\cot^2\psi I_n'(\gamma_{rn}a)K_n'(\gamma_{rn}a) \right\} \frac{\sin\frac{n\pi\delta}{p}}{\frac{n\pi\delta}{p}}$$

The factor outside the summation cannot be zero. Thus, the approximate determinantal equation is

$$(3.119)\quad 0 = \sum_n \left\{ \left[(\gamma_{rn}a)^2 - 2n\beta_n a\cot\psi + n^2\beta_n{}^2a^2\, \frac{\cot^2\psi}{\gamma_{rn}{}^2a^2} \right] I_n(\gamma_{rn}a)K_n(\gamma_{rn}a) \right.$$

$$\left. + K^2a^2\cot^2\psi I_n'(\gamma_{rn}a)K_n'(\gamma_{rn}a) \right\} \frac{\sin\frac{n\pi\delta}{p}}{\frac{n\pi\delta}{p}}$$

Equation (3.119) is solved by using the following approximations[10] for $n \neq 0$:

$$I_n(\gamma_{rn}a)K_n(\gamma_{rn}a) \approx \frac{1}{2}\,\frac{1}{(n^2 + \gamma_{rn}{}^2a^2)^{\frac{1}{2}}}$$

$$I_n'(\gamma_{rn}a)\, K_n'(\gamma_{rn}a) \approx -\frac{1}{2}\,\frac{(n^2 + \gamma_{rn}{}^2a^2)^{\frac{1}{2}}}{\gamma_{rn}{}^2a^2}$$

Subtracting out the terms for n = o from the summation in (3.119), the approximations lead to

$$(3.120)\qquad 0 = \{(\beta_o{}^2a^2-K^2a^2)\ I_o(\gamma_{ro}a)\ K_o\ (\gamma_{ro}a)$$

$$+\ K^2a^2\cot^2\psi\ I_o'(\gamma_{ro}a)\ K_o'\ (\gamma_{ro}a)\}$$

$$+\sum_{\substack{n\\ n\neq o}} \{(\beta_o{}^2a^2-K^2a^2+K^2a^2\ \frac{n^2\cot^2\psi}{\beta_n{}^2a^2-K^2a^2})\frac{1}{2(n^2+\gamma_{rn}{}^2a^2)^{\frac{1}{2}}}$$

$$-K^2a^2\cot^2\psi\ \frac{(n^2+\gamma_{rn}{}^2a^2)^{\frac{1}{2}}}{2\gamma_{rn}{}^2a^2}\}\ \frac{\sin\frac{n\pi\delta}{p}}{\frac{n\pi\delta}{p}}$$

$\beta_n a$ as a function of Ka is solved as follows. Having chosen δ/p and cot ψ, we next choose a value of Ka, and utilizing equations (3.113) and (3.114), we plot the entire function versus $\beta_o a$ looking for a zero. This yields $\beta_o a$ for the chosen Ka. It can be noted that the first terms outside the summation in equation (3.120) when set equal to zero is the determinantal equation for the n = o mode of the sheath helix. After determining $\beta_o a$ as a function of Ka, the ω-β diagram for the space harmonic components can be plotted utilizing equation (3.114). (Note that since $\omega = Kc$, where c is the velocity of light in the medium, ω is proportional to K.) The ω-β plot of of the space harmonic components for the single-tape helix, with $\pi\delta/p = 0.1$ and cot $\psi = 10$, is shown in Figure 3-9(a). Curves are given both for the modes traveling in the +z direction and those

traveling in the opposite direction. All space harmonic components belonging to the same mode have the same group velocity (the same slope of the ω-β diagram) at a particular frequency, ω. The various propagation modes of a single-tape helix have been previously plotted by Sensiper[6]. The various branches of the space harmonics in Figure 3-9(a) actually have a slight concave downward curvature, but have been approximated with straight lines to simplify the diagram. It is interesting to note that the third and higher branches of the space harmonic components do not merge into components starting at $ka/\cot\psi = o$ as do the first two.

The solutions for the bifilar helix with unbalanced (++) feed are shown in Figure 3-9(b). Only the n = even components can exist in this case.

The determinantal equation for the bifilar helix with balanced (+-) feed can be simplified because only n = odd components can exist. In equation (3.120), the terms outside the summation correspond to n = o (n even), so that these terms do not exist for n only odd. The determinantal equation then becomes

$$(3.121) \qquad 0 = \sum_{\substack{n \\ n\ \text{odd}}} (\beta_o{}^2a^2 - K^2a^2 - K^2a^2\cot^2\psi)\left[\mp\frac{1}{2(n^2+\gamma_{rn}{}^2a^2)^{1/2}}\right]\frac{\sin\frac{n\pi\delta}{p}}{\frac{n\pi\delta}{p}}$$

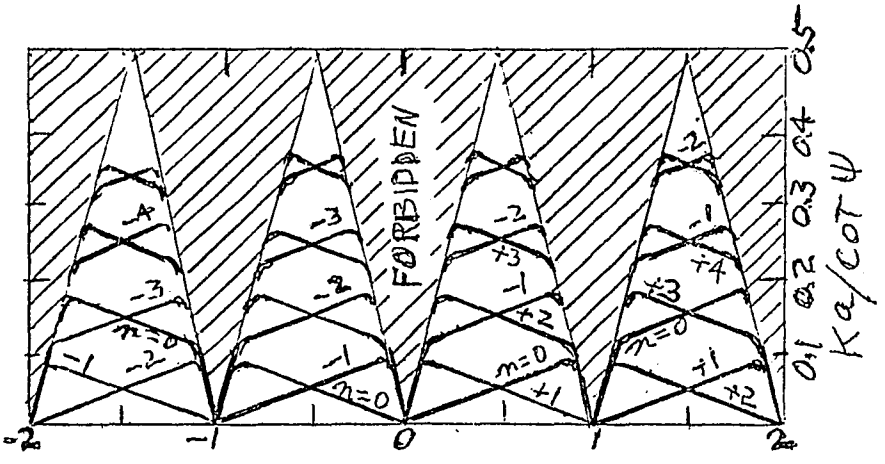

(a) Single helix

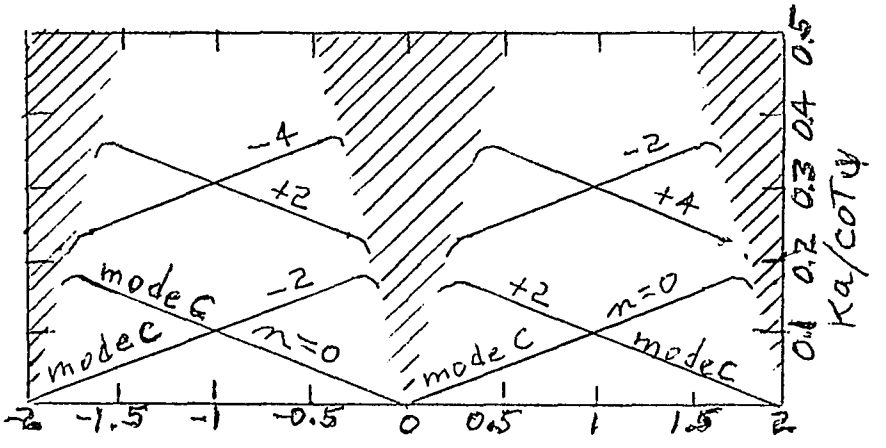

(b) Bifilar helix with unbalanced (++) feed

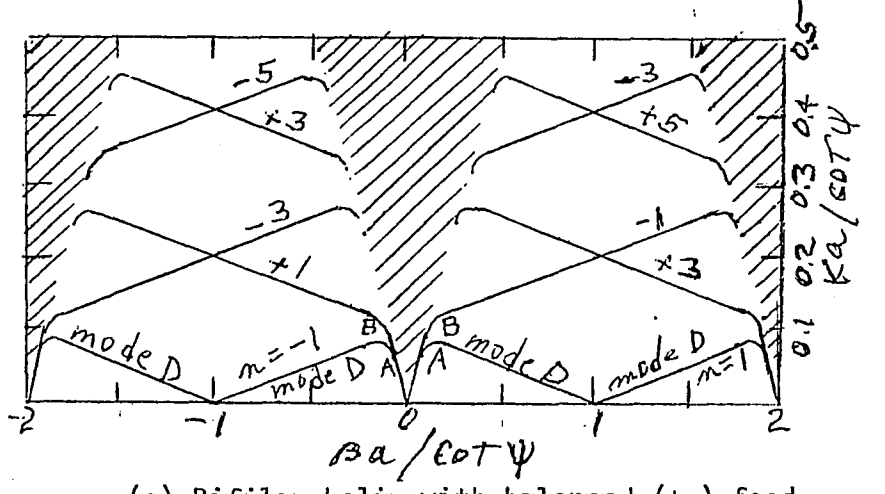

(c) Bifilar helix with balanced (+-) feed

Figure 3-9 Propagation characteristics of single and bifilar helices. (Forbidden regions are shaded.)

Equation (3.121) consists of an infinite number of terms all containing the common factor $(\beta_0^2a^2-K^2a^2-K^2a^2\cot^2\psi)$. One of the solutions must then be

$$\beta_0^2a^2-K^2a^2-K^2a^2\cot^2\psi = 0$$

$$\beta_0^2a^2-K^2a^2\ (1 + \cot^2\psi) = 0$$

$$\beta_0^2a^2- \frac{K^2a^2}{\sin^2\psi} = 0$$

$$\beta_0 a = \pm \frac{Ka}{\sin\psi} \tag{3.122}$$

Since the group velocity is $v_g = \frac{\omega}{\beta_0}$, and the velocity of light is $c = \frac{\omega}{K}$, equation (3.122) can be expressed as

$$v_g = \pm c \sin\psi \tag{3.123}$$

Equation (3.123) indicates that the group velocity can be obtained by taking the longitudinal component of the velocity of a wave traveling along the tape with the velocity of light.

From equation (3.93), the space harmonic propagation constants are given by

$$\beta_n a = \pm \frac{Ka}{\sin\psi} + n \cot\psi \tag{3.124}$$

The solutions for the bifilar helix with balanced (+-) feed are shown in Figure 3-9(c). Only n = odd components can exist in this case. In equation (3.122), β_0 is a linear function of frequency, so that the group velocity for the mode labeled D is constant (non-dispersive) with frequency away from the forbidden regions. In the case of the single-tape helix and the bifilar helix with unbalanced feed, there is some velocity dispersion with frequency for all the space harmonics. All the branches for the different harmonic components in Figures 3-8(a) and (b) have a slight concave downward curvature.

The different modes have been labeled A, B, C and D. Using a more detailed analysis of equation (3.119), Tien[8] has obtained the additional modes labeled A and B. The space harmonic components have been labeled with numbers. In Figure 3-8(a) for the single tape helix, modes A, B and C can be excited, but mode D cannot, because mode D cannot contain the n = o component which must be excited in the case of the single helix. For the single helix, even and odd space harmonics of mode C can be excited, whereas for the bifilar helix with unbalanced (++) feed, the odd harmonics of mode C are eliminated.

At low frequencies, Tien[8] has studied the field patterns of the n = o components of modes A and B. These components are circularly polarized plane waves. The component for mode A rotates in the direction of the helical wires, while that for mode B rotates in the reverse direction.

The n = o space harmonic component of mode C can be used to interact with longitudinal beam space charge waves, while the n = ± 1 components of mode C for the single helix and mode D of the bifilar helix can be used to interact with transverse beam synchronous and cyclotron waves. Because modes A and B are fast waves, they are not useful for interaction with beam waves.

3.6.5 Power and Impedance Calcuation for the Tape Helix[10].

The average power carried by a mode on the tape helix is given by the real part of the integral of the Poynting vector over the cross section:

$$P_{av} = \frac{1}{2} \text{Re} \int_0^{\infty} \int_0^{2\pi} (E_r H_\phi^* - E_\phi H_r^*) r d\phi dr \tag{3.125}$$

When the total field components are written in terms of their space harmonics, this becomes

$$P_{av} = \frac{1}{2} \text{Re} \sum_{n,m} \int_0^{\infty} \int_0^{2\pi} (E_{rn} H_{\phi m}^* - E_{\phi n} H_{rn}^*) r d\phi dr \tag{3.126}$$

Consider the integration of a typical term over ϕ for $n \neq m$. E_{rn}, $E_{\phi n}$, H_{rm} and $H_{\phi m}$ have the forms

$$E_{rn} = f_1(r,z)\, e^{jn\phi}$$

$$E_{\phi n} = f_2(r,z)\, e^{jn\phi}$$

$$H_{rm} = f_3(r,z)\, e^{jm\phi}$$

$$H_{\phi m} = f_4(r,z)\, e^{jm\phi}$$

where f_1, f_2, f_3 and f_4 are complex amplitude functions of r and z. Hence, over any z-plane,

$$\int_0^{2\pi} (E_{rn}H_{\phi m}^* - E_{\phi n}H_{rm}^*)\, d\phi$$

$$= \int_0^{2\pi} (f_1 \cdot f_4^* \, e^{j(n-m)} - f_2 \, f_3^* \, e^{j(n-m)})_{n \neq m} d\phi = 0$$

Equation (3.126) then simplifies to

$$P_{av} = \sum_n P_{av\ n} \tag{3.127}$$

where

$$P_{av\ n} = \frac{1}{2} \mathrm{Re} \int_0^{\infty} (E_{rn}H_{\phi n}^* - H_{\phi n}H_{rn}^*)\, 2\pi r dr \tag{3.128}$$

Thus the total power of the wave is the sum of the powers carried by the individual space harmonics. There are no cross terms because the individual space harmonics are orthogonal over the cross-section.

An expression which is useful in the calculation of the gain of a transverse wave traveling-wave tube is given by

$$K_{Tn} = \frac{E_{Tn}^2\ (0)}{2\beta_n{}^2 P_{av}} \tag{3.129}$$

where

K_{Tn} is called the transverse-wave interaction impedance for the n'th space harmonic

E_{Tn} (0) is the amplitude of the transverse electric field at the tube axis for the n'th space harmonic

β_n = propagation constant for the n'th space harmonic

P_{av} = the total average power carried by all the space harmonics of the mode.

K_{Tn} has the dimension of an impedance. It is a measure of the square of the strength of the transverse electric field of the n'th space harmonic when a given total average power flows. K_{Tn} is decreased if the total average power is increased by the presence of power carried by other space harmonics of the mode.

CHAPTER IV

THEORY OF TRANSVERSE-WAVE TUBES

4.1 Filamentary Beam Theory of Transverse-Wave Traveling-Wave Tubes

Of the four beam transverse waves originally introduced by Siegman[7], the slow cyclotron wave with right-hand polarization and the synchronous wave with left-hand polarization (with the d.c. longitudinal magnetic field in the +z direction for both waves) are the so-called negative energy waves. (See section 2.1 of this dissertation.) As in ordinary longitudinal space-charge wave traveling-wave tubes, the coupling of negative-energy beam waves with waves propagating along a slow wave circuit leads to traveling-wave amplification. Therefore, there are two possible types of transverse-wave traveling-wave amplifiers: A negative synchronous wave tube and a slow cyclotron wave tube. Figure 4-1 shows ω-β diagrams and the synchronism conditions required for the two types of traveling-wave amplifiers. Theoretical analyses of these amplifiers for gain and power output have been given by Siegman[7], Louiselle[4] and others. The analysis here will follow that of previous authors, but the emphasis will be on the physical mechanism of energy transfer and the question of longitudinal velocity spread. A filamentary beam of infinitesimal thickness is assumed in the following.

4.1.1 Effect of Circuit Field on the Electron Beam.

Throughout this dissertation, the circuit field "E_c" refers only to the space harmonic that is synchronous with the beam wave. The radius of the

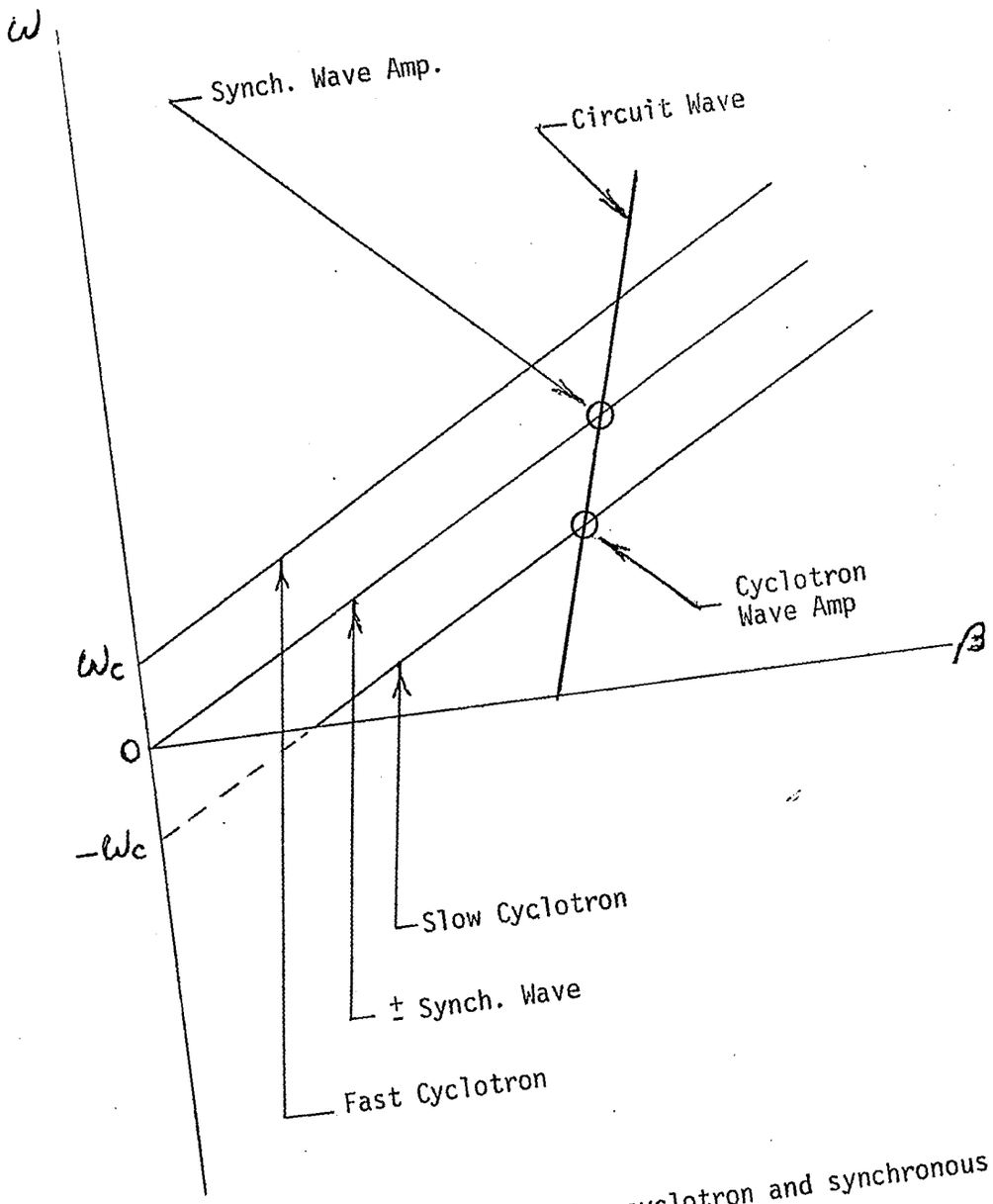

Figure 4-1 ω-β diagram for cyclotron and synchronous wave amplifiers.

beam wave is related to the transverse (radial) circuit electric field by means of the force equations on an electron which moves within the beam wave pattern. The force equation for an electron acted upon by a circuit field that is purely transverse at the unperturbed beam position ($x = y = o$), and with a uniform axial magnetic field, B_o, in the positive -z direction is

$$F = ma \tag{4.1}$$

$$-|e|E_c - |e|\bar{v}_o \times \bar{B}_o = m \frac{d^2 v_o}{dt^2} \tag{4.2}$$

where F = force on electron

m = mass of electron

a = acceleration of electron

e = electron charge

v_o = velocity of electron

B_o = longitudinal magnetic flux density

E_c = transverse circuit electric field

In the x-direction,

$$\ddot{x} + \omega_c \dot{y} = -\eta E_{xc} \tag{4.3}$$

In the y-direction,

$$\ddot{y} - \omega_c \dot{x} = -\eta E_{yc} \tag{4.4}$$

where E_{xc} = x-component of circuit field

E_{yc} = y-component of circuit field

$$\eta = \frac{|e|}{m}$$

$\omega_c = \eta B_o$ = cyclotron frequency

In (4.3) and (4.4), $\dot{x}$ and $\dot{y}$ are total time derivatives of x and y,

$$\dot{x} = \frac{dx}{dt} = \frac{\partial x}{\partial t} + \frac{\partial x}{\partial z}\frac{dz}{dt}$$

$$= \left(\frac{\partial}{\partial t} + v_o\frac{\partial}{\partial z}\right) x$$

$$\dot{y} = \left(\frac{\partial}{\partial t} + v_o\frac{\partial}{\partial z}\right) y$$

For analytical convenience, the circularly polarized variables r and E_c are introduced, where

(4.5) $$r = x + jy$$

(4.6) $$E_c = E_{xc} + j\,E_{yc}$$

In (4.5) and (4.6), x, y, E_{xc}, and E_{yc} are sinusoidally varying quantities.

The force equation can be written in terms of these variables by multiplying equation (4.4) by j, adding to equation (4.3) and using equations (4.5) and (4.6). Thus,

(4.7) $$\boxed{\ddot{r} - j\omega_c\dot{r} = -\eta E_c}$$

To illustrate the meaning of the circularly polarized variables in (4.5) and (4.6), note that a left-hand polarized forward traveling-wave field is described by

$$E_c = E_1 e^{j(\omega t - \beta z + \phi)} \tag{4.8}$$

because the angular agreement varies as $(-j\beta z)$ so that the angle becomes more negative with increasing z, i.e., E_c rotates clockwise with increasing z as viewed on a right-hand x-y coordinate system. A right-hand polarized wave, on the other hand, would rotate counter-clockwise with increasing z and be described by

$$E_c = E_1 e^{-j(\omega t - \beta z + \phi)} \tag{4.9}$$

For completeness and comparison, both the negative synchronous and slow cyclotron wave interactions will be considered. In the following sections, a small signal approximation, $dz/dt = v_z \approx v_0$, is made. In other words, it is assumed that v_z does not change very much from the injection velocity, v_0, and is considered to be approximately constant. The effect of a changing velocity due to loss of longitudinal velocity energy of the electrons as they give up energy to the circuit will be considered later.

4.1.2 Negative Synchronous-Wave Interaction. In equation (4.7), for synchronous-wave interaction, the beam and circuit waves are left-hand polarized with the magnetic field, B_0, in the $+z$ direction and in velocity synchronism. Thus,

(4.10) $$r(z,t) = r_1(z)\, e^{j(\omega t - \beta z)}$$

(4.11) $$E_c = E_1(z)\, e^{j(\omega t - \beta z)}$$

(4.12) $$\omega = \beta v_o$$

where $r_1(z)$ and $E_1(z)$ are complex amplitude functions of z only.

From (4.10),

$$\dot{r} = \frac{\partial r}{dt} + v_o \frac{\partial r}{\partial z}$$

(4.13) $$\dot{r} = \left[j(\omega - \beta v_o) r_1 + v_o r_1' \right] e^{j(\omega t - \beta z)}$$

where dot $\equiv \frac{d}{dt}$

prime $\equiv \frac{d}{dz}$

Using (4.12) in (4.13),

(4.14) $$\dot{r} = v_o r_1'\, e^{j(\omega t - \beta z)}$$

$$\ddot{r} = \frac{\partial \dot{r}}{\partial t} + v_o \frac{\partial \dot{r}}{\partial z}$$

(4.15) $$\ddot{r} = v_o^2 r_1''\, e^{j(\omega t - \beta z)}$$

Substituting (4.11), (4.14) and (4.15) into (4.7), the equation for the radius of the beam pattern as a function of z becomes

(4.16) $$v_o^2 r_1'' - j\omega c v_o r_1' = -\eta E_1(z)$$

A solution of (4.16) is

(4.17) $$r_1(z) = A\, e^{\alpha z} + B\, e^{-\alpha z}$$

where A and B are constants determined by boundary conditions

Thus,

(4.18) $$r_1' = \alpha A\, e^{\alpha z} - \alpha B\, e^{-\alpha z}$$

(4.19) $$r_1'' = \alpha^2 A\, e^{\alpha z} + \alpha^2 B\, e^{-\alpha z}$$

Substituting (4.18) and (4.19) into (4.16),

(4.20) $$-\eta E_1 = A\alpha v_o e^{\alpha z}(\alpha v_o - j\omega c) + B\alpha\, v_o e^{-\alpha z}(\alpha v_o + j\omega c)$$

In practical tubes where gain per unit length is low,

(4.21) $$\alpha v_o \ll \omega_c$$

Using approximation (4.21) in (4.20),

(4.22) $$-\eta E_1 = -j\omega c v_o (A\alpha e^{\alpha z} - B\alpha e^{\alpha z})$$

Using (4.18) in (4.22)

(4.23) $$\boxed{E_1(z) = \frac{j\omega_c v_o r_1'(z)}{\eta}}$$

For the synchronous wave case with $\alpha v_o \ll \omega_c$

Comparing (4.23) with (4.16), it is seent that (4.21) allows dropping of the first term on the left side of (4.16).

For the negative synchronous wave interaction, the solutions for $r_1(z)$ and $E_1(z)$ are:

(4.24) $$r_1(z) = A\, e^{\alpha z} + B\, e^{-\alpha z}$$

$$E_1(z) = \frac{j\omega_c v_o r_1'(z)}{\eta}$$

(4.25) $$E_1(z) = \frac{j\omega_c v_o}{\eta} (\alpha A e^{\alpha z} - \alpha B e^{-\alpha z})$$

The constants A and B are determined from the boundary conditions for $r_1(z)$ and $E_1(z)$.

At $z = 0$,

(4.26) $$r_1(z = 0) = 0$$

(4.27) $$E_1(z = 0) = E_1(0)$$

Substituting (4.26) and (4.27) into (4.24) and (4.25),

(4.28) $$A + B = 0$$

(4.29) $$j \frac{\omega_c \alpha v_o (A-B)}{\eta} = E_1(0)$$

From (4.28)

(4.30) $$B = -A$$

Substitute (4.30) into (4.29),

$$A = \frac{\eta E_1(0)}{j2\omega_c \alpha v_o} \tag{4.31}$$

$$B = \frac{-\eta E_1(0)}{j2\omega_c \alpha v_o} \tag{4.32}$$

Substitute (4.31) and (4.32) into (4.24) and (4.25),

$$r_1(z) = \frac{-j\eta E_1(0)}{2\ \omega_c \alpha v_o} \left(e^{\alpha z} - e^{-\alpha z}\right) \tag{4.33}$$

$$E_1(z) = \frac{E_1(0)}{2} \left(e^{\alpha z} + e^{-\alpha z}\right) \tag{4.34}$$

Equations (4.33) and (4.34) show that $E_1(z)$ is directed 90^o ahead of $r_1(z)$ in right-hand coordinate space. In the synchronous wave interaction, the electrons do not rotate at ω_c about the tube axis because the θ-component of the electric field force on an electron is exactly counterbalanced by the force caused by the longitudinal magnetic field crossed with the radial velocity of the electron. The electrons are slowly moved outward radially by a small radial component of the electric field.

The solutions for $r(z,t)$ and $E_c(z,t)$ are:

$$\boxed{r(z,t) = \frac{-j\eta E_1(0)}{2\omega_c \alpha v_o} \left(e^{\alpha z} - e^{-\alpha z}\right) e^{j(\omega t - \beta z)}} \tag{4.35}$$

$$E_c(z,t) = \frac{E_1(0)}{2}(e^{\alpha z} + e^{-\alpha z})\, e^{j(\omega t - \beta z)} \tag{4.36}$$

An expression for the gain constant, α, will be derived later.

4.1.2.1 Relation Between Longitudinal and Transverse Electric Circuit Fields for LH Polarization of Negative Synchronous Wave Interaction. In the linear theory of transverse wave interactions, the longitudinal electric field at the beam does not usually appear explicitly. All physical descriptions of the gain mechanism, however, show that it is the longitudinal field that is responsible for slowing down the longitudinal velocity of the electrons in converting energy from the beam to the circuit wave. If the beam displacement from the tube axis is much less than a wavelength, the longitudinal circuit field at the beam position is approximately

$$E_{zb} = \frac{\partial E_z}{\partial x}\, x + \frac{\partial E_z}{\partial y}\, y \tag{4.37}$$

since $E_z(0,0) = 0$. (x,y) describes the beam position. An electric field of a slow wave circuit with a phase velocity much smaller than the velocity of light, i.e., $\omega/\beta \ll c$, has $\nabla \times \bar{E} \approx 0$. Therefore,

$$\frac{\partial E_z}{\partial x} \approx \frac{\partial E_x}{\partial z} \tag{4.38}$$

$$\frac{\partial E_z}{\partial y} \approx \frac{\partial E_y}{\partial z} \tag{4.39}$$

Substituting (4.38) and (4.39) into (4.37),

$$E_{zb} = x \frac{\partial E_{xc}}{\partial z} + y \frac{\partial E_{yc}}{\partial z} \tag{4.40}$$

Since $r = x + jy$

$$\text{and } \frac{\partial E_c}{\partial z} = \frac{\partial E_{xc}}{\partial z} + j \frac{\partial E_{yc}}{\partial z}$$

Then (4.40) can be written

$$E_{zb} = \text{Re}\left(r^* \frac{\partial E_c}{\partial z}\right) \tag{4.41}$$

For $\alpha << \beta$, which is the case for practical tubes, and for LH polarization, equation (4.41) becomes

$$E_{zb} = \text{Re}(-j\beta r^* E_c) \tag{4.42}$$

4.1.2.2 Absence of R-F Velocity Modulation of Electrons in the Negative Synchronous Wave Interaction. Inserting equations (4.35) and (4.36) into (4.42), the longitudinal electric field at the beam is

$$E_{zb} = \frac{n\beta |E_1(0)|^2}{4\omega_c \alpha V_o} \left(e^{2\alpha z} - e^{-2\alpha z}\right) \tag{4.43}$$

The significance of equation (4.43) is that the axial electric field seen by an electron is monotonically varying during its motion through the tube and does not contain r-f modulation, Moreover, it is the same for all electrons, independent of their entrance phase with respect to the circuit field.

The axial equation of motion along the electron trajectory is

$$\frac{dv_z}{dt} = -\eta E_{zb} \tag{4.44}$$

Integrating (4.44) and noting that $dt = \frac{dz}{v_o}$,

$$\int_{v_o}^{v_z} dv_z = \int_{o}^{z} -\eta E_{zb} \frac{dz}{v_o} \tag{4.45}$$

Using equation (4.43) in (4.45),

$$v_z(z) - v_o = \frac{-\eta^2 \beta |E_1|^2}{4\alpha^2 v_o^2 \omega_c} \sinh^2 \alpha z \tag{4.46}$$

where v_o is the injection velocity. Thus, a monoenergetic beam injected at $z = 0$ remains monoenergetic at the output, $z = L$. Therefore, a theoretical efficiency of 100% would be obtained by depressing the collector voltage below the circuit voltage by an amount corresponding to the remaining energy in each and every electron that has given up the same energy to the circuit wave.

The way in which the electrons give up energy to the circuit is now physically clear. A small component of the transverse electric field in the r-direction causes displacement of the electrons off axis where there is a longitudinal electric field to extract energy from the electrons. With a circularly polarized transverse electric field, all electrons arriving at a given position, z, are located the same distance from the axis, and since the electrons move in

synchronism with the circuit field, they also see a constant phase of the longitudinal electric field during their transit through the tube.

4.1.2.3 Determination of the Growth Constant, α, for the Negative Synchronous Wave Interaction. Energy conservation requires

$$\frac{\partial P_C(z)}{\partial z} = P_B \tag{4.47}$$

where P_B is the net power lost by the electron beam to the circuit field per unit length, and P_C is the power on the circuit. All of the net longitudinal power lost by the beam is acquired by the circuit wave. The transverse energy acquired by the electrons is only in the r-direction and is negligibly small.

$$P_B = |I_o| E_{zb} \tag{4.48}$$

Thus,

$$\frac{\partial P_C(z)}{\partial z} = |I_o| E_{zb} \tag{4.49}$$

The time average circuit power is given by

$$P_C(z) = \frac{|E_C(z)|^2}{2\beta^2 K_T} \tag{4.50}$$

where K_T = transverse interaction impedance

$$\frac{\partial P_C(z)}{\partial z} = \left(\frac{|E_C(z)|}{\beta^2 K_T}\right) \left(\frac{\partial |E_C(z)|}{\partial z}\right) \tag{4.51}$$

The longitudinal electric field is given by (4.43) and is

$$E_{zb} = \frac{n\beta|E_1(0)|^2}{4\omega_c\alpha V_o}\left(e^{2\alpha z}-e^{-2\alpha z}\right) \tag{4.52}$$

Also, from equation (4.34),

$$|E_c(z)| = \frac{|E_1(0)|}{2}\left(e^{\alpha z}+e^{-\alpha z}\right) \tag{4.53}$$

$$\frac{\partial|E_c(z)|}{\partial z} = \frac{\alpha|E_1(0)|}{2}\left(e^{\alpha z}-e^{-\alpha z}\right) \tag{4.54}$$

Substituting (4.51), (4.52), (4.53) and (4.54) into (4.49),

$$\frac{\alpha|E_1(0)|^2\left(e^{2\alpha z}-e^{-2\alpha z}\right)}{4\beta^2 K_T} = \frac{|I_o|n\beta|E_1(0)|^2\left(e^{2\alpha z}-e^{-2\alpha z}\right)}{4\omega_c\alpha V_o}$$

From which

$$\boxed{\alpha = \beta\left(\frac{1}{2}\frac{I_o}{V_o}\frac{\omega}{\omega_c}K_T\right)^{1/2}} \tag{4.55}$$

where $\frac{v_o^2}{2\eta} = V_o$, the beam voltage,

and where for synchronous waves, $v_o = \omega/\beta$.

4.1.2.4 Output Power for Negative Synchronous Wave Interaction. From equation (4.49), the power lost by the beam and given up to the circuit in an interaction region of length, L, is given by

$$\int_0^L dP_c(z) = \int_0^L I_o E_{zb}\, dz \tag{4.56}$$

From equation (4.43),

$$E_{zb} = \frac{n\beta|E_1(0)|^2}{4\omega_c\alpha V_o}\left(e^{2\alpha z}-e^{-2\alpha z}\right)$$

$$\int_0^L E_{zb}\,dz = \frac{n\beta|E_1(0)|^2}{4\omega_c\alpha V_o}\left[\frac{e^{2\alpha z}}{2\alpha}+\frac{e^{-2\alpha z}}{2\alpha}\right]_0^L$$

$$\int_0^L E_{zb}\,dz = \frac{n\beta|E_1(0)|^2}{8\omega_c\alpha^2 V_o}\left(e^{\alpha L}-e^{-\alpha L}\right)^2 \tag{4.57}$$

Using equations (4.57), (4.33), $\omega_c = \eta B_o$, and $\beta = \omega/c$ for synchronous waves, (4.56) becomes

$$\boxed{P_c(L) - P_c(0) = \frac{1}{2}\omega B_o\, I_o r_L^2} \tag{4.58}$$

where r_L = amplitude of beam displacement at end of interaction region = $r_1(L)$

$P_c(L)$ = output power

$P_c(0)$ = input power

4.1.3 Slow Cyclotron-Wave Interaction. In equation (4.7), for slow cyclotron-wave interaction, the beam and circuit waves are right-hand polarized and in velocity synchronism. Thus,

$$r(z,t) = r_1(z)\, e^{-j(\omega t-\beta z)} \tag{4.59}$$

$$E_c = E_1(z)\, e^{-j(\omega t-\beta z)} \tag{4.60}$$

$$\omega-\beta V_o = -\omega_c, \text{ since } \beta = \frac{\omega+\omega_c}{V_o} \tag{4.61}$$

for the cyclotron wave.

where $r_1(z)$ and $E_1(z)$ are complex amplitude functions of z only

Substituting (4.59), (4.60) and (4.61) into (4.7), similar to the development in section (4.1.2) for the synchronous wave, the equation for the radius of the beam pattern as a function of z becomes

$$v_0^2 r_1'' + j\omega_c v_0 r_1' = -\eta E_1(z) \tag{4.62}$$

A solution to (4.62) is

$$r_1(z) = Ae^{\alpha z} + Be^{-\alpha z} \tag{4.63}$$

Substituting approximation (4.21), i.e., ($\alpha v_0 << \omega_c$), and (4.63) into (4.62),

$$\boxed{E_1(z) = \frac{-j\omega_c v_0 r_1'(z)}{\eta}} \tag{4.64}$$

For the cyclotron wave case with $\alpha v_0 << \omega_c$

Comparing (4.64) with (4.62), it is seen that (4.21) allows dropping of the first term on the left side of (4.62). Note that (4.64) is the same as (4.23) for the synchronous wave with j replaced by (-j).

For the slow cyclotron wave interaction, the solutions for $r_1(z)$ and $E_1(z)$ are given by equations (4.63) and (4.64). The constants A and B are determined from the boundary conditions for $r_1(z)$ and $E_1(z)$. At $z = 0$,

(4.65) $$r_1(z = 0) = 0$$

(4.66) $$E_1(z = 0) = E_1(0)$$

Substituting (4.65) and (4.66) into (4.63) and (4.64) results in

(4.67) $$A = \frac{j\eta E_1(0)}{2\omega_c \alpha v_o}$$

(4.68) $$B = \frac{-j\eta E_1(0)}{2\omega_c \alpha v_o}$$

Substituting (4.67) and (4.68) into (4.63) and (4.64)

(4.69) $$r_1(z) = \frac{j\eta E_1(0)}{2\omega_c \alpha v_o} (e^{\alpha z} - e^{-\alpha z})$$

(4.70) $$E_1(z) = \frac{E_1(0)}{2} (e^{\alpha z} + e^{-\alpha z})$$

Equations (4.69) and (4.70) show that $E_1(z)$ is directed 90^o behind $r_1(z)$ in right-hand coordinate space for the cyclotron wave interaction. The θ-component of electric field accelerates electrons in the positive θ-direction at an angular velocity, ω_c, and a small radial component of electric field slowly moves the electrons radially outward. The radial acceleration of the circular θ-motion is provided by the force of the longitudinal magnetic field crossed with the θ-velocity.

The solutions for $r(z,t)$ and $E_c(z,t)$ are:

(4.71) $$\boxed{r(z,t) = \frac{j\eta E_1(0)}{2\omega_c \alpha v_o} (e^{\alpha z} - e^{-\alpha z})\, e^{-j(\omega t - \beta z)}}$$

$$E_c(z,t) = \frac{E_1(0)}{2}\left(e^{\alpha z}+e^{-\alpha z}\right) e^{-j(\omega t-\beta z)} \tag{4.72}$$

The expression for the gain constant, α, will be derived later.

4.1.3.1 Relation Between Longitudinal and Transverse Electric Circuit Fields for RH Polarization of the Slow Cyclotron Wave Interaction. The derivation for the z-component of electric field at the beam, E_{zb}, is the same as in section 4.1.2.1 and is given by equation (4.41),

$$E_{zb} = \mathrm{Re}\left(r^* \frac{\partial E_c}{\partial z}\right) \tag{4.41}$$

For $\alpha << \beta$, which is the case for practical tubes, and for RH polarization, equation (4.41) becomes

$$E_{zb} = \mathrm{Re}(j\beta r^* E_c) \tag{4.73}$$

Note that (4.73) is the same as (4.42) except j has been replaced by (-j).

4.1.3.2 Absence of R-F Velocity Modulation of Electrons in the Slow Cyclotron Wave Interaction. Inserting equations (4.71) and (4.72) into equation (4.73) results in equation (4.43), the same as for the negative synchronous wave interaction,

$$E_{zb} = \frac{n\beta |E_1(0)|^2}{4\omega_c \alpha V_o}\left(e^{2\alpha z}-e^{-2\alpha z}\right) \tag{4.43}$$

Again, equation (4.43) shows that the axial electric field seen by an electron is monotonically varying during its motion through the tube and does not contain r-f modulation. Moreover, it is the same for all electrons, independent of their entrance phase with respect to the circuit field. In the slow cyclotron wave interaction, the electrons rotate around the tube axis at an angular velocity, ω_c, and the θ-component of velocity is not zero as in the synchronous wave interaction. However, both the longitudinal electric field and the electrons rotate around the axis with the same pitch since the electrons stay within the beam pattern, so that the axial electric field seen by a particular electron is monotonic during transit.

The axial equation of motion along the electron trajectory is the same as equation (4.44),

$$\frac{dv_z}{dt} = -\eta E_{zb} \tag{4.44}$$

Similar to the case for synchronous waves, the integration of equation (4.44) leads to equation (4.46),

$$v_z(z) - v_0 = \frac{-\eta^2 \beta |E_1|^2}{4\alpha^2 v_0^2 \omega_c} \sinh^2 \alpha z$$

where v_0 is the injection velocity. The same conclusion is obtained as for synchronous waves, i.e., a monoenergetic beam injected at $z = 0$ remains monoenergetic at the output $z = L$.

In the cyclotron wave interaction, the θ-direction kinetic energy will be shown to be a factor $\omega c/\omega$ times the magnitude of the change in the axial kinetic energy. In operating a depressed collector to achieve high efficiency with cyclotron waves, therefore, the transverse energy must be converted back to longitudinal. This can be accomplished by the use of a divergent magnetic field at the collector.

4.1.3.3 Determination of the Growth Constant, α, for the Slow Cyclotron Wave Interaction

Power in Cyclotron Motion

$$P_T = (n_e)\ (K.E.)_e$$

where n_e = number of electrons/sec passing through a plane

$(K.E.)_e$ = kinetic energy/electron

P_T = total power

An electron with velocity, v, will travel a distance, v, in one second. The amount of charge in a cylinder of the beam with cross-section area, A, that has moved through a plane in one second is

$$q = \rho(Av)$$

where q = charge/sec

ρ = charge density

The number of electrons in q is

$$n_e = \frac{q}{e}$$

where e = charge of an electron

Thus,

$$n_e = \frac{\rho A v}{e} = \frac{I_o}{e}$$

where I_o = beam current

$$(K.E)_e = \frac{mv^2}{2}$$

where m = mass of electron

Hence,

$$P_T = (n_e)\ (K.E.)_e$$

$$= \frac{I_o}{e}\ (\frac{mv^2}{2})$$

The velocity, v, of the electron has two components, v_θ, and v_z.

Hence,

$$P_T = \frac{I_o}{e}\ \frac{m}{2}\ (v_\theta^2 + v_z^2)$$

The power in the cyclotron motion is in the direction of v_θ and is

$$P_{cyc} = (\frac{I_o}{e})\ (\frac{mv_o^2}{2})$$

$$v_\theta = \omega_c r$$

where ω_c = cyclotron frequency

r = radius of cyclotron motion

P_{cyc} = power in cyclotron motion of electrons

$$P_{cyc} = \frac{I_o \omega_c^2 r^2}{2\eta}$$

where $\eta = \frac{e}{m}$ = charge to mass ratio of an electron

(4.74) $$\boxed{P_{cyc} = \frac{I_o \omega_c B_o r^2}{2}}$$

where $B_o = \frac{\omega_c}{\eta}$ = longitudinal magnetic flux density in webers/met^2

I_o = beam current in amps

P_{cyc} = power in cyclotron motion in watts

ω_c = radians/sec

r = meters

Energy Conservation

In the cyclotron wave interaction, the power in the cyclotron motion of the electrons must be considered as well as the power on the circuit. Thus, energy conservation requires

(4.75) $$\frac{\partial P_c(z)}{\partial z} + \frac{\partial P_{cyc}(z)}{\partial z} = |I_o| E_{zb}$$

Again, from equation (4.50)

$$P_c(z) = \frac{|E_c(z)|^2}{2\beta^2 K_T}$$

$$\frac{\partial P_c(z)}{\partial z} = \frac{|E_c(z)|}{\beta^2 K_T} \frac{\partial |E_c(z)|}{\partial z}$$

From (4.72)

$$|E_c(z)| = \frac{E_1(0)}{2} (e^{\alpha z} + e^{-\alpha z})$$

$$\frac{\partial |E_c(z)|}{\partial z} = \frac{\alpha |E_1(0)|}{2} (e^{\alpha z} - e^{-\alpha z})$$

(4.76) $$\frac{\partial P_c(z)}{\partial z} = \frac{\alpha |E_1(0)|^2}{4\beta^2 K_T} (e^{2\alpha z} - e^{-2\alpha z})$$

From equation (4.74)

$$P_{cyc}(z) = \frac{I_o \omega_c B_o |r(z)|^2}{2}$$

$$\frac{\partial P_{cyc}(z)}{\partial z} = I_o \omega_c B_o |r(z)| \frac{\partial |r(z)|}{\partial z}$$

From equation (4.71)

$$|r(z)| = \frac{\eta |E_1(0)|}{2\omega_c \alpha V_o} (e^{\alpha z} - e^{\alpha z})$$

$$\frac{\partial |r(z)|}{\partial z} = \frac{\eta |E_1(0)| (e^{\alpha z} + e^{-\alpha z})}{2\omega_c V_o}$$

$$(4.77) \qquad \frac{\partial P_{cyc}(z)}{\partial z} = \frac{I_{on}|E_1(0)|^2}{4\alpha v_o^2} \left(e^{2\alpha z} - e^{-2\alpha z}\right)$$

Equation (4.43) is

$$(4.43) \qquad E_{zb} = \frac{n\beta|E_1(0)|^2}{4\omega_c \alpha v_o} \left(e^{2\alpha z} - e^{-2\alpha z}\right)$$

Substituting (4.76), (4.77) and (4.43) into (4.75) results in

$$(4.78) \qquad \boxed{\alpha = \beta\left(\frac{1}{2}\frac{I_o}{V_o}\frac{\omega}{\omega_c}K_T\right)^{\frac{1}{2}}}$$

where $\frac{v_o^2}{2\eta} = V_o$, the beam voltage

$$\omega_c = \eta B_o$$

and where for the slow cyclotron wave,

$$\beta = \frac{\omega + \omega_c}{v_o}$$

Note that equation (4.78) for the slow cyclotron wave is the same as equation (4.55) for the negative synchronous wave where $\beta = \omega/v_o$ and $P_{cyc} = 0$.

4.1.3.4 Output Power for Slow Cyclotron Wave Interaction. From equation (4.75) for the conservation of power, the power lost by the beam and given up to the circuit and cyclotron motion in an interaction region of length, L, is given by

$$(4.79) \qquad \int_0^L d\, P_c(z) + \int_0^L d\, P_{cyc}(z) = \int_0^L I_0 E_{zb}\, dz$$

Using equations (4.71) and (4.72), equation (4.43) can be put into the form

$$E_{zb} = \beta |r_1(z)||E_1(z)|$$

In equation (4.71) let

$$a_0 = \frac{nE_1(0)}{\omega_c \alpha v_0}$$

Then from (4.71) and (4.72)

$$|r_1(z)| = a_0 \frac{(e^{\alpha z} - e^{-\alpha z})}{2}$$

$$|E_1(z)| = a_0 \alpha v_0 B_0 \frac{(e^{\alpha z} + e^{-\alpha z})}{2}$$

$$E_{zb} = \frac{a_0^2}{4} \alpha\beta v_0 B_0 (e^{2\alpha z} - e^{-2\alpha z})$$

Then,

$$\int_0^L I_0 E_{zb}\, dz = \frac{I_0(\beta v_0) B_0 r_L^2}{2}$$

$$\text{where } r_L = |r_1(L)| = \frac{a_0(e^{\alpha L} - e^{-\alpha L})}{2}$$

Using this, equation (4.74) with $z = L$, and $\omega = \beta v_0 - \omega_c$ for the slow cyclotron wave, equation (4.79) becomes

$$(4.80) \qquad \boxed{P_c(L) - P_c(0) = \frac{1}{2} \omega I_0 B_0 r_L^2}$$

where r_L = amplitude of beam displacement at the end of the interaction region

$P_c(L)$ = Output power

$P_c(0)$ = Input power

$P_c(L) - P_c(0)$ = Power extracted from the beam by the circuit.

Equation (4.80) is the same as (4.58) for the negative synchronous wave. Note that since P_{cyc} is given by (4.74), then

$$\frac{P_c(L) - P_c(0)}{P_{cyc}(L)} = \frac{\omega}{\omega_c} \tag{4.81}$$

4.2 Effect of Reversing the Magnetic Field

4.2.1 Negative Synchronous Wave Case. If the magnetic field is reversed and the polarization is changed from LH to RH, the resulting equations for the synchronous wave case remains the same as shown below.

With ω_c replaced by $(-\omega_c)$ and LH replaced by RH polarization, the equation of motion (4.7) is changed to

$$\ddot{r} + j\omega_r \dot{r} = -\eta E_c \tag{4.82}$$

with

$$r(z,t) = r_1(z)\, e^{-j(\omega t - \beta z)} \tag{4.83}$$

$$E_c = E_1(z)\, e^{-j(\omega t - \beta z)} \tag{4.84}$$

(4.85) $\omega = \beta v_0$

The solution to (4.82) is the same as the previous solution to (4.7) for the negative synchronous wave, except that j is changed to (-j). The solution to (4.82) is

(4.86) $$r_1(z) = \frac{jnE_1(0)}{2\omega_c \alpha v_0} (e^{\alpha z} - e^{-\alpha z})$$

(4.87) $$E_1(z) = \frac{E_1(0)}{2} (e^{\alpha z} + e^{-\alpha z})$$

Equations (4.86) and (4.87) show that now $E_1(z)$ is directed 90^0 behind, instead of ahead, $r_1(z)$ in right-hand coordinate space. However, the force on an electron caused by the crossed magnetic field and small radial velocity has also been reversed by the reversed magnetic field, so that the 0-directed electric force is still balanced by the magnetic force. The electrons still do not rotate around the tube axis, but move slowly radially outward as before. Thus the negative synchronous wave character remains the same.

4.2.2 Slow Cyclotron Wave Case. With ω_c replaced by $(-\omega_c)$ and RH replaced by LH polarization, the equation of motion is again (4.82), with

(4.88) $$r(z,t) = r_1(z)\, e^{j(\omega t - \beta z)}$$

(4.89) $$E_c = E_1 e^{j(\omega t - \beta z)}$$

(4.90) $$\omega - \beta v_0 = -\omega_c$$

The solution to (4.82) is the same as the previous solution to (4.7) for the slow cyclotron wave, except the j is changed to (-j). The solution to (4.82) is

$$(4.91) \qquad r_1(z) = \frac{-j\eta E_1(0)}{2\omega_c \alpha V_o} \left(e^{\alpha z} - e^{-\alpha z}\right)$$

$$(4.92) \qquad E_1(z) = \frac{E_1(0)\left(e^{\alpha z} + e^{-\alpha z}\right)}{2}$$

Equations (4.91) and (4.92) show that now $E_1(z)$ is directed 90^o ahead, instead of behind, $r_1(z)$ in right-hand coordinate space. The θ-component of electric field now accelerates electrons in the negative θ-direction at an angular velocity, $(-\omega_c)$, and a small radial component of electric field slowly moves the electrons radially outward. (Note that the force on a negative charge electron is opposite to the electric field.) The radial acceleration of the negative circular θ-motion is provided by the force of the reversed magnetic field crossed with the θ-velocity. Thus the slow cyclotron wave character remains the same.

Similar results are obtained for the positive synchronous and fast cyclotron waves when the magnetic field is reversed. The conclusion is that all transverse beam waves are reversed in polarization when the longitudinal magnetic field is reversed.

For interaction between a beam wave and the circuit wave to occur, both must have the same polarization. Thus, if the circuit,

and hence the circuit wave, is fixed in polarization, any of the beam waves could be made to interact with the circuit wave by choosing the proper direction of the magnetic field to obtain the same polarizations for the beam and circuit waves.

4.3 Desynchronization

The voltage gain of the negative synchronous and slow cyclotron wave amplifiers as a function of z is given by equation (4.34) or (4.70), i.e.,

$$G_V = \frac{E_1(z)}{E_1(0)} = \cosh \alpha z$$

As energy is extracted by the circuit wave from a beam wave, the beam wave is slowed in velocity. If the beam and circuit waves slip out of velocity synchronism, there is a loss of gain. The coupled mode analysis given below obtains the effect of this desynchronization for the cyclotron wave interaction. Coupled mode analysis is applicable because the coupling between waves is small. A similar analysis could be used for the slow synchronous wave case. In coupled mode analysis, the rate of change with distance of the amplitude of each wave equals a linear combination of the amplitudes of all the waves.

Only waves with the same polarization and approximate velocity synchronism can couple. Since the slow cyclotron wave has RH polarization, only the RH polarized synchronous and circuit waves could couple to the slow cyclotron wave. Thus, Siegman's[7] coupled mode

equations for the slow cyclotron wave are

$$\frac{dA_1}{dz} + j(\beta_e + \beta_c)A_1 = j\alpha A_o \tag{4.94}$$

$$\frac{dA_3}{dz} + j\beta_e A_3 = j\alpha A_o \tag{4.95}$$

$$\frac{dA_o}{dz} + j\beta_o A_o = j\alpha(A_3 - A_1) \tag{4.96}$$

where,

A_1 = amplitude of slow cyclotron wave

A_o = amplitude of forward positively polarized circuit wave

A_3 = amplitude of positive synchronous wave

$\beta_{cy} = \beta_e + \beta_c$ = propagation constant for slow cyclotron wave

$\beta_e = \omega/v_o$

$\beta_c = \omega_c/v_o$

β_o = propagation constant for RH polarized circuit wave

α = growth rate constant in nepers/meter

ω = signal radian frequency

$\omega_c = \eta B_o$ = cyclotron radian frequency

B_o = d.c. longitudinal magnetic field in the positive -z direction

v_o = longitudinal velocity of electrons

The β's here are the β's for each mode without the presence of the other modes. The amplitudes, $A_n (n = 0, 1, 3)$, have been normalized

so that the power in each mode is $Pn = A_n A_n^*$, i.e., the square of the magnitude of the amplitude equals the power in the mode.

Louiselle (page 75)[4] gives a transfer factor which can be used to determine the relative importance of the various modes. The transfer factor between modes i and j is given by

$$F_{ji} = F_{ij} = \left[1 + \left(\frac{C_{ii} - C_{jj}}{2}\right)^2 \frac{1}{C_{ij}\, C_{ji}}\right]^{-1}$$

If $|F_{ij}| \approx 1$, coupling must be retained, but if $|F_{ij}| << 1$, the modes are little affected by one another.

The C_{ii} are the self-coupling coefficients and the C_{ij} are the mutual coupling coefficients.

Transfer factor between A_3 and A_o

For A_3, $C_{ii} = j\beta_e$

For A_o, $C_{jj} = j\beta_o \approx j(\beta_e + \beta_c)$

$$C_{ij} = C_{ji} = j\alpha$$

$$F_{A_3, A_o} = \left[1 - \frac{\beta_c^2}{4} \times \frac{1}{-\alpha^2}\right]^{-1}$$

$$\alpha << \beta_c$$

Hence $F_{A_3, A_o} \approx 0$

Transfer factor between A_3 and A_1

For A_3 $\quad C_{ii} = j\beta_e$

For A_1 $\quad C_{jj} = j(\beta_e + \beta_c)$

As above,

$$F_{A3,A1} \simeq 0$$

Transfer factor between A_1 and A_0

For A_1, $\quad C_{ii} = j(\beta_e + \beta_c) \simeq j\beta_0$

For A_0, $\quad C_{jj} = j\beta_0$

$$F_{A1,A0} \simeq 1$$

Hence, A_3 can be neglected and only coupling between A_0 and A_1 need be considered.

The coupled mode equations now become

$$\frac{dA_1}{dz} + j\beta_{cy} A_1 = j\alpha A_0 \tag{4.97}$$

$$\frac{dA_0}{dz} + j\beta_0 A_0 = -j\alpha A_1 \tag{4.98}$$

In (4.98), it is assumed the circuit is lossless. Loss in the circuit could be taken into account by replacing the self-coupling coefficient, $j\beta_0$, by $(\alpha_L + j\beta_0)$, where α_L is the loss in nepers/ meter. Incidentally, the fact that the mutual coupling coefficients are

complex conjugates indicates that the coupling is active.[4] On the other hand, if the mutual coupling coefficients are negative complex conjugates, the coupling is passive.

Method for Determining Mutual Coupling Coefficient

A general method is to determine rate of change of power flow in terms of known parameters, then in terms of the mutual coupling coefficient, and then obtain the mutual coupling coefficient by comparison. As an example express (4.97) as

$$\frac{dA_1}{dz} + j\beta_{cy}A_1 = cA_0 \tag{4.99}$$

where the coupling coefficient, c, is to be determined.

The normalized amplitudes are obtained as follows. The power in the circuit is

$$P_C = \frac{|E_1(z)|^2}{2\beta_0{}^2K_T} \tag{4.100}$$

Thus let

$$A_0 = \frac{E_1(z)}{\sqrt{2\beta_0{}^2K_T}} \quad ; \quad A_0{}^* = \frac{E_1{}^*(z)}{\sqrt{2\beta_0{}^2K_T}} \tag{4.101}$$

So that

$$P_C = A_0A_0{}^*$$

The power for the cyclotron wave is obtained from equation (4.80) and is

$$P_1 = \frac{-1}{2} I_0\omega B_0|r(z)|^2 \tag{4.102}$$

Thus let

$$A_1 = r(z)\sqrt{\tfrac{1}{2} I_0 \omega B_0} \quad ; \quad A_1^* = r_1^*(z)\sqrt{\tfrac{1}{2} I_0 \omega B_0} \tag{4.103}$$

So that

$$P_1 = -A_1 A_1^*$$

Using (4.70) and (4.69) in (4.101) and (4.103),

$$A_0 = \frac{E_1(0)\ (e^{\alpha z} + e^{-\alpha z})}{2\sqrt{2\ \beta_0^2 K_T}} \tag{4.104}$$

$$A_1 = \frac{jnE_1(0)(e^{\alpha z} - e^{-\alpha z})}{2\omega_c \alpha v_0} \sqrt{\tfrac{1}{2} I_0 \omega B_0} \tag{4.105}$$

Now, the rate of change of power for the cyclotron wave is

$$\frac{-d(A_1 A_1^*)}{dz} = -A_1 \frac{dA_1^*}{dz} - A_1^* \frac{dA_1}{dz} \tag{4.106}$$

Utilizing (4.99) and its complex conjugate, (4.106) becomes

$$\frac{d(A_1 A_1^*)}{dz} = CA_0 A_1^* + C^* A_0^* A_1 \tag{4.107}$$

Using (4.104) and (4.105), equation (4.106) becomes

$$\frac{d(A_1 A_1^*)}{dz} = j\alpha A_0 A_1^* - j\alpha A_0^* A_1 \tag{4.108}$$

where α is the same as given by (4.78) and is

$$\alpha = \beta_0 \left(\frac{1}{2} \frac{I_0}{V_0} \frac{\omega}{\omega_0} K_T\right)$$

Here, α is for the case of perfect synchronism between the beam and circuit waves, i.e, $\beta_0 = \beta_{cy}$.

Comparing (4.107) with (4.108)

$$c = j\alpha$$

Velocity Parameter

Returning to the coupled mode equations (4.97) and (4.98), the propagating solutions vary as $e^{\Gamma z}$, where Γ is loaded common Γ between the A_0 and A_1 modes. Thus assume

(4.109) $$A_1 = \hat{A}_1 e^{\Gamma z}$$

(4.110) $$A_0 = \hat{A}_0 e^{\Gamma z}$$

Substitute (4.109) and (4.110) into (4.97) and (4.98),

(4.111) $$(\Gamma + j\beta_{cy})\hat{A}_1 - j\alpha\hat{A}_0 = 0$$

(4.112) $$j\alpha A_1 + (\Gamma + j\beta_0)\hat{A}_0 = 0$$

For the solution A_1 and A_0 to exist, the characteristic equation must be satisfied and is given by

(4.113) $$\begin{vmatrix} \Gamma + j\beta_{cy} & -j\alpha \\ j\alpha & \Gamma + j\beta_0 \end{vmatrix} = 0$$

From which

(4.114) $$\Gamma = \frac{-j(\beta_{cy} + \beta_0)}{2} \pm \sqrt{\alpha^2 - \left(\frac{\beta_{cy} - \beta_0}{2}\right)^2}$$

Thus,

The coupled phase constant is

$$\beta = \frac{\beta_{cy} + \beta_0}{2} \tag{4.115}$$

Equation (4.115) can be put into the form

$$(\beta_0 - \beta) = (\beta - \beta_{cy}) \tag{4.116}$$

The coupled growth constant is

$$\alpha' = \left(\alpha^2 - \left(\frac{\beta_{cy}-\beta_0}{2}\right)^2\right)^{\frac{1}{2}} \tag{4.117}$$

In the above, $\alpha = \alpha_s$, the value obtained when the uncoupled circuit wave velocity is synchronous with the uncoupled cyclotron beam wave velocity at $z = 0$, so that $\beta = \beta_0 = \beta_{cy}$ at $z = 0$. α is given by

$$\alpha = \beta \left(\frac{1}{2} \frac{I_0}{V_0} \frac{\omega}{\omega_c} K_T\right) \tag{4.118}$$

where

V_0 = beam injection voltage

$\beta = \beta_0$

As a check whether the solution (4.114) gives the known growing and decaying solutions with α as the growth constant for perfect synchronism, let $\beta_0 = \beta_{cy}$. Then from (4.114),

$$\Gamma = -j\beta_o \pm \alpha$$

Then

$$A_o = \hat{A}_o e^{\Gamma z}$$

One solution is

$$A_o = \hat{A}_{o1}\, e^{-j\beta_o z} \cdot e^{\alpha z} \quad \text{(growing wave)}$$

Another solution is

$$A_o = \hat{A}_{o2}\, e^{-j\beta_o z} \cdot e^{-\alpha z} \quad \text{(decaying wave)}$$

Thus (4.114) gives correct solutions for perfect synchronism.

Define a velocity parameter

(4.119) $$\boxed{b = \frac{\beta_o - \beta_{cy}}{\beta_{cy}}}$$

Using (4.119) in (4.117), α' can be expressed as

(4.120) $$\boxed{\alpha' = \alpha \sqrt{1 - K^2}}$$

where

(4.121) $$\boxed{K = \frac{b}{2\alpha/\beta_{cy}}}$$

Equation (4.120) expresses α' as a correction on the synchronous α, the correction being a function of α, β_{cy} and the velocity parameter, b. There is no growth if $K > 1$, since α' become imaginary. The synchronous α is obtained when the circuit propagation constant,

β_o, and the cyclotron wave propagation constant, β_{cy}, are adjusted to be equal.

Equation (4.119) can be put into another form by using $\beta_o = \omega/v_{ckt}$ and $\beta_{cy} = \omega/v_{cy}$. Thus

$$b = \frac{v_{cy} - v_{ckt}}{v_{ckt}} \tag{4.122}$$

where

v_{cy} = decoupled phase velocity of the slow cyclotron wave.

v_{ckt} = decoupled velocity of the circuit wave.

Utilizing (4.121) and (4.119)

$$K = \frac{\beta_o - \beta_{cy}}{2\alpha} \tag{4.123}$$

4.4 Power Limitation Caused by Desynchronization

For the cyclotron wave, when power is extracted from the longitudinal velocity of the electrons by the circuit and by the cyclotron motion of the electrons, the longitudinal velocity of the electrons is decreased. The phase velocity of the cyclotron wave slips out of synchronism with that of the circuit wave. When sufficient desynchronization occurs, there is no longer any interaction between the cyclotron and circuit waves, so that there is no more amplification of the circuit wave.

Let,

v_{eff} = slowed longitudinal velocity of the electrons

V_{eff} = equivalent effective kinetic voltage of the electrons corresponding to v_{eff}

= $v_{eff}^2/2\eta$, where η = ratio of electron charge to mass

(V_{eff} is the voltage required to accelerate the electrons to velocity, v_{eff}, from zero velocity)

v_o = initial longitudinal velocity of the electrons

V_o = circuit voltage, which gives the electrons the initial velocity, v_o

I_o = beam current

The initial longitudinal velocity, v_o, of the electrons and the final longitudinal velocity, v_{eff}, of the electrons are given by

(4.124) $$v_o = \sqrt{2\eta V_o}$$

(4.125) $$v_{eff} = \sqrt{2\eta V_{eff}}$$

The longitudinal power in the electron beam is given by

(4.126) $$V_{eff}\, I_o = I_o V_o - \eta_{ec}\, I_o V_o$$

where η_{ec} = fraction of power extracted from the initial longitudinal velocity of the electrons by the circuit and cyclotron motion.

η_{ec} will be called "electronic cyclotron efficiency."

From (4.126)

$$V_{eff} = V_o (1 - \eta_{ec}) \tag{4.127}$$

From (4.119), the velocity parameter, b, is given by

$$b = \frac{\beta_o - \beta_{cy}}{\beta_{cy}} = \frac{\beta_o}{\beta_{cy}} - 1 \tag{4.128}$$

where β_o = circuit wave phase constant

β_{cy} = cyclotron wave phase constant

Now, from equation (2.6), Chapter II, the final β_{cy} is given by

$$\beta_{cy} = \frac{\omega + \omega_c}{v_{eff}} \tag{4.129}$$

Initially, let the cyclotron and circuit waves be in synchronism, so that the circuit phase constant is given by

$$\beta_o = \frac{\omega + \omega_c}{v_o} \tag{4.130}$$

Substitute (4.129) and (4.130) into (4.128),

$$b = \frac{v_{eff} - v_o}{v_o} \tag{4.131}$$

or,

$$|b| = \frac{V_o - V_{eff}}{V_o} \tag{4.132}$$

Substituting (4.124), (4.125) and (4.127) into (4.132) results in

$$|b| = \frac{\sqrt{2\eta V_o} - \sqrt{2\eta V_o(1 - \eta_{ec})}}{\sqrt{2\eta V_o}}$$

$$|b| = 1 - \sqrt{1 - \eta_{ec}} \tag{4.133}$$

From equations (4.120) and (4.121) there will be no more gain when $|K| = 1$, or when

$$|b| = \frac{2\alpha}{\beta_{cy}} \tag{4.134}$$

Combining (4.133) and (4.134), the maximum η_{ec} is given by

$$\eta_{ec_{max}} = \frac{4\alpha}{\beta_{cy}} - \frac{4\alpha^2}{\beta_{cy}^2}$$

In practical tubes, $\alpha/\beta_{cy} << 1$, so that

$$\boxed{\eta_{ec_{max}} \approx \frac{4\alpha}{\beta_{cy}}} \tag{4.135}$$

Equation (4.135) gives the maximum fraction of power than can be extracted from the longitudinal velocity of the electrons when the cyclotron and circuit waves start in synchronism.

If the electron beam is initially overvoltaged, the cyclotron wave can slow down to synchronism with the circuit wave as energy is

extracted from the beam, and then slip out of synchronism as above. In this case of an overvoltaged beam, the maximum η_{ec} can be doubled so that

(4.136) $$\boxed{\eta_{ec}\underset{max}{} \simeq \frac{8\alpha}{\beta_{cy}}}$$

In (4.135) and (4.136), α is the growth constant for perfect synchronism between circuit and beam waves, and β_{cy} is the final uncoupled propagation constant for the cyclotron wave given by (4.129).

4.5 Formulation of Nonlinear Interaction Equations for the Cyclotron Wave

For a filamentary beam, the equation of motion for the beam electrons is given by equation (4.7) and is

(4.137) $$\ddot{r} - j\omega_c\dot{r} = -\eta E_c$$

For the slow cyclotron wave interaction, the beam and circuit waves are right-hand polarized when the d.c. magnetic focusing field is in the +z direction. For an interaction which has a small growth per wavelength (a basic assumption here), the circuit transverse electric field at the beam can be written as

(4.138) $$E_c = e^{-j(\omega t - \int_0^z \beta(z)dz)}\ (Ae^{\gamma(z)} + De^{-\gamma(z)})$$

where $\beta(z)$ is the coupled propagation constant and $\gamma(z)$ is real. E_c consists of the sum of growing and decaying waves. It will be shown

the constant coefficients A and B are equal when the beam is injected on the axis of the tube with the cyclotron wave in synchronism with the circuit wave. A quantity $\alpha(z)$ is defined by the relation

$$\frac{d\gamma(z)}{dz} = \alpha(z) \tag{4.139}$$

or,

$$\gamma(z) = \int_0^z \alpha(z)\, dz \tag{4.140}$$

The motivation for choosing the form E_c in (4.138) is that moderately slow changes in the longitudinal velocity of the electrons, $v_z(z)$, will lead to slow changes in the gain constant, α, and the net gain would be expected to accumulate in the way indicated by equation (4.140). (Compare equation (4.138) with equation (4.72).)

The radial beam displacement off-axis can be written as

$$r = e^{-j(\omega t - \int_0^z \beta(z)dz)}(Fe^{\gamma(z)} + Ge^{-\gamma(z)}) \tag{4.141}$$

Then,

$$\dot{r} = \frac{\partial r}{\partial t} + v_z \frac{\partial r}{\partial z} \tag{4.142}$$

where $v_z = \frac{dz}{dt}$

It is convenient to consider the growing and decaying waves separately. Substitution of the growing part of (4.141) into (4.142) results in

$$\dot{r} = F(-j(\omega - \beta v_z) + \alpha v_z)\, e^{\gamma(z)}\, e^{-j(\omega t - \int_0^z \beta dz)} \tag{4.143}$$

Since the amplitude function of z in (4.143) is slowly varying compared to the exponential functions of z,

$$\ddot{r} = \frac{\partial \dot{r}}{\partial t} + v_z \frac{\partial \dot{r}}{\partial z}$$

$$\ddot{r} = F(-j\,(\omega - \beta v_z) + \alpha v_z)^2\, e^{\gamma(z)}\, e^{-j(\omega t - \int_0^z \beta dz)} \tag{4.144}$$

Substitution of the growing wave of equation (4.138), and (4.143) and (4.144) into (4.137) results in

$$F\{-j(\omega - \beta v_z) + \alpha v_z\}\{-j(\omega - \beta v_z) + \alpha v_z - j\omega_c\} = -nA \tag{4.145}$$

For practical tubes,

$$\alpha v_z << \omega_c \tag{4.146}$$

Also, for slow cyclotron waves, if the beam and circuit waves are close to synchronism,

$$\beta \simeq \beta_{cy} = \frac{\omega + \omega_c}{v_z}$$

or,

$$\omega - \beta v_z \simeq -\omega_c \tag{4.147}$$

Then, also

$$\alpha v_z << |\omega - \beta v_z| \tag{4.148}$$

Using (4.146), (4.147), and (4.148) in (4.145),

$$F = \frac{\frac{j\eta A}{\omega_c}}{\alpha v_z - j(\omega - \beta v_z + \omega_c)} \tag{4.149}$$

The imaginary part of the denominator of (4.149) has not been set equal to zero in accordance with (4.147) because αv_z is also a small quantity.

Similarly, for the decaying waves, F is replaced by G, A is replaced by B, and $\gamma(z)$ is replaced by $(-\gamma(z))$

$$G = \frac{\frac{-j\eta B}{\omega_c}}{\alpha v_z + j(\omega - \beta v_z + \omega_c)} \tag{4.150}$$

The coefficients A, B, F and G are determined from the boundary conditions for the amplitudes of r and E_c at $z = 0$. Let the beam be injected on the tube axis with the slow cyclotron wave in synchronism with the circuit wave.

From (4.141),

$$r(0) = Fe^{\gamma(0)} + Ge^{-\gamma(0)} = 0$$

$$r(0) = F + G = 0 \tag{4.151}$$

Substituting (4.149) and (4.150) into (4.151),

$$\frac{j\eta(A - B)\alpha v_z}{\omega_c} - \frac{\eta(\omega - \beta v_z + \omega_c)(A + B)}{\omega_c} = 0 \tag{4.152}$$

For the cyclotron wave injected in synchronism with the circuit wave at $z = 0$, $\beta_{cy} = \beta_0 = \beta$, so that

$$\omega - \beta(0)v_z(0) + \omega_c = 0$$

Thus, the imaginary part of (4.152) = 0, and

(4.153) $$A = B$$

From (4.138), the amplitude of E_c at $z = 0$ is

$$E_c(0) = Ae^{\gamma(0)} + Ae^{-\gamma(0)}$$
$$= 2A$$

Thus

(4.154) $$A = \frac{E_c(0)}{2}$$

The solutions for E_c and r are

(4.155) $$\boxed{E_c = E_c(0)e^{-j\left(\omega t - \int_0^z \beta(z)dz\right)}\left(\frac{e^{\gamma(z)} + e^{-\gamma(z)}}{2}\right)}$$

(4.156) $$\boxed{r = e^{-j(\omega t - \int_0^z \beta(z)dz)}\left(Fe^{\gamma(z)} + F^*e^{-\gamma(z)}\right)}$$

where

$$F = \frac{\frac{jnE_c(0)}{2\omega_c}}{\alpha(z)v_z(z) - j(\omega - \beta(z)v_z(z) + \omega_c)}$$

$$\gamma(z) = \int_0^z \alpha(z)\, dz$$

Note that we have now allowed for a variation in the axial velocity, $v_z(z)$, of the electrons.

4.5.1 The Growth Parameter, $\alpha(z)$. An expression for the growth parameter, $\alpha(z)$, as a function of z, will now be derived. From energy conservation, for the cyclotron wave,

$$\frac{\partial P_c(z)}{\partial z} + \frac{\partial P_{cy}(z)}{\partial z} = |I_o| E_{zb} \tag{4.157}$$

where I_o is the d.c. beam current and the other variables are the same as before. (Equation (4.157) is the same as equation (4.75).

Similar to section 4.1.3.3 for determining the growth constant, α, for the slow cyclotron wave interaction where v_z was assumed contant, equal to v_o, the power carried by the circuit at the position z, by definition of K_T, is

$$P_c(z) = \frac{|E_c(z)|^2}{2\beta_o^2 K_T} \tag{4.158}$$

where β_o is the uncoupled circuit propagation constant at z, and K_T is the transverse wave interaction impedance. β_o can vary with z.

Using (4.155) in (4.158),

$$P_c(z) = \frac{|E_c(0)|^2}{2\beta_o^2 K_T} \left(\frac{e^{2\gamma(z)} + e^{-2\gamma(z)} + 2}{4}\right) \tag{4.159}$$

Since the coefficient of the exponential function varies slowly with z,

$$\frac{\partial P_c(z)}{\partial z} = \frac{\alpha |E_c(0)|^2}{4\beta_o^2 K_T} (e^{2\gamma} - e^{-2\gamma}) \tag{4.160}$$

The power in the cyclotron motion of the electrons is given by equation (4.74) and is

$$P_{cy}(z) = \frac{I_o \omega_c B_o |r(z)|^2}{2} \tag{4.161}$$

Using (4.156) and $\omega_c = \eta B_o$ in (4.161), and assuming slow variation of coefficients compared to the exponentials,

$$\frac{\partial P_{cy}(z)}{\partial z} = \frac{I_o \eta |E_c(0)|^2 \alpha \ (e^{2\gamma} - e^{-2\gamma})}{4 \{ (\alpha v)^2 + (\omega - \beta v_z + \omega_c)^2 \}} \tag{4.162}$$

The longitudinal electric field from the circuit at the beam is given by equation (4.43) and is

$$E_{zb} = \text{Re} \ (r \frac{\partial E_c^*}{\partial z}) \tag{4.163}$$

From (4.155)

$$\frac{\partial E_c^*}{\partial z} = \frac{E_c^*(0)}{2} \{ (\alpha - j\beta) e^{\gamma} - (\alpha + j\beta) e^{-\gamma} \} e^{j(\omega t - \int_o^z \beta dz)}$$

Since $\alpha << \beta$,

$$\frac{\partial E_c^*}{\partial z} = \frac{-j\beta E_c^*(0)}{2} (e^{\gamma} + e^{-\gamma}) e^{j(\omega t - \int_o^z \beta dz)} \tag{4.164}$$

This is equivalent to stating that $e^{\pm\gamma(z)}$ is slowly varying compared to $e^{-j\int_o^z \beta dz}$

Inserting (4.156) and (4.164) into (4.163),

$$E_{zb} = \frac{\eta\left(\frac{|E_c(0)|^2}{4}\alpha\beta v_z(e^{2\gamma}-e^{-2\gamma})\right.}{\omega_c\{\alpha v_z)^2 + (\omega-\beta v_z + \omega_c)^2\}} \tag{4.165}$$

Inserting (4.160), (4.162) and (4.165) into (4.157) results in

$$\alpha^2(z) = \frac{\beta_o{}^2 K_T I_o(\beta v_z-\omega_c)}{v_z{}^2\omega_c} - (\beta_{cy} - \beta)^2 \tag{4.166}$$

Close to synchronism,

$$\beta \simeq \beta_{cy} = \frac{\omega+\omega_c}{v_z}$$

or,

$$\beta v_z - \omega_c \simeq \omega \tag{4.167}$$

Also, from coupled mode theory, equation (4.115),

$$\beta = \frac{\beta_{cy} + \beta_o}{2} \tag{4.168}$$

Substituting (4.167) and (4.168) into (4.166),

$$\boxed{\alpha^2(z) = \frac{\beta_o{}^2 I_o \omega}{2V_{eff}\omega_c} K_T - \left(\frac{\beta_{cy} - \beta_o}{2}\right)^2} \tag{4.169}$$

where $V_{eff} = \frac{v_z{}^2(z)}{2\eta}$

Equation (4.169) holds when the uncoupled cyclotron and circuit waves are close to synchronism. Note the similarity of (4.169) and (4.117). The electron velocity, v_0, used in obtaining (4.117) has been replaced by $v_z(z)$ in (4.169). This is a result of assuming $v_z(z)$ is slowly varying.

If synchronism is maintained by tapering the circuit or by changing the beam voltage with z, then $\beta_{cy} = \beta_0$, and (4.169) becomes

$$\alpha^2(z) = \frac{\beta_0^2 I_0 \omega}{2V_{eff}\omega_c} K_T \tag{4.170}$$

4.5.2 Output Power

From equation (4.157) for energy conservation,

$$\int_0^z dP_c(z) + \int_0^z dP_{cy}(z) = \int_0^z I_0 E_{zb} dz \tag{4.171}$$

Or, since $P_{cy}(0) = 0$ in (4.161) when $r(0) = 0$,

$$(P_c(z) - P_c(0)) + P_{cy}(z) = \int_0^z I_0 E_{zb} dz \tag{4.172}$$

Using (4.1$\int_0^z I_0 E_{zb} dz$ ing that $\alpha = d\gamma/dz$,

$$\int_0^z I_0 E_{zb} dz = \frac{I_0 \eta |E_c(0)|^2 \beta v_z (e^{\gamma} - e^{-\gamma})^2}{8\omega_c \{(\alpha v_z)^2 + (\Omega)^2\}} \tag{4.173}$$

where $\Omega = \omega - \beta v + \omega_c$

Now, from (4.156)

$$|r(z)| = \frac{\eta^2 |E_c(0)|^2 \{(\alpha v_z)^2 (e^{\gamma} - e^{-\gamma})^2 + (\Omega)^2 (e^{\gamma} + e^{-\gamma})^2\}}{4\omega_c^2 \{(\alpha v_z)^2 + (\Omega)^2\}^2} \tag{4.174}$$

If exact synchronism is maintained,

(4.175) $$\Omega = 0$$

Using (4.174) and (4.175), equation (4.173) can be expressed as

(4.176) $$\int_0^z I_0 E_z b dz = \frac{1}{2} I_0 B_0 (\beta v_z) |r(z)|^2$$

where $B_0 = \omega c/\eta$

Substituting (4.161) and (4.176) into (4.172),

(4.177) $$P_c(z) - P_c(0) = \frac{1}{2} I_0 B_0 (\beta v_z - \omega_c) |r(z)|^2$$

Close to synchronism,

(4.178) $$\beta v_z - \omega_c = \omega$$

Using 4.178 in (4.177)

(4.179) $$\boxed{P_c(z) - P_c(0) = \frac{1}{2} I_0 B_0 \omega |r_z|^2}$$

From (4.161) and (4.179),

(4.180) $$\boxed{\frac{P_c(z) - P_c(0)}{P_{cy}(z)} = \frac{\omega}{\omega_c}}$$

Equation (4.179) and (4.180) are the same as equation (4.80) and (4.81) respectively. It can be noted from (4.173) and (4.174) that if z is large enough to make $e^{\gamma(z)} >> e^{-\gamma(z)}$, say $e^{\gamma(z)} = 5$, then (4.179) and (4.180) still hold even if exact synchronism is not maintained.

4.5.3 Determination of $v_z(z)$. The slow down of the longitudinal velocity, v_z, of the beam electrons is determined by the amount of power extracted from the longitudinal velocity. Thus,

$$P_e = (P_c(z) - P_c(0)) + P_{cy}(z) \tag{4.181}$$

where P_e = power extracted from longitudinal velocity of electrons

The power on the circuit is given by (4.158) and is

$$P_c(z) = \frac{|E_1(0)|^2}{2\beta_0^2 K_T} \left(\frac{e^{\gamma(z)} + e^{-\gamma(z)}}{2}\right)^2$$

$$\boxed{P_c(z) = P_c(0) \left(\frac{e^{\gamma(z)} + e^{-\gamma(z)}}{2}\right)^2} \tag{4.182}$$

where $P_c(0)$ is the power on the circuit at $z = 0$.

Using (4.180) and (4.182), (4.181) becomes

$$P_e = \left(\frac{\omega + \omega_c}{\omega}\right) P_c(0) \left(\frac{e^{\gamma(z)} - e^{-\gamma(z)}}{2}\right)^2 \tag{4.183}$$

Now from power conservation,

$$V_{eff}\, I_o = V_o I_o - P_e \tag{4.184}$$

where V_{eff} is the effective d.c. kinetic voltage of the slowed-down electrons to v_z

V_o = initial voltage of electrons = $v_o^2/2\eta$

I_o = beam current

Substituting (4.183) into (4.184)

$$V_{eff} = V_o - \left(\frac{\omega + \omega_c}{\omega}\right)\left(\frac{P_c(0)}{I_o}\right)\left(\frac{e^{\gamma(z)} - e^{-\gamma(z)}}{2}\right)^2 \tag{4.185}$$

where $V_{eff} = \frac{v_z^2}{2\eta}$

or $v_z = \sqrt{2\eta V_{eff}}$

$$\gamma(z) = \int_0^z \alpha(z)dz$$

The analysis of the growth of the circuit power with z involves a simultaneous solution of equations (4.169), (4.185), and (4.182). If synchronism is maintained by appropriately tapering the circuit wave velocity or by appropriately varying the applied d.c. beam voltage, equation (4.169) is replaced by (4.170).

4.5.4 Numerical Analysis of Non-Linear Interaction. The simultaneous solution of (4.169), (4.185) and (4.182) can be accomplished numerically. A typical calculation is given below.

The cumulative growth constant is

$$\gamma(z) = \int_0^z \alpha(z)\, dz$$

This can be expressed as a summation

$$\gamma(z) = \sum_0^z \alpha(z)\Delta z$$

where the Δz are small increments of z.

Start with $z = 0$ in (4.182)

$$P_c(0) = \frac{|E_1(0)|^2}{2\beta_o^2 K_T}$$

$\beta_{cy} = \beta_o$ for synchronism at $z = 0$

$V_{eff} = V_o$, the injection voltage

$\alpha_o(z = 0)$ is calculated from (4.169)

Move an increment Δz_1 in the z-direction

$z = \Delta z_1$

$\gamma_1 = \alpha_o \Delta z_1$

$P_c(z)$ is calculated from (4.182) using γ_1

$V_{eff1}(z)$ is calculated from (4.185) using γ_1

$$\beta_{cy1} = \frac{\omega + \omega_c}{\sqrt{2nV_{eff}}}$$

$\alpha_1(z)$ is calculated from (4.169) using β_{cy1} and V_{eff1}

Move another increment Δz_2

$z = \Delta z_1 + \Delta z_2$

$\gamma_2 = \alpha_o \Delta z_1 + \alpha_1 \Delta z_2$

$P_c(z)$ is calculated from (4.182) using γ_2

$V_{eff2}(z)$ is calculated from (4.185) using γ_2

$$\beta_{cy2} = \frac{\omega + \omega_c}{2\eta V_{eff2}}$$

$\alpha_2(z)$ is calculated from (4.169) using

β_{cy2} and V_{eff2}

Continue moving increments Δz to obtain $P_c(z)$ point by point.

4.5.5 Compensation for Loss of Synchronism. In section 4.4, equation (4.135) gives a maximum fraction of power that can be extracted from the beam by the circuit and the cyclotron motion of the electrons when the cyclotron and circuit waves start in synchronism and are allowed to slip out of synchronism. From equation (4.135), the maximum power that can be extracted in this case is

$$(P_c(z) - P_c(0) + P_{cy}(z))_{max} = 4V_0I_0(\frac{\alpha_0}{\beta_{cy}})$$

where β_{cy} is the final uncoupled cyclotron wave propagation constant, and α_0 is the injection gain constant.

Using equation (4.180), the maximum power extracted by the circuit is

$$(P_c(z) - P_c(0))_{max} = (\frac{\omega}{\omega + \omega_c}) (\frac{4\alpha_0}{\beta_{cy}}) V_0I_0$$

For typical design parameters, α_0/β_{cy}, is of the order of 1% and $\omega/(\omega + \omega_c)$ is of the order of 1/2, so that the order of 2% of the beam

power can be converted to RF circuit power.

This limitation on output power can be overcome by three methods for maintaining synchronism as follows.

(1) Tapering of Applied Beam Voltage. If a d.c. potential, $V_o(z)$, were imposed along the axis of the interaction region by some means, then equation (4.185) indicates how to choose this potential profile to maintain synchronism. Let the second term on the right side of (4.185) equal a reduction voltage, V_{red}. Then (4.185) becomes

$$V_{eff} = V_o - V_{red} \tag{4.186}$$

Now, if the applied voltage, $V_o(z)$ is chosen as

$$V_o(z) = V_o + V_{red}$$

Then,

$$\begin{aligned} V_{eff} &= V_o(z) - V_{red} \\ &= (V_o + V_{red}) - V_{red} \\ &= V_o \end{aligned}$$

Thus, choose $V_o(z)$ given by

$$V_o(z) = V_o + \left(\frac{\omega + \omega_c}{\omega}\right)\left(\frac{P_c(0)}{I_o}\right)\left(\frac{e^{\gamma(z)} - e^{-\gamma(z)}}{2}\right)^2 \tag{4.187}$$

where V_o = the injection voltage

Then $V_{eff} = V_o$ for all z and $\alpha(z) = \alpha_o$, the injection gain constant. $\gamma(z)$ then becomes $\gamma(z) = \alpha_o z$. The beam is simply accelerated by the potential gradient an amount that precisely compensates the loss of energy by the RF interaction. The cyclotron wave then maintains synchronism with the circuit wave.

It may be difficult to implement this method because the d.c. potential profile would require d.c. isolation of sections of the circuit with no RF isolation. In the case of a bifilar helix circuit, it may be possible to obtain the d.c. potential profile at the beam by means of an external d.c. source which "leaks" the d.c. potential through the spaces between the turns of the helix.

(2) Tapering of the Circuit Phase Velocity. Another method to maintain synchronism is to taper the circuit. β_o would then be given by $(\omega + \omega_c)/(2\eta V_z)^{\frac{1}{2}}$ and $\alpha(z)$ would be given by equation (4.170). A disadvantage of this solution is that the tube would be designed for only a single value of output power since the circuit taper is fixed inside the tube and cannot be adjusted.

(3) Adjustment of the D.C. Magnetic Focusing Field. The uncoupled phase velocity of the cyclotron wave is given by

$$v_{Pcy} = \frac{\omega}{\beta_{cy}}$$

where β_{cy} = cyclotron uncoupled progation constant

β_{cy} is given by

$$\beta_{cy} = \frac{\omega^{+}\omega_c}{v_z(z)}$$

As $v_z(z)$ decreases, ω_c, or the magnetic focusing field $B_o = \omega_c/\eta$, can be decreased to maintain v_{pcy} or β_{cy} constant so as to maintain synchronism with the circuit wave. ω_c has a lower limit dictated by focusing requirements and can not be less than the value corresponding to minimum Brillouin focusing field. This method for resynchronization has the advantage of being easily adjustable external to the tube.

There is another advantage to this method of resynchronization. A decreasing magnetic field with z converts rotational energy to longitudinal energy. Thus some of the undesired power in the cyclotron motion is used to help increase v_z to maintain synchronism.

4.6 Effects of Finite Beam Radius and Space Charge

In previous sections, it was shown how the energy exchange mechanism with a filamentary beam involves motion of the beam electrons off axis into a region of a finite longitudinal electric field. For a beam of zero spot size, all of the electrons see the same longitudinal decelerating field, and hence the amplification of the circuit field proceeds by removing an identical amount of energy from each electron. For a finite size beam, electrons initially at different radii would see different decelerating fields during their transit, and the beam would not be monoenergetic at the output. The purpose of this section is to quantitatively assess this effect.

The configuration of the beam is a helical displacement in the transverse direction (Figure 4-2) with the center of the beam located at $x_1(z,t)$, $y_1(z,t)$. It will be assumed the cross-section of the beam in any x-y plane (perpendicular to the z-directed magnetic focusing field) is a circle. The beam distorts into an ellipse in planes perpendicular to the beam axis. However, when using Gauss' theorem in estimating the average d.c. electric field from the space charge of the beam, a circular cross-section perpendicular to the beam axis will also be assumed. This distortion in the cross-section should have no substantial effect on estimation of energy spread. For the cyclotron wave, it will be found the motion of the electrons is a rotation around the beam center at a frequency, ω_R, superimposed on the rotation of the beam center around the tube axis at cyclotron frequency. It will be assumed the deflection of the beam center off axis is small enough so that the beam is within a uniform transverse electric field of the circuit wave. This will be true if $\beta a_L < 1$ and $\beta b < 1$, where a_L is the deflection of the beam center off the tube axis, and where b is the radius of the beam, so that a_L or $b < 1/\beta = \lambda/2\pi$, with λ = coupled wavelength. For this case, the uncoupled beam waves have velocity dispersion characteristics that are closely approximated by the predictions of the filamentary beam model.

From Gauss' Law, the electric field inside the beam is given by

$$E_x = \frac{\rho_0}{2\varepsilon_0}(x-x_1) + E_{xc} \tag{4.188}$$

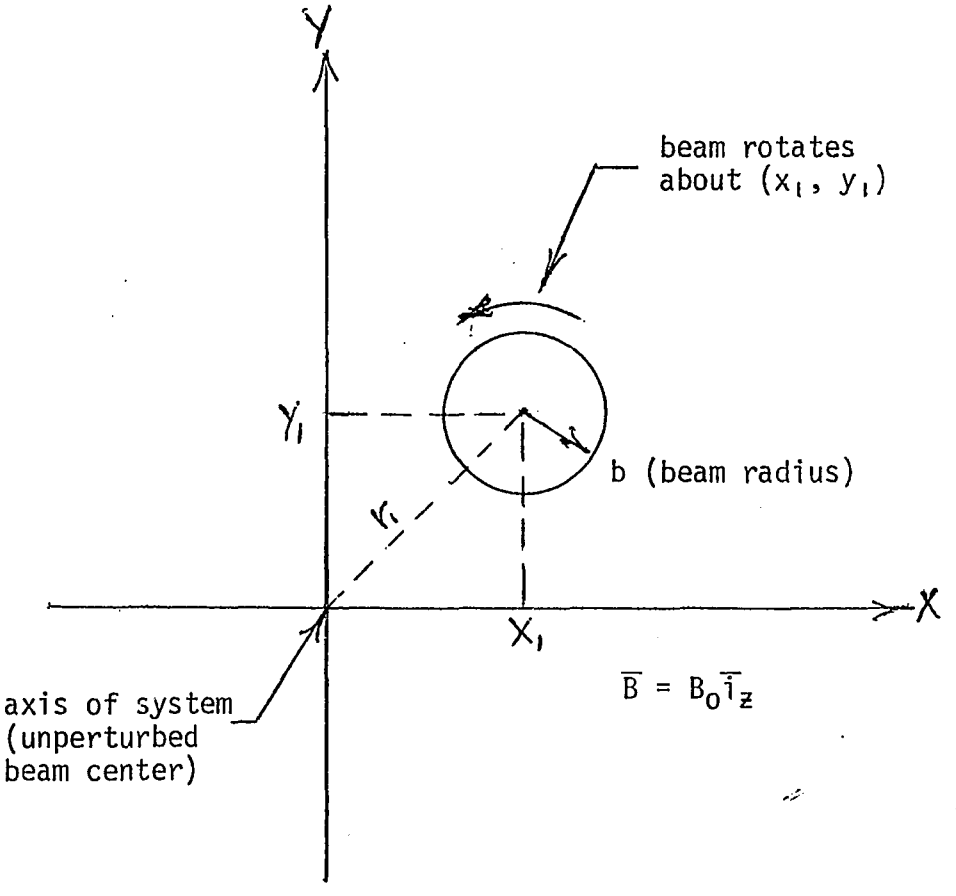

Figure 4-2 Beam displacement variables

$$E_y = \frac{\rho_o}{2\varepsilon_o}(y-y_1) + E_{yc} \tag{4.189}$$

where ρ_o = charge density in the beam and is negative for electrons

ε_o = free space dielectric constant

E_{xc} and E_{yc} are the x and y components of the transverse circuit field E_c (the field arising from charges on the circuit structure)

Now introduce circularly polarized variables with $r(z,t)$ now describing the position of a particular electron in the beam cross-section.

The force equation for the electrons is

$$\ddot{r} - j\omega_c\dot{r} = \frac{\omega_p^2}{2}(r-r_1) - \eta E_c \tag{4.190}$$

where $r_1 = x_1 + jy_1$ describes the beam center position

$\omega_p = (-\eta\rho_o/\varepsilon_o)^{\frac{1}{2}}$ is the plasma frequency

Comparing equation (4.190) with (4.137), it is seen that (4.190) contains an additional space charge term.

For the cyclotron wave interaction, the circuit field is taken to be circularly polarized in the right-hand sense and is given by (4.155).

$$\boxed{E_c = \frac{E_c(0)}{2} e^{-j(\omega t - \int_0^z \beta dz)}(e^{\gamma(z)} + e^{-\gamma(z)})} \tag{4.191}$$

With $r = r_1 + r_0$, equation (4.190) can be put in the form

$$(\ddot{r}_0 - j\omega_c\dot{r}_0 - \frac{\omega_p^2}{2} r_0) + \ddot{r}_1 - j\omega_c\dot{r}_1 = -\eta E_c \tag{4.192}$$

First consider the beam in the region before it enters the circuit field and where the circuit field, $E_c = 0$, and where $r_1 = 0$. Then (4.192) becomes

$$\ddot{r}_0 - j\omega_c\dot{r}_0 - \frac{\omega_p^2}{2} r_0 = 0 \tag{4.193}$$

The solution to (4.193) is of the form

$$r_0 = Ae^{\Gamma t} \tag{4.194}$$

Substitution of (4.194) into (4.193) results in

$$\Gamma^2 - j\omega_c\Gamma - \frac{\omega_p^2}{2} = 0 \tag{4.195}$$

From (4.195)

$$\Gamma = j\left(\frac{\omega_c \pm \sqrt{\omega_c^2 - 2\omega_p^2}}{2}\right) = j\omega_R \tag{4.196}$$

If

$$\omega_c^2 = 2\omega_p^2 \tag{4.197}$$

Then

$$\omega_R = \frac{\omega_c}{2} \tag{4.198}$$

This is the solution with Brillouin focusing. In Brillouin focusing, the d.c. magnetic field at the cathode is zero. It can be shown[11] that when the beam is injected into the magnetic field with a beam radius equal to the Brillouin radius, then in the uniform magnetic field, all the electrons rotate around the beam center at a frequency $\omega_c/2$, and all electrons have the same longitudinal velocity. The Brillouin field, given by (4.197) in the uniform field region, is the minimum field required to focus the beam for a given beam radius and a given charge density in the beam.

If

$$\omega_c^2 >> \omega_p^2 \tag{4.199}$$

Then the square root in (4.196) can be approximated by

$$(\omega_c^2 - 2\omega_p^2)^{\frac{1}{2}} \approx \omega_c - \frac{\omega_p^2}{\omega_c} \tag{4.200}$$

The solutions (4.196) then become

$$\omega_{R1} = \frac{\omega_p^2}{2\omega_c} \tag{4.201}$$

$$\omega_{R2} = \omega_c - \frac{\omega_p^2}{2\omega_c} \tag{4.202}$$

The solution to (4.193) is then

$$r_o = Ae^{j\omega_{R1}t} + Be^{j\omega_{R2}t} \tag{4.203}$$

This is the solution with confined flow focusing. Confined flow requires that the magnetic field link the cathode and that the magnetic field in the uniform region be greater than the Brillouin field.

It will now be shown that if (4.199) holds, then solution (4.202) is not allowed in practical tubes, i.e., B = 0 in (4.203).

A useful theorm, which is obtained by setting torque on an electron about the beam center equal to the rate of change of momentum, called Busch's theorem[11], states that for constant magnetic flux density with r,

$$\omega_R = \frac{1}{2}\left(\omega_C - \omega_{CO}\frac{r_o^2}{r^2}\right) \tag{4.204}$$

where

ω_R = angular velocity of an electron about the beam center at $z = z$

$\omega_C = \eta B_z$, the cyclotron frequency at $z = z$

B_z = longitudinal magnetic flux density at $z = z$

$\omega_{CO} = \eta B_{zo}$

B_{zo} = magnetic flux density linking the cathode (assumed uniform over the cathode area) at $z = 0$

r_o = radial distance of electron off axis at the cathode ($z = 0$)

r = radial distance of electron at $z = z$

In obtaining (4.204), it is assumed that the initial angular velocity of the electrons at the cathode equals zero.

Equation (4.204) can be used to estimate the flux density, or ω_{co}, linking the cathode in order to obtain a given ω_R. Let $r = r_o$ and solve for ω_{co}.

(4.205) $$\omega_{co} = \omega_c - 2\omega_R$$

If $\omega_c >> \omega_{cB}$

where $\omega_{cB} = \eta B_B$

B_B = Brillouin field

$\omega_{cB}^2 = 2\omega_p^2$

Then from (4.201)

(4.206) $$\omega_{R1} << \omega_c$$

Using (4.206) in (4.205) for ω_R, then

(4.207) $$\omega_{co} \approx \omega_c$$

From (4.202)

(4.208) $$\omega_{R2} \approx \omega_c$$

Using (4.208) in (4.205) for ω_R, then

(4.209) $$\omega_{co} \approx -\omega_c$$

Equation (4.209) states that to obtain ω_{R2} given by (4.202), the field at the cathode would have to be in the reverse direction to that of the rest of the field. This is physically not the case, so that ω_{R2} is not allowed as a solution.

As an example, let the magnetic field in the uniform region (at $z = \bar{z}$) be twice Brillouin, i.e.,

$$\omega_c = 2\sqrt{2}\,\omega_p \tag{4.210}$$

Substitution of (4.210) into (4.201) and (4.202) results in

$$\omega_{R1} = \frac{\omega_c}{16} \tag{4.211}$$

$$\omega_{R2} = \frac{15}{16}\,\omega_c \tag{4.212}$$

Also let

$$r = r_o \tag{4.213}$$

Substitution of (4.211) and (4.213) into (4.204) results in

$$\omega_{co} = \frac{7}{8}\,\omega_c \quad \text{(to obtain } \omega_{R1}\text{)}$$

Substitution of (4.212) and (4.213) into (4.204) results in

$$\omega_{co} = -\frac{7}{8}\,\omega_c \quad \text{(to obtain } \omega_{R2}\text{)}$$

Thus, in practical tubes with confined flow focusing, solution (4.203) to equation (4.193) becomes

$$r_o = a_o\, e^{j\omega_R t} \tag{4.214}$$

$$\text{where } \omega_R = \frac{\omega_p^2}{2\omega_c}$$

$$a_o = \text{complex amplitude}$$

$$= |a_o| e^{j\phi}$$

It can be noted that in (4.204), if the cathode is immersed in the uniform field, i.e., $\omega_c = \omega_{co}$, and if the beam (outer electrons) is constant in radius, i.e., $r = r_o$, then $\omega_R = 0$. In order for $\omega_R \to 0$, $\omega_c \to \infty$ for the stable beam condition given by equation (4.201). In other words, as ω_c becomes very large with the cathode immersed in the uniform field, all electrons follow the field lines and do not rotate.

If in (4.204), $\omega_{co} = 0$, (zero field at the cathode), $\omega_R = \omega_c/2$, the Brillouin flow solution.

In (4.204), for given values of ω_c and ω_{co}, r (radius of beam) would have to adjust in relation to r_o (radius of beam at cathode) so that stable beam condition (4.201) is attained. The adjustment of r changes the charge density in the beam and changes ω_p^2 in (4.201).

Returning to (4.192), the term in brackets on the left side is the homogeneous part of the equation and is equal to zero. The motion of the beam center at r_1 is then given by

$$\ddot{r}_1 - j\omega_c r_1 = -\eta E_c \tag{4.215}$$

Equation (4.215) is the same as (4.137), and with E_c given by (4.191), the solution for r_1 is given by (4.156). Thus, the complete solution of (4.190) is the sum of the homogeneous and particular solutions and is given by

$$\boxed{r(z,t) = r_o e^{j\omega_R t} + e^{-j(\omega t - \int_o^z \beta dz)}\left(Fe^{\gamma(z)} + F^* e^{-\gamma(z)}\right)} \tag{4.216}$$

where

$$\omega_R = \frac{\omega_p^2}{2\omega_c}$$

ω_c = cyclotron frequency = ηB_0

$$\omega p^2 = \frac{|\eta \rho_0|}{\varepsilon_0}$$

$$F = \frac{\frac{j\eta E_c(0)}{2\omega_c}}{\alpha(z)v_z(z) - j\,(\omega - \beta(z)v_z(z) + \omega_c)}$$

$$\gamma(z) = \int_0^z \alpha(z)\, dz$$

r_0 is complex = $a_0 e^{j\phi}$, where a_0 is real

The solution is a beam rotating around its center at a frequency, ω_R, with the center of the beam following the solution for the filamentary beam. Note that for synchronism,

$$-j(\omega t - \int_0^z \beta dz) = -j(\omega t - \int_0^t \frac{\omega + \omega_c}{v_z} v_z dt)$$

$$= j(\omega t - (\omega + \omega_c)t)$$

$$= j\omega_c t$$

In the above, for the electrons in the beam pattern, $dz = v_z dt$. Thus, with the time, the electrons in the beam rotate around the tube axis at a frequency, ω_c.

In practice, the achievement of a stable beam with Brillouin flow is very difficult. It is much easier to control the beam with confined

flow. Therefore, a field which is greater than Brillouin will be used for focusing.

To calculate the axial energy lost or gained by a particular electron, expressions are needed for the axial component of the electric field. The axial component of the space-charge field (E_{zS}) can be determined by noting from integration of Gauss' Law that the equipotentials associated with the space-charge field inside the beam are approximately

$$V = \frac{-\rho_0}{4\varepsilon_0} \{(x-x_1)^2 + (y-y_1)^2\} \tag{4.217}$$

where ρ_0 is the charge density and is negative for electrons.

Therefore,

$$E_{zS} = - \frac{\partial V}{\partial z}$$

$$E_{zS} = \frac{-\rho_0}{2\varepsilon_0} \{(x-x_1) \frac{\partial x_1}{\partial z} + (y-y_1) \frac{\partial y_1}{\partial z} \}$$

$$E_{zS} = \frac{-\rho_0}{2\varepsilon_0} \text{Re} \{(r-r_1) \frac{\partial r_1^*}{\partial z} \} \tag{4.218}$$

where $(r-r_1) = a_0 e^{j\phi} e^{j\omega_R t}$

If synchronism is maintained for the cyclotron wave,

$$\omega - \beta(z) v_z(z) + \omega_C = 0 \tag{4.219}$$

For an electron, with z representing the position of an electron

$$\int_0^z \beta dz = \int_0^z \frac{\omega+\omega_c}{v_z} v_z \, dt$$

$$= \int_0^t (\omega+\omega_c) \, dt$$

$$\int_0^z \beta dz = (\omega+\omega_c) \, t$$

(4.220) $$\omega t - \int_0^z \beta dz = - \omega_c t$$

Using (4.216), (4.219), (4.220) and $\alpha << \beta$, equation (4.218) becomes

(4.221) $$E_{zs} = \frac{-\omega_R \beta a_o}{\alpha v_z} \frac{|E_c(0)|}{2} (e^{\gamma(z)} - e^{-\gamma(z)}) \cdot \cos \{(\omega_c-\omega_R) \, t - (\phi_o-\theta_o)\}$$

where

$$\omega_R = \frac{\omega_p^2}{2\omega_c}$$

$$E_c(0) = |E_c(0)| e^{j\theta_o}$$

Equation (4.221) gives the longitudinal space charge field seen by the electron at synchronism ($\omega = \beta v_z - \omega_c$). This field oscillates with time at a frequency ($\omega_c-\omega_R$).

The longitudinal circuit field at the beam position is given by (4.163) and can be expressed by

(4.222) $$E_{zc} = \mathrm{Re}\ (r^* \frac{\partial E_c}{\partial z})$$

Using (4.191), (4.216) and $\alpha << \beta$ in (4.222),

(4.223) $$E_{zc} = \frac{|E_c(0)|^2 \eta\beta (e^{2\gamma} - e^{-2\gamma})}{4\alpha v_z \omega_c}$$

$$-\beta a_o \frac{|E_c(0)|}{2}(e^{\gamma} + e^{-\gamma}) \sin\{(\omega_c - \omega_R)t - (\phi_o - \theta_o)\}$$

Typically, $\omega_R >> \alpha v_z$, so that with $e^{\gamma} >> e^{-\gamma}$, the amplitude of the sinusoidal term in (4.223) can be neglected compared to that in (4.221). Thus the oscillating space charge field at an electron dominates the energy spread generation.

The total field seen by an electron effectively consists of a d.c. term due to the circuit field and an oscillating term due to space charge.

The longitudinal force equation is

$$\frac{dv_z}{dt} = -\eta(E_{zs} + E_{zc})$$

or,

(4.224) $$dv_z = -\eta(E_{zs} + E_{zc})\, dt$$

For an electron, $dt = dz/v_z$

Equation (4.224) becomes

(4.225) $$\int_{v_o}^{v_z} v_z\, dz = \int_0^z -\eta(E_{zs} + E_{zc})\, dz$$

Inserting (4.221) and the d.c. part of (4.223) into (4.225), assuming v_z is slowly varying and v_z differs from v_0 by a small amount results in

$$W_K = \frac{v_z^2}{2\eta}$$

$$= \frac{v_0^2}{2\eta} - \left|\frac{E_c(0)}{2}\right|^2 \frac{\eta\beta(e^{\gamma}-e^{-\gamma})^2}{2\alpha^2 v_z \omega_c} \tag{4.226}$$

$$+ \frac{\omega_R \beta a_0}{\omega_c \alpha} \frac{|E_c(0)|}{2}(e^{\gamma}-e^{-\gamma}) \left[\sin\{(\omega_c-\omega_R)t-(\phi_0-\theta_0)\} + \sin(\phi_0-\theta_0)\right]$$

In the integration, the exponentials in (4.221) are slowly varying compared to the sinusoidal function, so that the exponentials can be pulled out of the integral.

The ratio of the second term on the right side of (4.226) to the amplitude of the third term is $r\omega_c/2a_0\omega_R$. Since $\omega_c >> \omega_R$, the amplitude of the d.c. part of the third term is small compared to the second term, so that $\sin(\phi_0-\theta_0)$ in the third term can be neglected.

Equation (4.226) gives the longitudinal kinetic energy in electron volts, W_K, of the electron described by the initial position a_0, ϕ_0. Note that the first term on the right side of (4.226) is the initial kinetic energy of the electrons. The second term is the average energy lost by the electrons. The third term changes sign over the beam cross-section. That is, at a given instant of time and a given position z, electrons in a particular sector of the beam have lost

more than the average energy while those in the opposite sector have lost less than the average (Figure 4-3). As time goes on, the center of the beam electrons rotates around the tube axis at ω_c while the electrons rotate around the center at ω_R. With time, the sectors in Figure 4-3 rotate around the beam center.

The mean energy loss of all electrons is the relevant quantity when computing the gain and power output. This mean energy extracted from the longitudinal energy of the beam goes to the circuit and to cyclotron motion of the electrons, and is given by the second term on the right side of (4.226).

$$\Delta\varepsilon_L = \left|\frac{E_c(0)}{2}\right|^2 \frac{n\beta(e^{\gamma} - e^{-\gamma})}{2\alpha^2 v_z \omega_c} \tag{4.227}$$

The power extracted from the beam is thus

$$P_e = P_c(z) - P_c(0) + P_{cyc} = I_0 \Delta\varepsilon_L \tag{4.228}$$

At synchronism, using $\beta = (\omega+\omega_c)/v_z$, (4.227), and (4.156), equation (4.228) can be expressed as

$$P_e = I_0\Delta\varepsilon_L = \frac{1}{2}(\omega+\omega_c)\, I_0 B_0 \left|a_L\right|^2 \tag{4.229}$$

where $\left|a_L\right| = \left|r_1(L)\right|$ = final beam deflection

This result checks with (4.161), (4.179) and (4.180)

From (4.229)

$$\Delta\varepsilon_L = \frac{1}{2}(\omega+\omega_c)\, B_0 \left|a_L\right|^2 \tag{4.230}$$

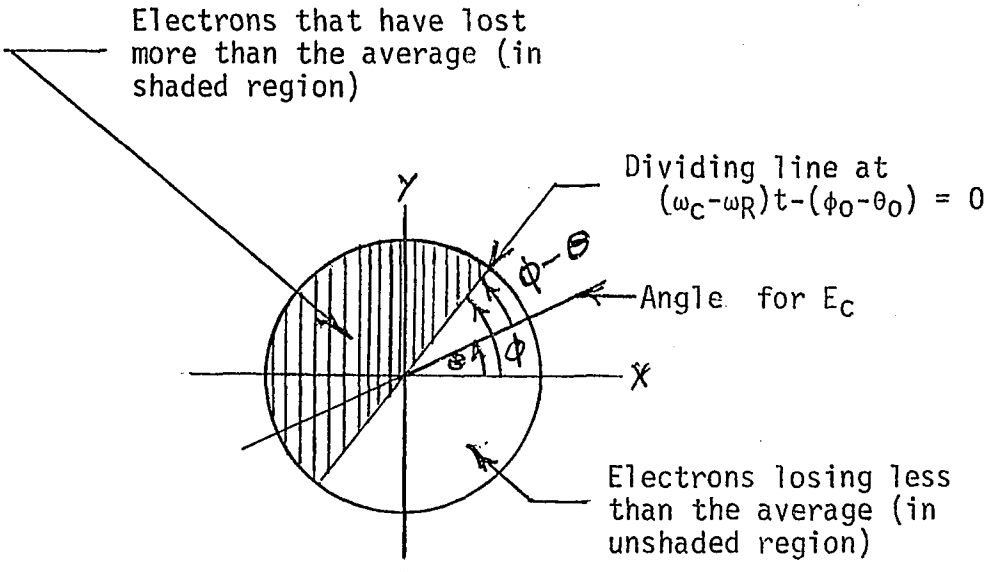

Figure 4-3 Illustration of the Energy Distribution of Electrons Over the Beam Cross-Section

$\Delta\varepsilon_L$ is the sum of the electron kinetic voltages representing the energy extracted from the beam by the circuit and by the cyclotron motion of the electrons.

In considering the enhancement of amplifier efficiency by collector depression, the distribution of electron energies is of importance. From (4.226), the energy loss of any particular electron can differ from the mean loss ($\Delta\varepsilon_L$) by as much as $\pm\ \Delta\varepsilon_S$, with

$$\Delta\varepsilon_S = \frac{\omega R}{\omega_C}\frac{\beta b}{\alpha}\frac{|E_C(0)|}{2}(e^{\gamma}-e^{-\gamma}) \tag{4.231}$$

where b = beam radius

Using (4.156) and $\beta = (\omega+\omega_C)/v_z$, equation (4.231) can be expressed by

$$\Delta\varepsilon_S = \frac{(\omega+\omega_C)\omega_R b|a_L|}{\eta} \tag{4.232}$$

The energy distribution of the electrons at the output would look roughly as shwon in Figure 4-4. The significance of $\Delta\varepsilon_S$ is as follows. A properly designed collector could be depressed below the circuit voltage by an amount that would not return the slowest electrons.

Thus,

$$V_{ckt.} - V_{coll} = V_z \tag{4.233}$$

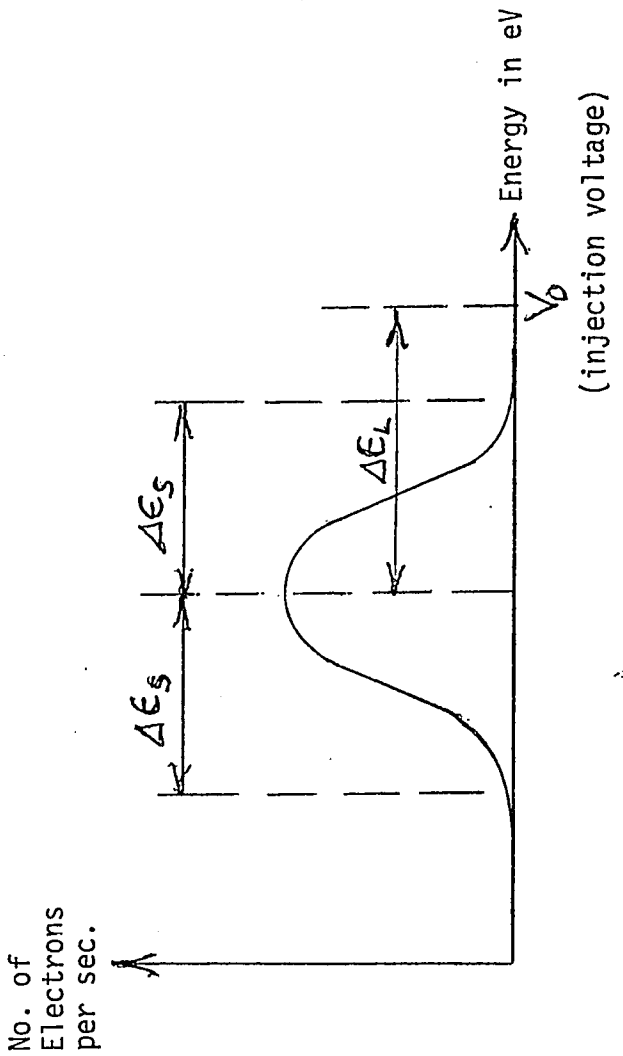

Figure 4-4 Electron energy distribution at the output of the r.f. interaction region

where V_{ckt} = circuit voltage with respect to cathode at the collector end

V_{coll} = voltage at collector with respect to the cathode

V_z = longitudinal kinetic voltage of slowest electrons at the end of the circuit near the collector

If circuit tapering is used to maintain synchronism,

$$V_{ckt} = V_o = \text{injection voltage}$$

$$V_z = V_o - \Delta\varepsilon_L - \Delta\varepsilon_S$$

Equation (4.233) becomes

$$V_o - V_{coll} = V_o - \Delta\varepsilon_L - \Delta\varepsilon_S$$

or,

$$V_{coll} = \Delta\varepsilon_L + \Delta\varepsilon_S \tag{4.234}$$

If voltage tapering is used to maintain synchronism,

$$V_{ckt} = V_o + \Delta\varepsilon_L$$

$$V_z = V_o - \Delta\varepsilon_S$$

Equation (4.233) becomes

$$(V_o + \Delta\varepsilon_L) - V_{coll} = V_o - \Delta\varepsilon_S$$

or,

$$V_{coll} = \Delta\varepsilon_L + \Delta\varepsilon_S, \text{ which is again equation (4.234).}$$

With no interception of the beam on the circuit, the d.c. power supplied to the beam by the collector is

$$P_{dc} = I_o V_{coll}$$

$$P_{dc} = I_o (\Delta\varepsilon_L + \Delta\varepsilon_S) \tag{4.235}$$

The power supplied to the circuit is

$$P_c(z) - P_c(0) = \frac{\omega}{\omega+\omega_c} I_o \Delta\varepsilon_L \tag{4.236}$$

Using (4.235) and (4.236), the depressed collector efficiency is

$$\eta_{opt} = \frac{P_c(z) - P_c(0)}{P_{dc}} = \frac{\omega/(\omega+\omega_c)}{1 + \Delta\varepsilon_S/\Delta\varepsilon_L} \tag{4.237}$$

From (4.230) and (4.232),

$$\frac{\Delta\varepsilon_S}{\Delta\varepsilon_L} = \frac{\omega R}{\omega_c} \frac{2b}{a_L} \tag{4.238}$$

Inserting (4.238) into (4.237) results in

$$\eta_{opt} = \frac{\omega/(\omega+\omega_c)}{1 + \frac{\omega R}{\omega_c} \frac{2b}{a_L}} \tag{4.239}$$

As the beam becomes filamentary, i.e., $b \ll a_L$, the depressed collector efficiency becomes greater. The cyclotron motion of the electrons causes them to see an oscillating longitudinal field, which

tends to average out the effect of velocity spread as the electrons travel through the tube; the factor ω_R/ω_c indicates this effect.

The depressed collector efficiency indicated by (4.239) can be increased by converting some of the energy of the cyclotron motion to longitudinal energy which can then be recouped by further collector depression.

The depressed collector efficiency can be put into the form

$$\eta_{opt} = \frac{Pc(z) - Pc(0)}{(Pc(z)-Pc(0)) + P_{cyc} + P_s}$$

where P_s = d.c. power supplied due to velocity spread

Equation (4.237) can then be expressed as

(4.240)
$$\eta_{opt} = \frac{\frac{\omega}{\omega+\omega_c}\Delta\varepsilon_L}{\frac{\omega}{\omega+\omega_c}\Delta\varepsilon_L + \left(\frac{\omega_c}{\omega+\omega_c}\right)\Delta\varepsilon_L + \Delta\varepsilon_s}$$

If P_{cyc} is reduced to KP_{cyc} (where $K<1$) by means of a divergent magnetic field between circuit and collector, (4.240) becomes

(4.241)
$$\boxed{\eta_{opt} = \frac{1}{1 + \frac{K\omega_c}{\omega} + \left(\frac{\omega+\omega_c}{\omega}\right)\left(\frac{\omega R}{\omega_c}\right)\left(\frac{2b}{a_L}\right)}}$$

In (4.241) if $K = 1$, equation (4.239) is obtained. As $2b/a_L \to 0$ and $K \to 0$, $\eta_{opt} \to 100\%$.

The relation of the factor, K, in (4.241) to the flux densities at the circuit output and at the collector can be obtained as follows. Setting torque on an electron about the tube axis equal to the rate of of change of angular momentum,

$$|e|\dot{r}B_z - |e|\dot{z}B_r = \frac{d(mr^2\dot{\theta})}{dt} \tag{4.242}$$

If the radial velocity is small, $\dot{r} \simeq 0$, and if B_z changes slowly with z, $B_r \simeq 0$. Then (4.242) becomes

$$\frac{d(mr^2\dot{\theta})}{dt} \simeq 0$$

or,

$r^2\dot{\theta} \simeq$ constant. (angular momentum is approximately conserved)

Thus, since $\dot{\theta} \simeq \omega_c$, the cyclotron frequency, because $\dot{r}$ is small,

$$r_1^2\,\omega_{c1} = r_2^2\,\omega_{c2} \tag{4.243}$$

where subscripts 1 and 2 indicate z-positions 1 and 2.

Now from (4.161), the kinetic potential corresponding to the kinetic energy in the cyclotron motion of the electrons is

$$V_{cy} = \frac{P_{cyc}}{I_o} = \frac{\omega_c^2 r^2}{2\eta}$$

Thus,

$$\frac{V_{cy2}}{V_{cy1}} = \frac{(\omega_{c2}r_2)^2}{(\omega_{c1}r_1)^2} \tag{4.244}$$

From (4.243) and (4.244)

$$\frac{V_{cy2}}{V_{cy1}} = \frac{\omega_{c2}}{\omega_{c1}} = \frac{B_{z2}}{B_{z1}} \tag{4.245}$$

Thus,

$$\boxed{K = \frac{B_{z2}}{B_{z1}}} \tag{4.246}$$

where B_{z2} = magnetic flux density at the collector

B_{z1} = magnetic flux density at the end of the circuit.

Equation (4.246) gives the reduction factor K in (4.241) when a divergent magnetic field is used between the output end of the circuit and the entrance to the collector to convert cyclotron motion energy to longitudinal energy.

Equation (4.246) has been checked for K = 0.1 and for the initial values at the circuit output in the 10-watt tube that has been constructed. The electron trajectories in a divergent magnetic field were computed to determine the conversion of cyclotron motion energy to longitudinal energy. It was found that (4.246) is a good approximation for $L>50R_0$, when L = distance between circuit and collector, and R_0 = deflection radius of the beam at the circuit. A small amount of the θ-motion energy is converted to radial-motion energy (about 3%). 87% is converted to longitudinal energy, and 10% is left in the cyclotron motion when K = 0.1.

The trajectories were calculated by a numerical technique on a computer utilizing a typical divergent magnetic field generated at the end of a solenoid and the equations of motion for the r, θ, and z directions. The equation of motion in the θ-direction was Busch's theorem.

CHAPTER V

DESIGN CONSIDERATIONS FOR CYCLOTRON WAVE AMPLIFIERS

5.1 The Circuit

A twisted transmission line (bifilar helix) circuit has been chosen for the design of cyclotron wave amplifiers. This circuit is relatively easy to construct and can readily be phase tapered to maintain synchronism of the cyclotron wave with the circuit wave, as indicated in section (4.55). Figures 5-1a, b show the circuit and ω-β diagram. The twist of the circuit is right-hand, the pitch angle is ψ, the longitudinal pitch is p, the mean helix radius is a and the inner radius is a_i, and ρ is the radius of the wire. The n = +1 space harmonic component of the forward wave is used for interaction with the cyclotron wave. Balanced (+-) feed is used to excite the transverse mode.

5.1.1 Circuit Propagation Constant. It was shown in Chapter 3 that the propagation constant for this circuit is given by

$$\beta_{ckt} = \beta_o \pm n \frac{2\pi}{p} \tag{5.1}$$

$$\beta_o = \frac{\omega}{c \sin \psi} = \frac{\beta_f}{\sin \psi} \tag{5.2}$$

where c = velocity of light

β_f = free space propagation constant = ω/c

n = an integer

The group velocity is

(5.3) $$v_g = c\sin\psi$$

The group velocity is equivalent to the longitudinal velocity component of a wave traveling along the wire of the circuit at a velocity of light, as indicated by equation (3.123).

For n = + 1, equation (5.1) becomes

(5.4) $$\boxed{\beta_1 = \beta_0 + \beta_T}$$

where

(5.5) $\beta_T = 2\pi/p$ = the part of the propagation constant due to the twist of the circuit

$\beta_1 = \beta_{ckt}$ for the n = + 1 space harmonic component of the forward wave.

A developed (unraveled) turn of the helix is shown in Figure 5-1c. It can be seen that

(5.6) $$\cot\psi = \frac{2\pi a}{p}$$

(5.7) $$\cot\psi = \beta_T a$$

From (5.2) and (5.7), (5.4) becomes

(5.8) $$\boxed{\beta_1 = \frac{\beta f}{\sin\psi} + \frac{\cot\psi}{a}}$$

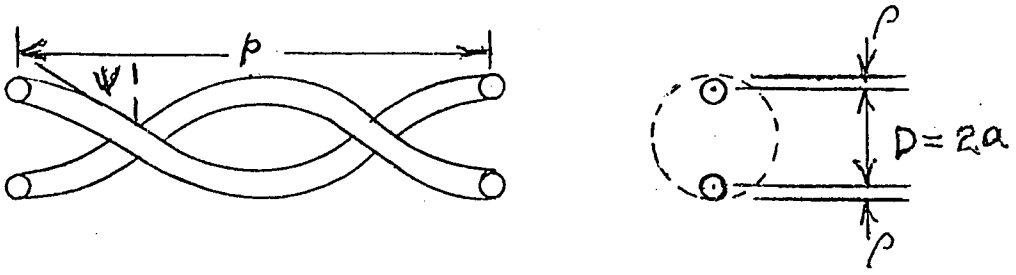

(a) Circuit Dimensions

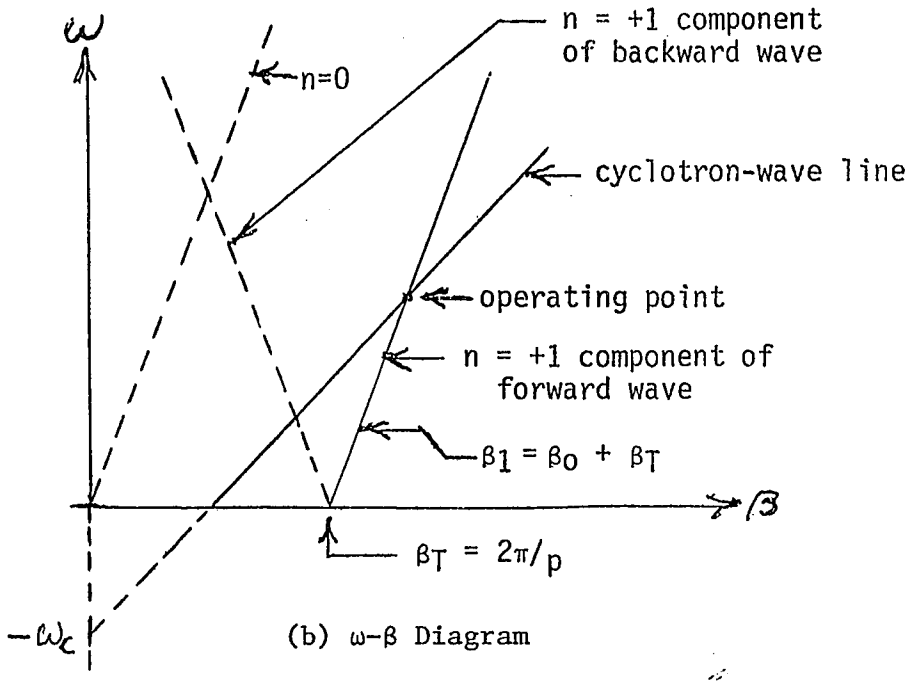

(b) ω-β Diagram

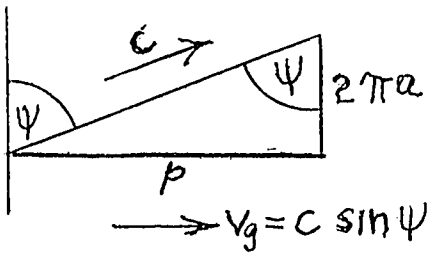

(c) Developed Helix Turn

Figure 5-1 Twisted Two-Wire Line and ω-β Diagrams

From Figure 5-1c, equation (5.8) can be put into the form

$$\beta_1 = \frac{\omega}{c}\frac{\sqrt{(2\pi a)^2 + p^2}}{p} + \frac{2\pi}{p} \tag{5.9}$$

For a given operating point (ω, β_1) for the circuit, equation (5.8) can be solved for the pitch angle, ψ. Thus,

$$\boxed{\psi = \sin^{-1}\left\{\frac{(\beta_1 a)\ (\beta_f a) + \sqrt{(\beta_1 a)^2 - (\beta_f a)^2 + 1}}{1 + (\beta_1 a)^2}\right\}} \tag{5.10}$$

Then,

$$\beta_T = \frac{\cot \psi}{a} \tag{5.11}$$

and the circuit pitch is

$$\boxed{p = \frac{2\pi}{\beta_T}} \tag{5.12}$$

5.1.2 Transverse Interaction Impedance of the Circuit. The transverse interaction impedance, K_T, may be estimated from the characteristic impedance of the two-wire line, assuming a gentle right-hand twist ($p/a \geq 1$). The characteristic impedance of the two-wire line is

$$z_0 = \sqrt{\mu_0/\epsilon_0}\ \frac{\ln\ (d/\rho)}{\pi} \tag{5.13}$$

where μ_0 = permeability of free space

ϵ_0 = dielectric constant of free space

d = mean distance between the two wires

ρ = wire radius

The approximate amplitude of the right-hand polarized electric field, $|E_{+1}(r=0)|$, of the n = +1 space harmonic of the forward mode of the twisted circuit can be obtained as follows. Consider a plane wave traveling along the untwisted circuit. The plane wave consists of the sum of equal amplitude RH and LH polarized waves. The transverse electric field at the midpoint between the wires is related to the "circuit" voltage by

$$E_T(0) = \frac{|V|}{d \ln(d/p)} \tag{5.14}$$

The transverse electric field of one of the circularly polarized components (with RH polarization) is

$$|E_{+1}(0)| = \frac{1}{2} E_T(0) = \frac{|V|}{2d \ln(d/p)} \tag{5.15}$$

For a slow RF twist, the LH polarized wave is suppressed and its power is distributed among the space harmonic components of the forward wave. Equation (5.15) gives the approximate amplitude of the RH polarized, n = +1 space harmonic of the forward wave.

The total power flow along the circuit may be expressed by

$$P_c = \frac{|V|^2}{2z_0} = \frac{2d^2 \ln^2(d/\rho)|E_{+1}(0)|^2}{z_0} \tag{5.16}$$

The transverse interaction impedance is, therefore, given by

$$K_T = \frac{|E_{+1}(0)|^2}{2\beta^2 P_c} = \{4\pi\beta^2 d^2 \ln\left(\frac{d}{p}\right)\sqrt{\varepsilon_0/\mu_0}\}^{-1} \tag{5.17}$$

(5.18)
$$K_T = \frac{377}{4\pi\beta^2 d^2 \ln(d/\rho)}$$

where $\sqrt{\mu_0/\varepsilon_0}$ = 377 ohms = free space impedance

It should be noted that (5.18) was derived with the implied assumption that $|E_{+1}(0)|$ was the amplitude of one of two equal circularly polarized modes, and that $|E_{+1}(0)|$ and the total power, P_C, remained constant when the circuit was twisted. Also, it was implied that the n = +1 component carried half the total power on the circuit.

A possibly more accurate analysis has been made by Tien[9] utilizing field theory rather than the transmission line analogue. His analysis of the infinitesimally thin tape helix circuit is given in Appendix A. Tien's results, which include all space harmonics, have been utilized to obtain the interaction impedance of the bifilar circuit of the one-watt tube that has been constructed. The interaction impedance was calculated utilizing a computer to obtain the power carried by all odd space harmonic components up to n = ±23. (See Appendix A.) For balanced (+-) feed, the even harmonics equal zero.

It was found that the interaction impedance with Tien's analysis was 1.109 ohms, while with the transmission line analysis, the impedance was 0.776 ohms. This result indicates that for the same total power flow, the effective value of $|E_{1+}(0)|$ with Tien's analysis is somewhat greater than that with the transmission line analysis. In Tien's

analysis, the n = +1 component carries 35.7% of the total power, and the n = -1 component carries 41.8%. The remainder of the power is carried by the other components. It is deduced that the characteristic impedance for the n = +1 component must increase when the wires are twisted, so that $|E_{1+}(0)|$ can increase although the power in the n = +1 component decreases from 50% to 35.7% of the total power.

The approximate value of K_T given by (5.18) has been used in the initial design of the cyclotron wave amplifiers because (5.18) provides a much simpler analytic relation than Tien's analysis, and gives a better insight into the relationship between various parameters and such characteristics as gain and power output.

Using equation (5.18), K_T can be maximized with respect to ρ, keeping the inner diameter of the bifilar helix circuit constant. The inner diameter determines clearance for the deflected beam.

The inner diameter of the circuit is

$$d_i = d-2\rho \tag{5.19}$$

In (5.18) let

$$F = d^2 \ln \frac{d}{\rho} = (d_i+2\rho)^2 \ln\left(\frac{d_i+2\rho}{\rho}\right) \tag{5.20}$$

If d_i and β are constant, then for maximum K_T,

$$\frac{dF}{d\rho} = .0 \tag{5.21}$$

Using (5.20) and (5.21), the condition for maximum K_T is

$$\frac{d}{\rho} = \frac{d_i+2\rho}{\rho} = 12 \tag{5.22}$$

From which

$$\frac{d_i}{\rho} = 10 \tag{5.23}$$

It should be noted from (5.18) that K_T does not vary rapidly with the d/ρ ratio.

5.1.3 Tapering of the Circuit Pitch. To maintain synchronism of the cyclotron and circuit waves, the pitch can be tapered as indicated in section (4.5.4). The incremental longitudinal distance, Δz, in section (4.5.4) is made equal to the pitch of the helix turn. The pitch is calculated turn by turn by utilizing equations (5.10), (5.11) and (5.12). For synchronism, the magnitude of β_1 in (5.10) is made equal to β_{cy} computed in section (4.5.4), depending on the slow down of the electrons as energy is extracted from the beam. In equations (5.10) and (5.18) where $d = 2a$, the mean radius, a, of the helix can be tapered as discussed in the next section (5.1.4).

5.1.4 Tapering of Circuit Mean Diameter. The interaction impedance, K_T, and therefore the growth constant, α, can be increased by making the mean circuit diameter as small as possible. The beam deflection is zero at the beginning of the circuit, and varies as $\sinh \alpha z$ up to a_L at the end of the circuit. To increase K_T, the diameter of the circuit can be tapered to increase from the beginning to the end of the circuit to provide clearance for the beam. The

simplest taper to construct is a linear one. If the filling factor, K_f, for the beam is 0.8, then

(5.24) $$a_{i1} = \frac{b}{0.8} = 1.25b$$

(5.25) $$a_{i2} = \frac{b+a_L}{0.8} = 1.25(b+a_L)$$

where b = beam radius

a_{i1} = initial inside radius of the helix

a_{i2} = final inside radius of the helix

a_L = final deflection of beam

The inside radius of the circuit as a function of z is then given by

(5.26) $$a_i = 1.25b + 1.25\, a_L \frac{z}{L}$$

where L = length of the circuit

The mean radius, a, of the circuit is given by

(5.27) $$a = a_i + \rho$$

where ρ = radius of the wire of the circuit

ρ is chosen to obtain optimum K_T at $z = L$, i.e., equation (5.23) is satisfied. Thus $\rho = 2a_{i2}/10$. Then the relation between the mean radius, a, and the inner radius, a_i, at $z = L$ is $a = 1.2a_i$.

With circuit diameter tapering, it should be possible to shorten the circuit length for a given total gain with a given beam voltage and

current. To determine how much shortening of the circuit length could be accomplished, a computer calculation for a 13 db gain was made for a tapered pitch circuit with a constant diameter, and then for a tapered pitch circuit with a tapered diameter, the final diameter being the same as the constant diameter for the first case.

The total gain calculation for both cases was accomplished as indicated in section (5.1.3), with $\Delta z = p$, where p is the variable pitch turn by turn, to maintain synchronism. The following were the parameters for the circuit with constant mean diameter.

$P_o = 0.5$ W	$d = 3.48X10^{-3}$ met
$P = 10$ W	$\rho = 0.381X10^{-3}$ met
$V_o = 1300$ V	$f = 3$ GHz
$I_o = 29.7$ ma	$fc = 2.8$ GHz

where P_o = input r.f. power

P = output r.f. power

V_o = d.c. injection voltage for the beam

I_o = d.c. beam current

d = mean diameter of circuit

ρ = radius of the circuit wire

f = operating frequency

f_c = cyclotron frequency

The parameters for the circuit with diameter taper were the same as for the circuit with constant mean diameter, except that the mean diameter of the circuit varied linearly with z given by

(5.28) $$d = 1.74X10^{-3} + 1.74X10^{-3}\,\frac{z}{L}\ \text{meters}$$

where L = length of the diameter-tapered circuit.

At $z = L$, the diameter of the tapered circuit equals the diameter of the untapered circuit.

In (5.28), to determine the value of L, an initial value is assumed and the z to obtain 13 db gain is determined by means of the computer program. The program is then re-run with L equal to this z, and a new z is computed. This procedure is re-iterated until $|z-L|<.001$. The final value of z gives the required L.

It was found that for 10 W output and 13 db gain, the length of circuit needed without diameter tapering was 22", while that needed with diameter tapering was 14.3". The 10-watt tube was designed with circuit diameter tapering since a considerable reduction in circuit length is accomplished.

5.1.5 Tolerance for Pitch of Circuit. The effect of accuracy of pitch of the helices on gain can be estimated from the relation between the reduced growth parameter, α', and the velocity parameter, b_V given by equations (4.119), (4.120), and (4.121)

which are

(5.29) $$\alpha' = \alpha\sqrt{1-K^2}$$

(5.30) $$K = \frac{b_V}{2\alpha/\beta_{cy}}$$

$$b_V = \frac{\beta_1 - \beta_{cy}}{\beta_{cy}} \tag{5.31}$$

Also, from equations (5.4) and (5.5)

$$\beta_1 = \beta_o + \beta_T \tag{5.32}$$

$$\beta_T = \frac{2\pi}{p} \tag{5.33}$$

where p = pitch

Let p_o = pitch for synchronism. From (5.31), for synchronism,

$$b_V = 0 = \frac{(\beta_o + \frac{2\pi}{p_o}) - \beta_{cy}}{\beta_{cy}} \tag{5.34}$$

Let p_o be in error by Δp, so that the pitch is now $p_o + \Delta p$. The velocity parameter then is

$$b_V = \frac{(\beta_o + \frac{2\pi}{p_o + \Delta p} - \beta_{cy}) - (\beta_o + \frac{2\pi}{p_o} - \beta_{cy})}{\beta_{cy}} \tag{5.35}$$

(The second bracketed term equals zero.)

$$b_V = \frac{\frac{-2\pi}{p_o}\frac{\Delta p}{p_o}}{\beta_{cy}}$$

$$\left|b_V\right| = \frac{\beta_T}{\beta_{cy}} \left|\frac{\Delta p}{p_o}\right| \tag{5.36}$$

At synchronism,

$$\beta_o << \beta_T$$

So that

$$\beta_T = \beta_1 - \beta_0 \approx \beta_1 \approx \beta_{cy}$$

Thus (5.36) becomes

(5.37) $\left|b_v\right| \approx \left|\frac{\Delta p}{p_0}\right|$ = fractional change in pitch from the value of the pitch for synchronism.

If the velocity of the electrons does not deviate greatly from the injection velocity, then at synchronism, for voltage gains >10 (then $e^{\alpha z} >> e^{-\alpha z}$), the total gain parameter for a circuit length, L, is

(5.38) $$G = \Sigma \alpha p_0 = \alpha \Sigma p_0 = \alpha L \text{ nepers}$$

If there is error in p_0, the total gain parameter is

(5.39) $$G' \approx \Sigma \alpha' p_0 = \alpha' L, \text{ if } \Delta p << p_0$$

Thus

(5.40) $$\frac{G}{G'} = \frac{\alpha}{\alpha'}$$

For the 10-watt tube,

Pitch, $p \approx 0.2"$

$\alpha \approx 4$ nepers/met

$\beta_T \approx \beta_{cy} \approx 1300$ rad/met

If the pitch is maintained to an accuracy of 0.5 mil, the maximum $b_v \simeq 5/2000 = .0025$, $2\alpha/\beta_{cy} \simeq 8/1300 \simeq .006$. Then maximum $K \simeq .0025/.006 \simeq 0.4$. Then

$$\alpha' = \alpha\sqrt{1-K^2} = \alpha\sqrt{1-.16} = .92\alpha$$

Thus in a tube which would have 13 db gain for perfect synchronism, the gain would be reduced to 0.92X13 = 12 db (a 1 db loss) if the pitch of every turn of the helices were inaccurate by 0.5 mil.

5.2 Focusing

The Brillouin d.c. magnetic focusing field, B_B, is the minimum field required to focus the beam. The Brillouin condition is given by equation (4.197) and is

(5.41) $$\omega_c 2 = 2\omega_p^2$$

Now,

(5.42) $$\omega_c = \eta B_B$$

(5.43) $$\omega_p^2 = \frac{\eta|\rho|}{\varepsilon_0}$$

where ω_c = cyclotron frequency corresponding to B_B

ρ = space charge density

ε_0 = dielectric constant of free space

= $8.854\text{X}10^{-12}$ Farad/met

Also,

$$\rho = \frac{J_o}{v_o} = \frac{I_o}{\pi b^2 v_o}$$

$$\rho = \frac{I_o}{\pi b^2 (2\eta V_o)^{\frac{1}{2}}} \tag{5.44}$$

where J_o = beam current density

v_o = electron velocity

I_o = beam current

b = beam radius

V_o = beam voltage

η = electron charge to mass ratio

= 1.759×10^{11} coulomb/kgm

Using (5.42), (5.43) and (5.44) in (5.41) results in

$$\boxed{B_B = \frac{8.32 \times 10^{-3} \ (I_o)^{\frac{1}{2}}}{V_o^{\frac{1}{4}} \ b}} \tag{5.45}$$

where I_o = beam current, amps

V_o = beam voltage, volts

b = beam radius, meters

B_B = Brillouin magnetic field, kilogauss

5.3 Minimum Voltage for Focusing

The minimum beam voltage required for a choice of particular design parameters can be obtained by means of the Brillouin focusing equation (5.45). It will be assumed that the velocity of the electrons does not deviate very much from the injection velocity, v_o.

For $B_O = 2B_\beta$, from equation (5.45),

$$b = \frac{16.64 \times 10^{-3} \; I_O^{\frac{1}{2}}}{V_O^{\frac{1}{4}} \; B_O} \tag{5.46}$$

where the units are the same as in (5.45).

Let,

$$K = \beta b \tag{5.47}$$

$$b = K/\beta \tag{5.48}$$

$$a_L = mb \tag{5.49}$$

where β = propagation constant

b = beam radius

a_L = final deflection radius of beam

For the slow cyclotron wave

$$\beta = \frac{\omega + \omega_C}{V_O} \tag{5.50}$$

$$\beta = \frac{\omega + \omega_C}{\sqrt{2\eta V_O}} \tag{5.51}$$

$$b = \frac{K}{\beta} = \frac{K\sqrt{2\eta V_O}}{\omega + \omega_C} \tag{5.52}$$

where ω = signal radian frequency

ω_C = cyclotron radian frequency

V_O = beam electron velocity

η = electron charge/mass ratio

V_O = beam voltage

Also,

(5.53) $$P_{ckt} = \eta_e I_o V_o$$

(5.54) $$I_o = \frac{P_{ckt}}{\eta_e V_o}$$

where P_{ckt} = r.f. power extracted from electron beam by the circuit

$P_{ckt} = P - P_o$

P = final r.f. power on circuit

P_o = initial r.f. power on circuit

η_e = electronic efficiency

Using (5.52) and (5.54) in (5.46) results in

(5.55) $$V_o^{5/4} = \frac{17.59X10^{9}X16.64X10^{-3}\ P_{ckt}^{\frac{1}{2}}\ (\omega+\omega_c)}{K\sqrt{2\eta}\ \ \omega_c\ \eta_e^{\frac{1}{2}}}$$

Now, the power extracted from the beam by the circuit and cyclotron motion of the electrons is given by

(5.56) $$P_{ckt+cyc} = \frac{1}{2}\ (\omega+\omega_c)\ I_o B_o a_L^{\,2}$$

$$a_L = mb = \frac{mK}{\beta} = \frac{mK\sqrt{2\eta V_o}}{\omega+\omega_c}$$

(5.57) $$a_L^{\,2} = \frac{m^2K^2\ (2\eta V_o)}{(\omega+\omega_c)^2}$$

Using (5.57) and $\eta B_o = \omega_c$ in (5.56),

$$P_{ckt+cyc} = \frac{m2K^2\omega_c}{\omega+\omega_c}\ I_o\ V_o$$

Hence,

(5.58) $$\boxed{\eta_{ec} = \frac{m^2K^2\omega_c}{\omega+\omega_c}}$$

Since,

$$\eta_e = \frac{P_{ckt}}{P_{Dc}} \quad ; \quad \eta_{ec} = \frac{P_{ckt+cyc}}{P_{Dc}}$$

Then,

(5.59) $$\boxed{\eta_e = \eta_{ec}\,\frac{\omega}{\omega+\omega_c}}$$

From which

(5.60) $$\boxed{\omega_c = \omega\left(\frac{\eta_{ec}}{\eta_e} - 1\right)}$$

Combining (5.58) and (5.59),

(5.61) $$\boxed{\eta_e = \eta_{ec}\left(1 - \frac{\eta_{ec}}{m^2K^2}\right)}$$

Using (5.59) and (5.61) in (5.55) results in

(5.62) $$\boxed{V_{o\ min} = \frac{142.88(m^2K)^{\frac{4}{5}}\,P_{ckt}^{\frac{2}{5}}}{(\eta_{ec})^{6/5}\,\left(1-\frac{\eta_{ec}}{m^2K^2}\right)^{2/5}}}$$

In (5.62),

$$K = \beta b$$

$$m = \frac{a_L}{b}$$

V_o min is the minimum V_o for focusing the beam if $B_o = 2B_B$.

5.4 The Collector

5.4.1 Effect of Space-Charge on Collector Depression. A simplified problem will be solved to determine qualitative effects. A parallel-plane diode (Figure 5-2) will be analyzed to determine the current limiting effects caused by space charge, and the relationship of spacing between collector and circuit and circuit-collector voltage to limited current. It will be assumed the beam is focused so that it does not spread.

An electron beam exits the circuit at a velocity v_o. The collector is depressed to collect the electrons at zero velocity.

Voltage differences rather than absolute voltages, determine the shape of the voltage, V_z, as a function of z. Hence, without loss of generality, the circuit voltage V_1, can be set to the kinetic voltage of the electrons exiting the circuit.

(5.63) $$V_1 = V_o$$

where $V_o = \frac{v_o^2}{2\eta}$

η = charge to mass ratio for an electron

The collector is set to $V_2 = 0$, since the electrons will be collected at velocity $v_z = 0$, so that the kinetic energy equals zero. In the potential drop of V_o from the circuit to collector, the electon gives up all its kinetic energy.

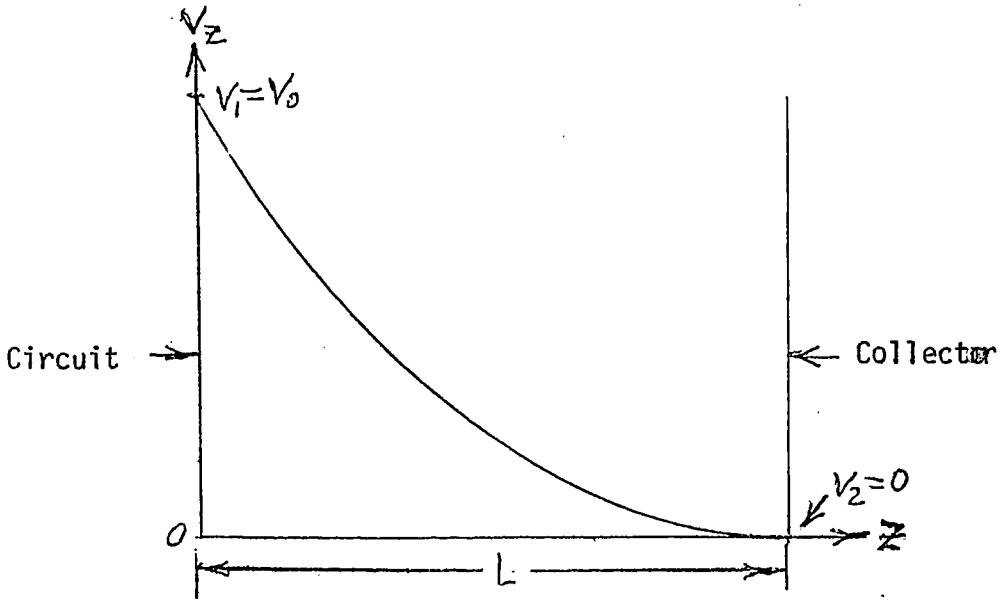

Figure 5-2 Voltage variation with distance for planar diode

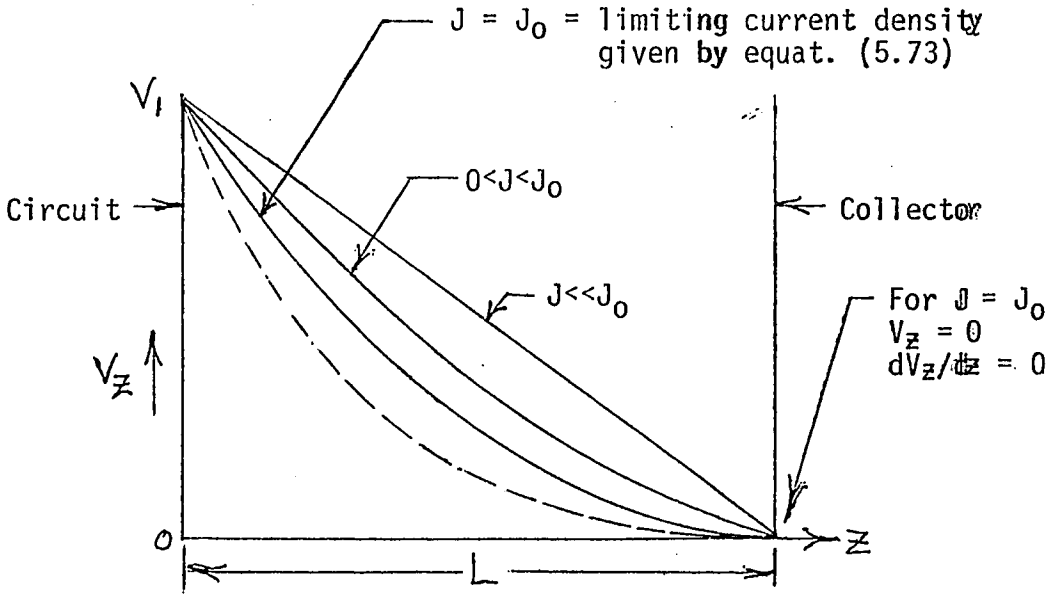

Figure 5-3 Voltage variation with distance for planar diode with various current densities

The following are the equations (similar to the equations used to obtain Child's Law).

$$\frac{d^2V_z}{dz^2} = \frac{-\rho}{\varepsilon_0} = \frac{-J_0/v_z}{\varepsilon_0} = \frac{|J_0|}{\varepsilon_0 v_z} \tag{5.64}$$

where ρ = charge density

ε_0 = dielectric constant of free space

v_z = velocity at point z

J_0 = current density (assumed constant because of continuity of current)

For electrons, $J_0<0$

Using $v_z = \sqrt{2\eta V_z}$ in (5.64) results in

$$\boxed{\frac{d^2V_z}{dz^2} = \frac{|J_0|}{\varepsilon_0\sqrt{2\eta V_z}}} \tag{5.65}$$

A first integration is achieved by multiplying (5.65) by $2\frac{dV_z}{dz}$ and integrating

$$(\frac{dV_z}{dz})^2 = \frac{4|J_0|}{\varepsilon_0}\ \frac{V_z^{\frac{1}{2}}}{\sqrt{2\eta}} + C_1 \tag{5.66}$$

Let the distance between circuit and collector be equal to L. The current density, $|J_0|$, can not be greater than the limiting current density because then a potential well with $V_z<0$ would exist somewhere for $0<z<L$ so that electrons would be reflected until the potential well would be eliminated. The current density would automatically adjust

to the limiting value, any excess current being reflected back toward the circuit.

When $z=L$, and when the limiting current density flows,

$$\frac{dV_z}{dz} = 0 \tag{5.67}$$

$$V_z = 0 \tag{5.68}$$

Substituting conditions (5.67) and (5.68) into (5.66) gives $C_1 = 0$ when $|J_o|$ is the limiting current density.

A second integration gives

$$\frac{4V_z^{3/4}}{3} = \left(\frac{4|J_o|}{\varepsilon_o\sqrt{2\eta}}\right)^{\frac{1}{2}} z + C_2 \tag{5.69}$$

At $z = L$, $V_z = 0$. Then

$$C_2 = -\left(\frac{4|I_c|}{\varepsilon_o\sqrt{2\eta}}\right)^{\frac{1}{2}} L \tag{5.70}$$

Substitute (5.70) into (5.69)

$$(z - L)^2 = \frac{4\varepsilon_o\sqrt{2\eta}V_z^{3/2}}{9|J_o|} \tag{5.71}$$

where $|J_o|$ is the limiting current density

Equation (5.71) gives V_z as a function of z. From equation (5.71), one can obtain an expression relating the circuit voltage, V_1, the limiting current density $|J_o|$, and the distance between circuit and

collector, L. (The collector voltage equals zero. Actually, V_1 equals the difference between circuit and collector voltages.)

In (5.71), when $z = 0$, $V_z = V_1$.

Thus,

$$|J_o| = \frac{4\varepsilon_o \sqrt{2\eta}\, V_1^{3/2}}{9L^2} \tag{5.72}$$

Numerically, (5.72) is equal to

$$\boxed{|J_o| = \frac{2.335\text{X}10^{-6}\, V_1^{3/2}}{L^2}} \text{ amps/unit area} \tag{5.73}$$

where J_o = limiting current density

V_1 = circuit-collector voltage

L = distance between circuit and collector

If L is in centimeters, the limiting current density is in amperes/square centimeter.

Any current density, J, less than the limiting current density, J_o, can be pushed through the diode without reflection of current. Thus,

$$J \leq \frac{2.335\text{X}10^{-6}\, V_1^{3/2}}{L^2} \tag{5.74}$$

or,

$$\boxed{L^2 \leq \frac{2.335\text{X}10^{-6}\, V_1^{3/2}}{J}} \tag{5.75}$$

Equation (5.75) gives the value of L to be able to push the current density, J, through the depressed collector diode.

The curves in Figure 5-3 show how V_z varies with z for ranges of current density, J, between zero and the limiting current density, J_0, given by (5.73).

The dotted curve in Figure 5-3 shows what happens if one attempts to make $J>J_0$. In this case, the excess current above J_0 is reflected. This causes additional space charge before the voltage minimum and causes the voltage to depress faster before the voltage minimum.

One can raise the collector voltage above zero so that more current density than the limiting current density given by equation (5.73) can flow. Then no current will be reflected. The curves in Figure 5-4 show the variation of V_z with z for this case.

In Figure 5-4, J_1 is the maximum current density that can be pushed through the diode without current reflection when the collector voltage is V_2. Raising V_2 above zero makes $V_z>0$ everywhere except at the minimum of V_z where $V_z = 0$. Thus J_1 can be greater than J_0 given by equation (5.73). If V_2 were lowered, there would be a tendency for V_z to drop below zero somewhere for $0<z<L$, thus causing electrons to be reflected until the minimum $V_z = 0$. In the above figure, any current density in excess of J_1 would be reflected until minimum $V_z = 0$. The dotted curve in Figure 5-4 shows what happens if one attempts to make $J>J_1$. The voltage depression effect is similar to that indicated by the dotted line in Figure 5-3.

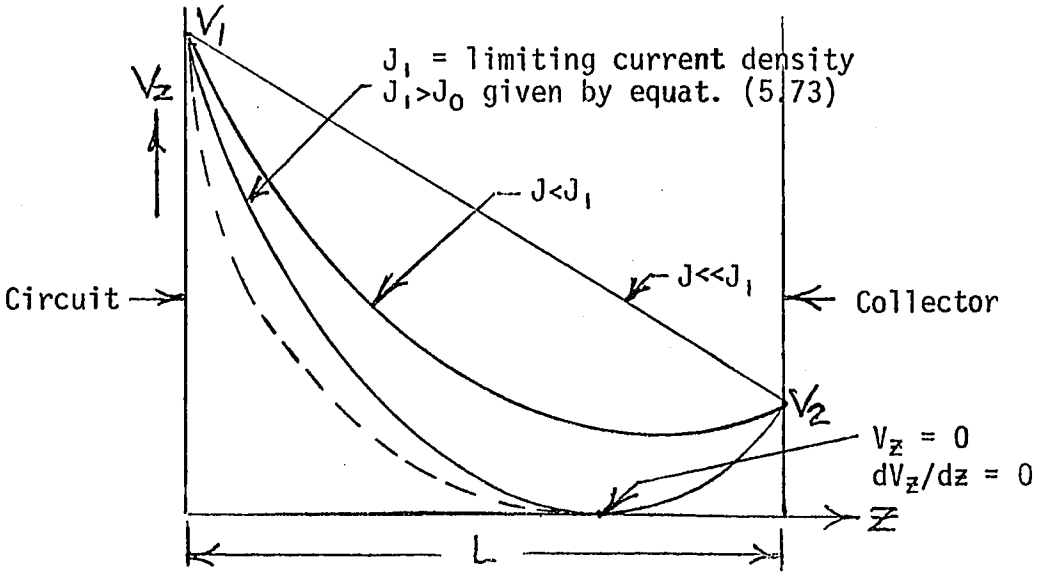

Figure 5-4 Voltage variation for planar diode with raised collector voltage

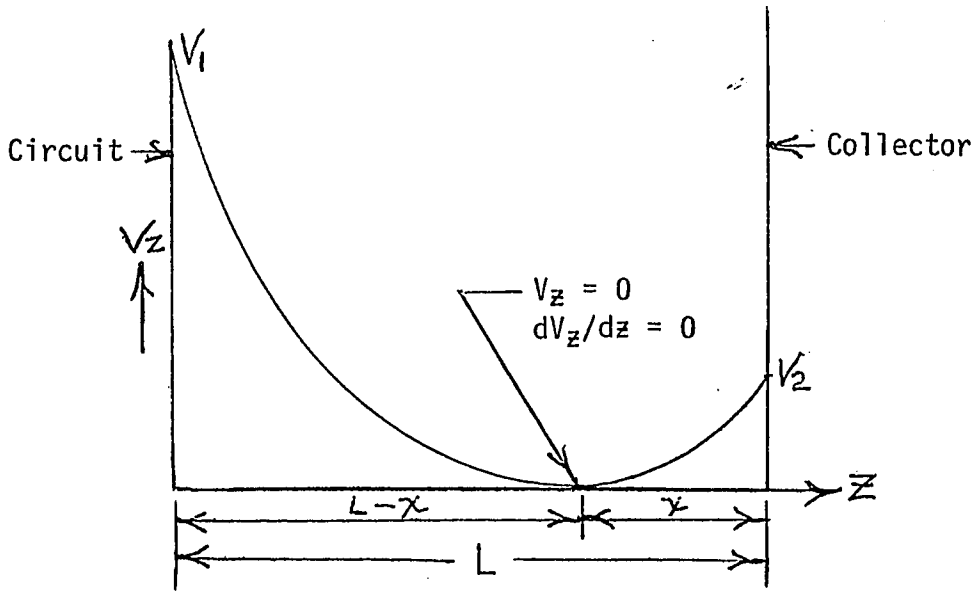

Figure 5-5 Diagram for analyzing effect of raised collector voltage

Thus, if one attempts to push more current through the diode than J_0 given in equation (5.73), the collector voltage can not be depressed to zero without causing some of the current to be reflected.

A relation between V_1, V_2, the distance between circuit and collector L, and the maximum current density J_1 can be obtained as follows.

In Figure 5-5, the limiting current density, J_1, flows. There is no reflected current. $V_z = 0$ and $dV_z/dz = 0$ at $z = L - x$.

For $0<z<L-x$, equation (5.73) holds with L replaced by L-x. Thus

$$J_1 = \frac{2.335X10^{-6}\ V_1^{\ 3/2}}{(L-x)^2} \tag{5.76}$$

For $L-x<z<L$, Child's law holds. Thus,

$$J_1 = \frac{2.335X10^{-6}\ V_2^{3/2}}{x^2} \tag{5.77}$$

Eliminating x between (5.76) and (5.77) results in

$$\boxed{J_1 = \frac{2.335X10^{-6}\ (V_1^{3/4} + V_2^{3/4})^2}{L^2}} \tag{5.78}$$

When $V_2 = 0$, equation (5.78) becomes equation (5.73).

5.4.2 Effect of Focusing on Collector Depression. An electron which enters the collector entrance region between circuit and collector at a velocity, $v_z = v_0$, should reach a potential line, V = 0, at the collector boundary if it is properly focused. If the electron ever

reaches a potential line V>0 tangentially, it will go no further but turn around because of the retarding fields. Its kinetic energy was not completely used to reach the V = 0 potential. This is analogous to rolling a ball up a hill. If the hill is 10 feet high and the ball initially is given a kinetic energy corresponding to the 10 foot height, it will reach the top of the hill only if it is rolled straight up the hill. If it is rolled at an angle, the ball will not reach the top even though it had sufficient energy to reach the top if rolled straight up.

Thus, to obtain optimum depressed collector operation, the beam trajectory must be focused into the collector so that all of the energy of each electron is expended in moving through the retarding field of the collector.

CHAPTER VI

DESIGN OF EXPERIMENTAL TUBES

6.1 It was decided to design a 2-kilowatt output, 5 GHz amplifier. Then, instead of constructing the 2 kW tube, a one-watt and 10-watt tube at 3 GHz were constructed. The latter tubes were scaled from the 2 kW design to verify the theory. The lower power tubes at the lower frequency simplify the experiments. A bifilar helix circuit is used. Some parameters are chosen and the rest calculated from the equations in Chapter V. To obtain a starting point for the designs of the one-watt and 10-watt tubes, in the design of the 2 kW tube, it is assumed that the beam velocity, v_z, does not deviate very much from the injection velocity, v_o.

6.2 Design of Two-Kilowatt Tube

Choose

P_{ckt} = 2 kW

P_{ckt} = P(L) -P(0)

= power extracted by the circuit from the beam

where

P(L) = r.f. power at end of circuit

P(0) = r.f. input power to circuit

f = 5 GHz

$\omega = 2\pi x5x10^9 = 31.41x10^9$ rad/sec

η_{ec} = 0.2 = electronic cyclotron efficiency

$= (P_{ckt} + P_{cyc}) / P_b$

where P_{cyc} = power in cyclotron motion of electrons at end of circuit

P_b = power in beam at entrance to circuit

$K = \beta_1 b = 1$

(Too large a value for K results in a large value for $\beta_1 d$ (d = mean diameter of circuit) and then results in a small interaction impedance as can be seen from equation (5.18))

$m = a_L/b = 0.7$

Inner circuit radius, a_i,

$= (a_L + b)/0.8 = 2.125b$

Mean circuit radius, a,

$= 1.2a_i = 2.55b$

Then calculate

V_o min (Equation 5.62)

$$V_o \text{ min} = \frac{142.88(m^2K)^{4/5} P_{ckt}}{(\eta_{ec})^{6/5} \left(1 - \frac{\eta_{ec}}{m^2K^2}\right)^{2/5}}$$

V_o min = 14369 volts

(Chosen parameters were used which resulted in this reasonable value for V_o min)

Electronic Efficiency, η_e (Equation 5.61)

$$\eta_e = \eta_{ec}\left(1 - \frac{\eta_{ec}}{m^2K^2}\right)$$

$\eta_e = 0.1184$

Cyclotron frequency, ω_c, and magnetic focusing, B_0 (Equat. 5.60)

$$\omega_c = \omega\left(\frac{\eta ec}{\eta e} - 1\right) = \omega(.690)$$

$$= 21.68 \times 10^9$$

$$f_c = \omega_c / 2\pi = f(.690)$$

$$= 3450 \text{ MHz}$$

$B_0 = fc(MHz)/2.8 = 1233$ Gauss (This B_0 is twice Brillouin)

$$\omega_c/\omega = fc/f = .690$$

Beam Current, I_0 (Equat. 5.54)

$$I_0 = \frac{P_{ckt}}{\eta e V_0} = 1.176 \text{ amps}$$

Propagation Constant, $\beta_1 = \beta_{cy}$ (Equat. 5.50)

$$\beta 1 = \frac{\omega + \omega_c}{v_0}$$

$$v_0 = \sqrt{2\eta V_0} = 5.93 \times 10^5 \sqrt{14369}$$

$$= 7.108 \times 10^7 \text{ met/sec}$$

$$\beta_1 = \frac{31.41 + 21.68}{7.108 \times 107} = 746.9 \text{ rad/met}$$

Beam Radius, b (Equat. 5.48)

$$\beta b = 1$$

$$b = 1/746.9 = 1.339 \text{ mm}$$

Beam Current Density, J_o

$$J_o = \frac{I_o}{\pi b^2} = \frac{1.176}{\pi(.1339)} = 20.9 A/cm^2$$

Area Compression of Beam, Comp

If the cathode loading is limited to $4A/cm^2$, the area compression for the beam is

$$Comp = \frac{20.9}{4A/cm^2} = 5.23$$

Final Deflection of Beam, a_L (Equat. 5.49)

$$a_L = .7b = .7(1.339) = .937 \text{ mm}$$

Mean Radius of Circuit, a

For assumed filling factor, $K_F = 0.8$,

$$a = 2.55b = 3.41 \text{ mm}$$

$$= .134"$$

Inner Circuit Radius, a_i

$$a_i = 2.125b = 2.84 \text{ mm}$$

$$= .112"$$

Pitch Angle of Helix, ψ (Equat 5.10)

$$\psi = \sin^{-1}\left\{\frac{(\beta_1 a)\ (\beta_f a) + \sqrt{(\beta_1 a)^2 - (\beta_f a)^2 + 1}}{1 + (\beta_1 a)^2}\right\}$$

$$\beta_1 = 746.9 \text{ rad/met}$$

$$\beta_f = \frac{\omega}{c} = \frac{5x10^9 x 2\pi}{3x10^8} = 104.72 \text{ rad/met}$$

$a = 3.41 \times 10^{-3}$ met

$\sin \psi = .48381$

$\psi = 28.93^{o}$

$\cot \psi = 1.80892$

Twist Propagation Constant, β_T (Equat. 5.11)

$$\beta_T = \frac{\cot \psi}{a} = 530.47 \text{ rad/met}$$

Pitch of Helix, p (Equat. 5.12)

$$p = \frac{2\pi}{\beta_T} = 11.84 \text{ mm} = .466" \text{ (for uniform pitch circuit)}$$

Group Propagation Constant, β_o (Equat. 5.2)

$$\beta_o = \frac{\beta_f}{\sin \psi} = \frac{104.72}{.48381} = 216.45 \text{ rad/met}$$

Check: $\beta_1 = \beta_o + \beta_T = 216.45 + 530.47 = 746.9$ rad/met

Interaction Impedance, K_T (Equat. 5.18)

$$K_T = \frac{377}{4\pi\beta_1^2 d^2 \ln(d/\rho_w)}$$

For maximum K_T,

$$d/\rho_w = 2a/\rho_w = 12$$

$K_T = .465$ ohms

Radius of helix wire, ρ_w (Equat. 5.22)

$$\rho_w = \frac{2a}{12} = .568 \text{ mm} = .0224"$$

Growth Constant, α (Equat. 4.78)

$$\alpha = \beta_1 \left(\frac{1}{2} \frac{\omega}{\omega_c} \frac{I_o}{V_o} K_T\right)^{\frac{1}{2}}$$

$$= 3.922 \text{ nep/met}$$

$$= 3.922 \times 8.69 = 34.1 \text{ dB/met}$$

Circuit length, L, for gain of 10 dB

$$\text{Voltage gain} = \frac{e^{\alpha L} + e^{-\alpha L}}{2} \approx \frac{e^{\alpha L}}{2}$$

$$\text{Gain in dB} = 10 \text{ db} = \alpha_{dB} L - 6 \text{ dB}$$

$$L = \frac{16 \text{ dB}}{\alpha_{dB}} = \frac{16}{34.1} = .47 \text{ met} = 18.5"$$

(Without circuit taper)

Depressed Collector Efficiency, η_{opt} (Equat. 4.241)

$$\eta_{opt} = \frac{1}{1 + K_\eta \frac{\omega_c}{\omega} + \left(\frac{\omega+\omega_c}{\omega}\right)\left(\frac{\omega_R}{\omega_c}\right)\left(\frac{2b}{a_L}\right)}$$

where

$$\omega_R = \frac{\omega_p^2}{2\omega_c} \quad \text{(From Chapter IV)}$$

For $B_o = 2B_B$, $\omega_c = 2\sqrt{2}\,\omega_p$

Thus,

$$\frac{\omega_R}{\omega_c} = \frac{1}{16}$$

K_η = reduction factor caused by the divergent magnetic field between circuit and collector

$= B$ at collector/B at circuit

$$\eta_{opt}\, K_n = 1/(1.3018 + .69\, K_n)$$

Values of η_{opt} for various values of K_n are given in Table 6-1 in the next paragraph.

Depressed Collector Voltage, V_{cn}

$V_{cn}I_o$ = total power supplied (assuming no beam interception on the circuit)

$$\eta_{optKn} = \frac{P_{ckt}}{\text{Total Power Supplied}}$$

where P_{ckt} = power extracted by the circuit from the beam

$$\eta_{optKn} = \frac{\eta_e V_o I_o}{V_{cn} I_o} = \frac{\eta_e V_o}{V_{cn}}$$

Thus,

$$V_{cn} = \frac{\eta_e V_o}{\eta_{optKn}}$$

Values of V_{cn} for various values of K_n are given in Table 6-1 below.

Table 6-1

K_n	η_{optKn}	V_{cn} Volts
1	.502	3389.0
.5	.607	2802.8
.1	.729	2342.9
0	.768	2215.2

To obtain the values in Table 6-1.

$$\frac{\omega_c}{\omega} = .690 \qquad \frac{2b}{a_L} = \frac{2b}{.7b} = 2.857$$

$$\frac{\omega+\omega_c}{\omega} + 1.69$$

$$\frac{\omega R}{\omega_c} = \frac{1}{16}$$

$$\eta_{opt} = \frac{1}{1.3018 + .69K_\eta}$$

$$\eta_e V_o = (.1184)\ (14369) - 1701.3 \text{ volts}$$

6.3 Design of 10-Watt Tube

The design of the 10-watt, 13 dB gain tube is scaled from the 2 kW design by utilizing the same K, m, and η_{ec}. Tapering of the circuit pitch is used to maintain synchronism as discussed in section (5.1.3). Tapering of the circuit diameter is used to increase interaction impedance, K_T, and thus decrease the length of the circuit for a given gain, as discussed in section (5.1.4).

Choose

$P_{ckt} = P(L)-P(0)$

$= 10$ watts

$f = 3$ GHz

$\omega = 2\pi f = 2\pi x 3x10^9$

$= 18.85x10^9$ rad/sec

$\eta_{ec} = 0.2$

$K = \beta_1 b = 1$

$m = a_L/b = 0.7$

Inner circuit radius, a_i,

$= \frac{a_L + b}{0.8} = 2.125b$

Mean circuit radius, a,

$= 1.2a_i = 2.55b$

Then calculate

V_o min (Equat. 5.62)

V_o min = 1725.88 volts

Electronic Efficiency, η_e (Equat. 5.61)

η_e = .1184 (Sames as for 2 kW tube)

Cyclotron Frequency, ω_c, and Magnetic Focusing Field, B_o (Equat. 5.60)

$$\omega_c = \omega\left(\frac{\eta ec}{\eta_e} - 1\right) = \omega(.690) = 13.01 \times 10^9 \text{ rad/sec}$$

$$f_c = f(.690) = 2.07 \times 10^3 \text{ MHz}$$

$$B_o = \frac{f_c(\text{MHz})}{2.8} = \frac{2070}{2.8} = 739.3 \text{ Gauss}$$

$$\frac{\omega_c}{\omega} = \frac{f_c}{f} = .690$$

Beam Current, I_o (Equat. 5.54)

$$I_o = \frac{P_{ckt}}{\eta_e V_o} = 48.94 \text{ ma}$$

Initial Value of Propagation Constant, $\beta_1 = \beta_{cy}$ (Equat. 5.50)

$$\beta_1 = \frac{\omega + \omega_c}{v_o}$$

$$v_o = \sqrt{2\eta V_o} = 5.93 \times 10^5 \sqrt{1725.88}$$

$$= 2.4635 \times 10^7 \text{ met/sec}$$

$$\beta_1 = \frac{31.86 \times 10^9}{2.4635 \times 10^7} = 1293.28 \text{ rad/met}$$

Beam Radius, b (Equat. 5.48)

$$\beta_1 b = 1$$

$$b = 1/1293.28 = .7725 \text{ mm} - .0304"$$

Beam Current Density, J_o

$$J_o = \frac{I_o}{\pi b^2} = \frac{.04894}{\pi(.0773)^2} = 2.61 A/cm^2$$

Final Deflection of Beam, a_L (Equat. 5.49)

$$a_L = .7b - .7(.7725) = .5411 \text{ mm} = .0213"$$

Final Inner Radius of Circuit, a_{if}

For assumed filling factor, $K_F = 0.8$,

$$a_{if} = 2.125b = (2.125)\ (.773)$$

$$= 1.6426 \text{ mm} = .0647"$$

$$d_{if} = 2a_{if} = 3.285 \text{ mm} = .1293"$$

Final Mean Radius of Circuit, a_f

$$a_f = 2.55b = (2.55)\ (.773) - 1.971 \text{ mm} = .0776"$$

$$d_f = 2a_f = 3.942 \text{ mm} = .1552"$$

Radius of Helix Wire, ρ_w (Equat. 5.22)

$$\rho_w = \frac{d_{if}}{10} = \frac{d_f}{12} = \frac{3.285}{10} = .3285 \text{ mm} = .01293"$$

$$d_w = 2\rho_w = .657 \text{ mm} = .0259"$$

Initial Inner Diameter of Circuit, d_{i1}

$$d_{i1} = \frac{2b}{0.8} = \frac{2x.7725}{.8} = 1.9313 \text{ mm} = .0760"$$

Initial Mean Diameter of Circuit, d_1

$$d_1 = d_{i1} + d_w = (1.9313 + .657) = 2.5883 \text{ mm} = .1019"$$

Equation for Mean Diameter of Linearly Tapered Circuit

(6.1) $$d = (2.5883 + 1.3537 \frac{z}{L}) \times 10^{-3} \text{ met}$$

z and L = met

When $z = 0$, $d = d_1$

When $z = L$, $d = d_f$

L is determined by the reiterative procedure described in section (5.1.3).

Effective Beam Voltage, V_{eff} (Equat. 4.185)

$$V_{eff} = V_o - V_{red}$$

(6.2) $$V_{red} = (\frac{\omega+\omega_c}{\omega}) \frac{P(0)}{I_o} \{\frac{e^{\Sigma\alpha\Delta z} - e^{-\Sigma\alpha\Delta z}}{2}\}^2$$

Here $P(0)$ = r.f. input power

Δz = pitch of a turn (which is a function of z)

Propagation Constant, β

$$\beta = \frac{\omega+\omega_c}{\sqrt{2\eta V_{eff}}} \qquad \sqrt{2\eta} = 5.93\times10^5$$

Interaction Impedance, K_T as a Function of z (Equat. 5.18)

$$K_T = \frac{377}{4\pi\beta^2 d^2 \ln(d/\rho_W)}$$

Here, d is given by equation (6.1), ρ_W is constant

Growth Parameter, α, as Function of z (Equat. 4.170)

(6.3) $$\alpha = \beta\left(\frac{1}{2}\frac{\omega}{\omega_c}\frac{I_o}{V_{eff}} K_T\right)^{\frac{1}{2}}$$

(6.4) $$\alpha = \frac{B}{d\left(V_{eff} \ln(d/\rho_W)\right)^{\frac{1}{2}}}$$

where

$$B = \left(\frac{377}{8\pi}\frac{\omega}{\omega_c} I_o\right)^{\frac{1}{2}} = \text{a constant}$$

Power on the Circuit, P

$$P = \frac{P(0)}{4}\left(e^{\Sigma\alpha\Delta z} + e^{-\Sigma\alpha\Delta z}\right)^2$$

Pitch Angle, ψ (Equat. 5.10)

$$\psi = \sin^{-1}\left\{\frac{(\beta a)\ (\beta_f a) + \sqrt{(\beta a)^2 - (\beta_f a)^2 + 1}}{1 + (\beta a)^2}\right\}$$

$$\beta_f = \omega/c$$

$$c = 3\times10^8 \text{ met/sec}$$

Twist Propagation Constant, β_T

$$\beta_T = \frac{\cot \psi}{a}$$

Pitch, p

$$p = \frac{2\pi}{\beta_T}$$

The pitch and diameter of the helix circuit are tapered turn by turn to maintain synchronism between the circuit and cyclotron waves as described in section (5.1.3). The method of computer calculation for the first three turns is given below.

Start (n = 0)

P_o = 0.5 W (Input r.f. power)

V_o = 1725.88 = V_{eff1}

p_o = 0 (pitch)

z = 0

L = 0.45 met (first estimate for length of circuit)

$$B = \left(\frac{377}{8\pi} \frac{\omega}{\omega_c} I_o\right)^{\frac{1}{2}}$$

$$\beta_f = \frac{\omega}{c} = \frac{3\times10^9 \times 2}{3\times10^8} = 62.83 \text{ rad/met}$$

(Free space propagation constant)

First Turn (n = 1)

z = 0

$$d_1 = (2.5883+1.3537\ z/L)\times10^{-3}\ \text{met}$$

(Diameter of first turn)

$$\alpha_1 = \frac{B}{d_1 V_{eff1} \ln(d_1/\rho_w)}$$ (At beginning of first turn)

$$\beta_1 = \frac{\omega+\omega_c}{\sqrt{2\eta}} \times \frac{1}{\sqrt{V_{eff1} - V_o}}$$

(Propagation constant for first turn)

Pitch Angle ψ_1

ψ_1 is computed from equat. (5.10) with $\beta = \beta_1$

$$a = a_1 = d_1/2$$

$$\beta_{T1} = \frac{\cot \psi_1}{a_1}$$ (Twist propagation constant for first turn)

$$p_1 = \frac{2\pi}{\beta_{T1}}$$ (pitch for first turn)

$$\gamma_1 = \Sigma\alpha p = \alpha_1 p_1$$ (cumulative)

$$P_1 = \frac{P_o}{4} (e^{\gamma 1} + e^{-\gamma 1})^2$$ (power at end of first turn)

$$n = 1$$

$$z_1 = \Sigma p = 0+p_1$$

$$\text{Gain, } G = 10 \log_{10} \frac{P_1}{P_o}\ \text{dB}$$

Second Turn (n = 2)

$$V_{red2} = \left(\frac{\omega+\omega_c}{\omega}\right) \frac{P_o}{I_o} \left(\frac{e^{\gamma_1} - e^{-\gamma_1}}{2}\right)^2$$

$V_{eff2} = V_o - V_{red2}$ (V_{eff} at beginning of second turn)

$$d_2 = (2.5883 + 1.3537\ \text{ƶ}_1/L) \times 10^{-3}$$

(Diameter of second turn)

$$\alpha_2 = \frac{2}{d_2\ V_{eff2}\ \ln\ (d_2/\rho\omega)}$$

(At beginning of second turn)

$$\beta_2 = \frac{\omega+\omega_c}{\sqrt{2\eta}} \quad \frac{1}{\sqrt{V_{eff2}}}$$ (Propagation constant for second turn)

Pitch angle, ψ_2

ψ_2 is computed from equat. (5.10) with $\beta = \beta_2$

$$a = a_2 = d_2/2$$

$$\beta_{T2} = \frac{\cot \psi_2}{a_2}$$ (Twist propagation constant for second turn)

$$p_2 = \frac{2\pi}{\beta_{T2}}$$ (Pitch for second turn)

$$\gamma_2 = \Sigma\alpha p = \alpha_1 p_1 + \alpha_2 p_2$$ (cumulative)

$$P_2 = \frac{P_o}{4} \left(e^{\gamma_2} + e^{-\gamma_2}\right)^2$$ (Power at end of second turn)

$n = 2$

$$\text{ƶ}_2 = \Sigma p = p_1 + p_2$$

$$\text{Gain, } G = 10 \log_{10} \frac{P_2}{P_o} \text{ dB}$$

Third Turn (n = 3)

$$V_{red3} = \left(\frac{\omega+\omega_c}{\omega}\right) \frac{P_o}{I_o} \left(\frac{e^{\gamma 2} - e^{-\gamma 2}}{2}\right)^2$$

$V_{eff3} = V_o - V_{red3}$ (V_{eff} at beginning of third turn)

$$d_3 = (2.5883 + 1.3537\, z_2/L) \times 10^{-3}$$

(Diameter of third turn)

$$\alpha_3 = \frac{B}{d_3\, V_{eff3}\, \ln (d_3/\rho_w)}$$

(At beginning of third turn)

$$\beta_3 = \frac{\omega+\omega_c}{\sqrt{2\eta}} \frac{1}{\sqrt{V_{eff3}}}$$ (Propagation constant for third turn)

Pitch angle, ψ_3

ψ_3 is computed from equat. (5.10) with $\beta = \beta_3$

$$a = a_3 = d_3/2$$

$$\beta_{T3} = \frac{\cot\psi_3}{a_3}$$ (Twist propagation constant for third turn)

$p_3 = 2\pi/\beta_{T3}$ (Pitch for third turn)

$\gamma_3 = \Sigma\alpha p = \alpha_1 p_1 + \alpha_2 p_2 + \alpha_3 p_3$ (cumulative)

$$P_3 = \frac{P_o}{4} \left(e^{\gamma 3} + e^{-\gamma 3}\right)^2$$ (Power at end of third turn)

$n = 3$

$z_3 = \Sigma p = p_1 + p_2 + p_3$

$$\text{Gain, } G = 10 \log_{10} \frac{P_3}{P_o} \text{ dB}$$

The above is reiterated for the complete helix turn by turn, and then is again reiterated for the complete helix using the new helix length, L, until $|L - z| < 0.001$ meters when $P_n \geq 10W$. The last z determines L, which originally was only estimated.

Table 6-2 tabulates the results of this computer program. The columns labeled "N" (the number of the turn) and "pitch" were used for winding the helices of the 10-watt tube. The mean diameter of each helix tapers linearly with distance, z, from 0.1019" at the cathode to 0.1552" at the collector in the total length of 16.422".

Check of Power Extracted, P_e, by the Circuit from the Beam in the 10-watt Tube

$$P_e = \frac{1}{2} I_o B_o \omega a_L^2, \text{ where } B_o \text{ is in webers/met}^2$$

$$= \frac{1}{2} (.04894) (.07393) (18.85 \times 10^9) (.5411 \times 10^{-3})^2$$

$$= 9.98 \text{ watts}$$

Depressed Collector Efficiency, η_{opt} (Equat. 4.241)

The values for η_{opt} are the same as for the 2 kW tube in Table 6-1 because the same constants are used in equat. (4.241). Values of η_{opt} for various values of K_n are given in Table 6-3 in the next paragraph.

Table 6-2

Longitudinal Pitch Taper for Each Helix of Bifilar Helix Circuit of the 10-Watt Tube

Preliminary Reiteration to Determine Length, L, of Circuit

L	Z	L-Z
0.4200	0.41702	0.00290
0.41702	0.41712	-0.00010

Thus L= 0.41712 meters

N	Z inches	Pitch inches	α nep/ met	V_{eff} Volts	P Watts	Gain dB	β_T rad/ met	β rad/ met
0	0.000				0.500			
1	0.210	0.2099	6.68	1726	0.501	0.0	1178	1293
2	0.419	0.2095	6.64	1719	0.503	0.0	1180	1296
3	0.629	0.2096	6.58	1719	0.506	0.0	1180	1296
4	0.839	0.2097	6.53	1719	0.510	0.1	1180	1296
5	1.049	0.2098	6.48	1718	0.516	0.1	1179	1296
6	1.258	0.2099	6.42	1718	0.522	0.2	1179	1296
7	1.468	0.2100	6.37	1718	0.530	0.3	1178	1296
8	1.678	0.2100	6.32	1718	0.539	0.3	1178	1296
9	1.889	0.2101	6.27	1717	0.550	0.4	1177	1296
10	2.099	0.2102	6.23	1717	0.562	0.5	1177	1296
11	2.309	0.2102	6.18	1717	0.574	0.6	1177	1297
12	2.519	0.2103	6.13	1716	0.589	0.7	1176	1297
13	2.730	0.2104	6.09	1716	0.604	0.8	1176	1297
14	2.940	0.2104	6.04	1715	0.621	0.9	1176	1297
15	3.150	0.2105	6.00	1715	0.640	1.1	1175	1297
16	3.361	0.2105	5.95	1714	0.659	1.2	1175	1298
17	3.572	0.2106	5.91	1713	0.681	1.3	1175	1298
18	3.782	0.2106	5.87	1713	0.704	1.5	1175	1298
19	3.993	0.2106	5.82	1712	0.728	1.6	1174	1298
20	4.203	0.2107	5.78	1711	0.754	1.8	1174	1299
21	4.414	0.2107	5.74	1710	0.782	1.9	1174	1299
22	4.625	0.2108	5.70	1709	0.812	2.1	1174	1299
23	4.836	0.2108	5.66	1708	0.843	2.3	1174	1300
24	5.047	0.2108	5.63	1707	0.877	2.4	1173	1300
25	5.257	0.2108	5.59	1706	0.913	2.6	1173	1301
26	5.468	0.2108	5.55	1705	0.950	2.8	1173	1301
27	5.679	0.2108	5.51	1703	0.990	3.0	1173	1302
28	5.890	0.2109	5.48	1702	1.032	3.1	1173	1302

Table 6-2 (cont.)

N	Z inches	Pitch inches	α nep/ met	V_{eff} Volts	P Watts	Gain dB	β_T rad/ met	β rad/ met
29	6.101	0.2109	5.44	1700	1.077	3.3	1173	1303
30	6.312	0.2109	5.41	1699	1.124	3.5	1173	1303
31	6.522	0.2108	5.37	1697	1.174	3.7	1173	1304
32	6.733	0.2108	5.34	1696	1.226	3.9	1173	1305
33	6.944	0.2108	5.31	1694	1.281	4.1	1173	1305
34	7.155	0.2108	5.27	1692	1.339	4.3	1174	1306
35	7.366	0.2107	5.24	1690	1.400	4.5	1174	1307
36	7.576	0.2107	5.21	1688	1.465	4.7	1174	1308
37	7.787	0.2106	5.18	1686	1.533	4.9	1174	1308
38	7.998	0.2106	5.15	1683	1.604	5.1	1175	1309
39	8.208	0.2105	5.12	1681	1.679	5.3	1175	1310
40	8.418	0.2105	5.09	1678	1.758	5.5	1175	1311
41	8.629	0.2104	5.06	1675	1.840	5.7	1176	1312
42	8.839	0.2103	5.03	1673	1.927	5.9	1176	1314
43	9.049	0.2102	5.00	1670	2.018	6.1	1177	1315
44	9.259	0.2101	4.98	1666	2.113	6.3	1178	1316
45	9.469	0.2100	4.95	1663	2.214	6.5	1178	1317
46	9.679	0.2098	4.93	1660	2.319	6.7	1179	1319
47	9.889	0.2097	4.90	1656	2.429	6.9	1180	1320
48	10.098	0.2095	4.88	1652	2.544	7.1	1181	1322
49	10.308	0.2094	4.85	1648	2.665	7.3	1182	1323
50	10.517	0.2092	4.83	1644	2.791	7.5	1183	1325
51	10.726	0.2090	4.81	1640	2.924	7.7	1184	1327
52	10.935	0.2088	4.78	1635	3.062	7.9	1185	1328
53	11.143	0.2086	4.76	1630	3.207	8.1	1186	1330
54	11.352	0.2083	4.74	1625	3.359	8.3	1187	1332
55	11.560	0.2081	4.72	1620	3.517	8.5	1189	1335
56	11.768	0.2078	4.70	1615	3.683	8.7	1190	1337
57	11.975	0.2075	4.68	1609	3.856	8.9	1192	1339
58	12.182	0.2072	4.66	1603	4.037	9.1	1194	1342
59	12.389	0.2069	4.65	1597	4.226	9.3	1196	1344
60	12.596	0.2066	4.63	1590	4.424	9.5	1198	1347
61	12.802	0.2062	4.61	1583	4.630	9.7	1200	1350
62	13.008	0.2058	4.60	1576	4.845	9.9	1202	1353
63	13.213	0.2054	4.58	1569	5.070	10.1	1204	1356
64	13.418	0.2050	4.57	1561	5.305	10.3	1207	1360
65	13.623	0.2045	4.55	1553	5.549	10.5	1209	1363
66	13.827	0.2041	4.54	1544	5.804	10.6	1212	1367
67	14.030	0.2036	4.53	1536	6.071	10.8	1215	1371
68	14.233	0.2030	4.52	1526	6.348	11.0	1218	1375
69	14.436	0.2025	4.51	1517	6.637	11.2	1222	1379
70	14.638	0.2019	4.50	1507	6.939	11.4	1225	1384
71	14.839	0.2012	4.49	1496	7.253	11.6	1229	1389
72	15.040	0.2006	4.48	1486	7.580	11.8	1233	1394

Table 6-2 (cont.)

N	Z inches	Pitch inches	α nep/ met	V_{eff} Volts	P Watts	Gain dB	β_T rad/ met	β rad/ met
73	15.239	0.1999	4.48	1474	7.921	12.0	1238	1399
74	15.439	0.1992	4.47	1463	8.275	12.2	1242	1405
75	15.637	0.1984	4.47	1450	8.645	12.4	1247	1411
76	15.835	0.1976	4.47	1438	9.030	12.6	1252	1417
77	16.031	0.1967	4.46	1424	9.430	12.8	1257	1423
78	16.227	0.1959	4.46	1410	9.847	12.9	1263	1430
79	16.422	0.1949	4.46	1396	10.280	13.1	1269	1438

V_{eff} at end of 79th turn = 1382 volts.

Depressed Collector Voltage, V_{cn}

$$V_{cn} = \frac{n_e V_o}{n_{opt} K_n}$$

where $n_e V_o = (.1184)\ (1725.88)$

$= 204.34$

Values of V_{cn} for various values of K_n are given in Table 6-3 below

Table 6-3

K_n	$n_{opt}K_n$	V_{cn} volts
1	.502	407.1
.5	.607	336.6
.1	.730	279.9
0	.768	266.1

6.3.1 Design of Collector of 10-Watt Tube. A minimum distance is needed between circuit and collector for conversion of cyclotron motion of the electrons to longitudinal velocity by means of a divergent magnetic field, as discussed in section (4.6). For the 10-watt tube, this distance should be greater than $50a_L \simeq 1"$. The needed distance is obtained by means of a drift tube at the potential of the circuit between circuit and collector.

Some information was obtained on collector design from the one-watt tube, which was the first tube constructed. To obtain an idea

of energy spread in the spent beam and to obtain more control on focusing the beam through the collector entrance, the collector in the one-watt tube was made with two isolated stages. The fraction of beam current to each collector stage could be measured. A diagram of the collector region is shown in Figure 6-1. The total beam current could be controlled by means of a grid control in the electron gun. It was originally intended that the cone potential be close to the circuit potential and that the collector cup be depressed. The total drift length would be the sum of the drift tube and cone lengths. The spacing between cone and cup was made equal to 0.1" in accordance with equation (5.75) to avoid space charge buildup in front of the collector. However, it was found that the cone had to be depressed in voltage together with the cup, rather than being maintained at circuit potential, in order to avoid space charge buildup and reflected current. The following is an explanation for this effect. Figure 6-1 shows that the effective spacing between cone and cup at the tube axis is greater than the actual distance of 0.1".

Although the gap at B is small (0.1"), when the cup is depressed with respect to the cone, the equipotential lines spread on the axis where the beam is located because of the large radius of the cup. Thus the effective spacing between cup and cone on the axis is greater than the spacing at the gap. In accordance with equation (5.75), the large effective L lowers the maximum current below the design value, so that the cup can not be depressed with respect to the cone if one wants to obtain the design current with the slowest electrons collected at zero velocity.

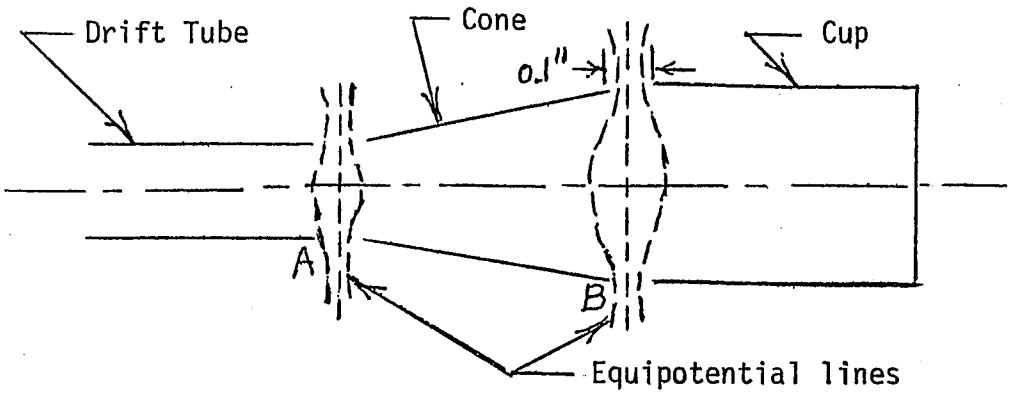

Figure 6-1 Collector region of one-watt tube

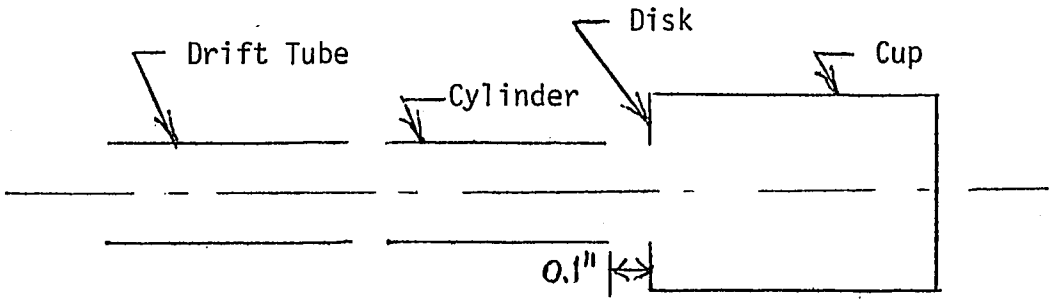

Figure 6-2 Collector region of ten-watt tube

The situation is better at gap A between drift tube and cone. Because of the smaller radius of the drift tube, the equipotential lines do not spread as much on the axis so that the effective L is smaller than that between cup and cone. This makes I_{max} larger so that the cone can be depressed with respect to the drift tube and still allow the design current to pass through.

In accordance with the above, the collector for the 10-watt tube has been redesigned as shown in Figure 6-2 so as to decrease the effective distance between cone and cup on the axis. The cone has been replaced by a cylinder with inner diameter equal to that of the drift tube. A disk with a hole in the center has been placed in front of the collector. The diameter of the hole equals the inner diameter of the cylinder. In this way, the spread of the equipotential lines has been reduced, thereby reducing the effective L.

Figure 6-3 shows the essential features of the 10-watt tube. Figure 6-4 shows the details of the bifilar helix support for both the 10-watt and one-watt tubes. Details of the electron gun, which is the same for the 10-watt and one-watt tubes, are shown in Figure 6-5.

The focusing solenoid for the ten-watt and one-watt tubes are shown in Figure 6-6A, and the longitudinal magnetic field distribution is shown in Figure 6-6B.

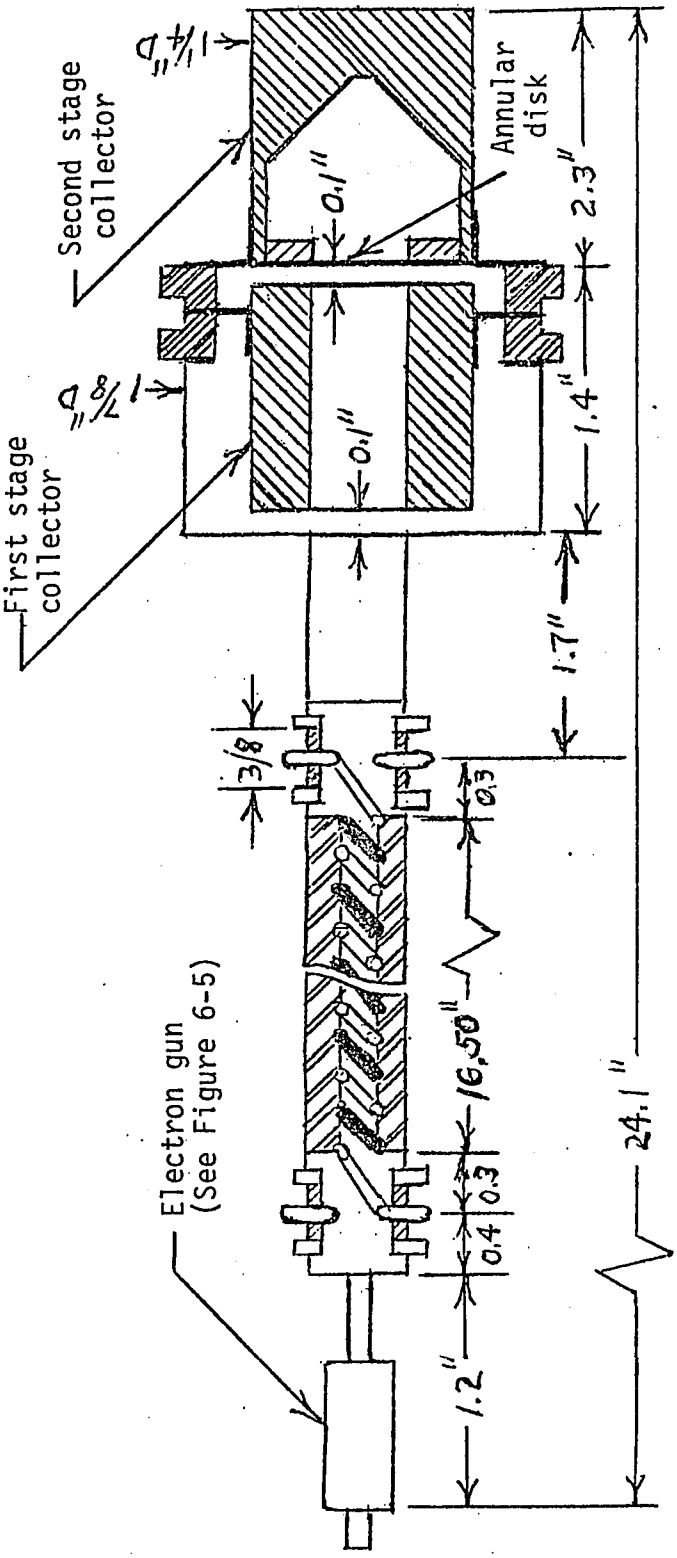

Figure 6-3 Sketch of experimental ten-watt cyclotron-wave amplifier

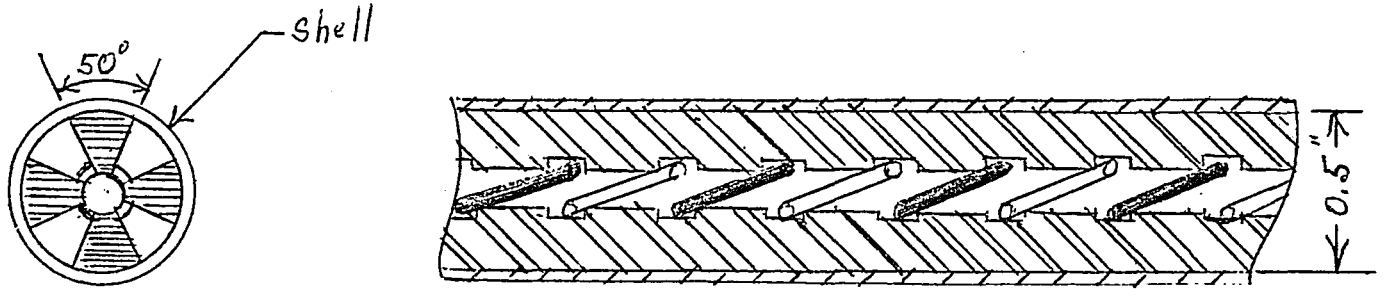

Figure 6-4 Dielectric supports for bifilar helices of one-watt and ten-watt tubes

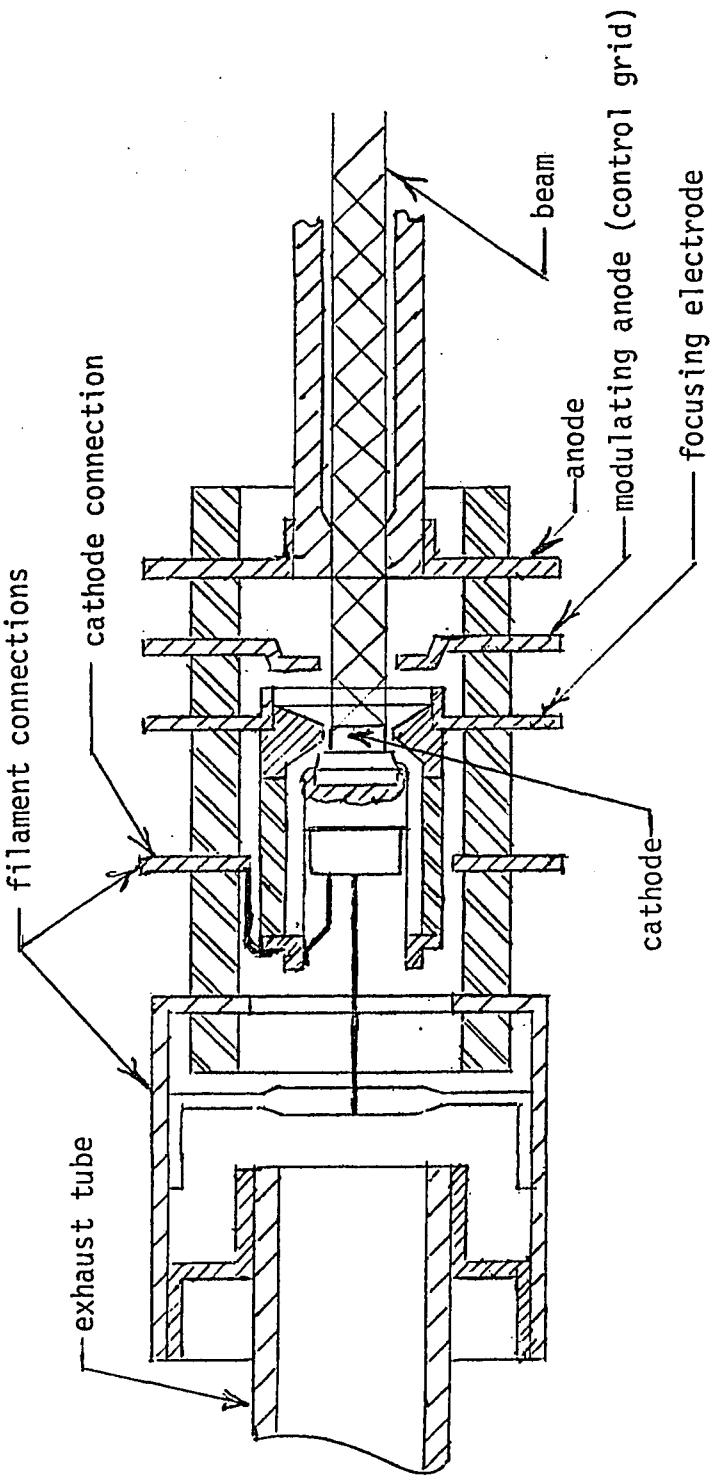

Figure 6-5 Electron gun for one-watt and ten-watt tubes

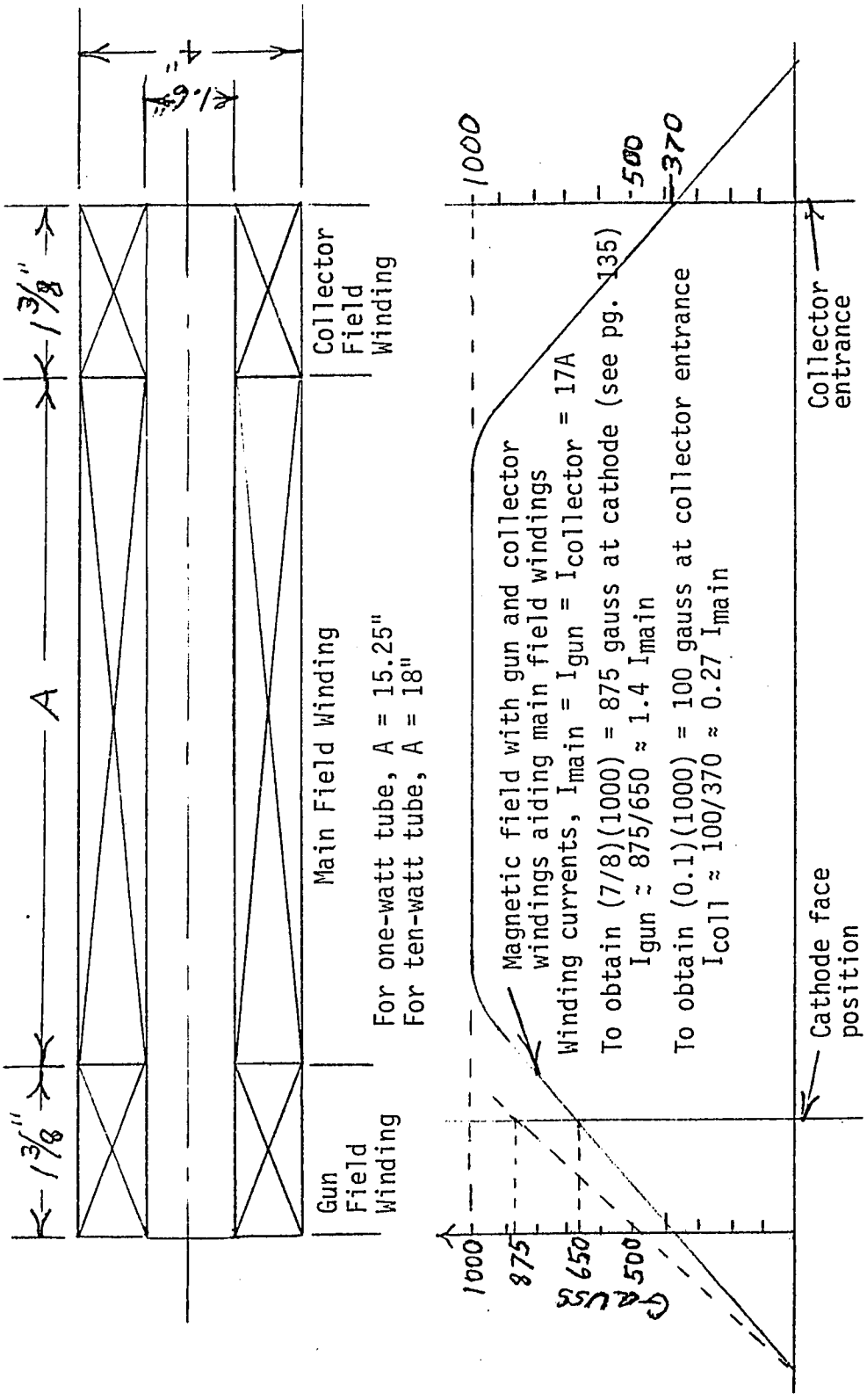

Figure 6-6 Focusing solenoid and magnetic field distribution for one-watt and ten-watt tubes

6.4 Design of One-Watt Tube

One of the purposes in constructing the one-watt tube was to experimentally verify equation (5.18) for the interaction impedance by means of gain measurements. The one-watt tube also served as a beam tester for the 10-watt tube, which uses the same electron gun. If a very small amount of power is extracted from the beam, the slow-down of the beam is small enough so that a constant pitch circuit can be used for the one-watt tube. The circuit and slow cyclotron waves will then be close to synchronism over the whole length of the circuit.

The circuit length of the one-watt tube was chosen the same as the length of a 10-watt tube with 10 dB gain. This length was obtained by utilizing the reiterative computer program described for the 10-watt tube when the input power was one watt instead of 0.5 W. The length, L, was determined to be

$$L = .3472 \text{ met} = 13.668"$$

The pitch, p, was chosen to be equal to the initial pitch of the 10-watt tube.

$$p = 5.3314X10^{-3} \text{ met} = .2099"$$

The mean diameter, d, and the inner diameter, d_i, of the bifilar helix were chosen between the minimum and maximum values for the helix of the 10-watt tube.

$$d = 3.0073X10^{-3} \text{ met} = .1184"$$

$$d_i = d/1.2 = 2.5061X10^{-3} \text{ met} = .09867"$$

The following parameters, equal to those of the 10-watt tube are chosen.

Operating Frequency

$f = 3$ GHz

$\omega = 2\pi f = 2\pi X3X10^9 = 18.85X10^9$ rad/sec

Cyclotron Frequency

$f_c = 2.07$ GHz

$\omega_c = 2\pi X2.07X10^9 = 13.01X10^9$ rad/sec

Magnetic Focusing Field

$B_o = f_c(mHz)/2.8 = 739$ gauss

ω/ω_c Ratio

$\omega/\omega_c = 3/2.07 = 1/.69 = 1.45$

d/ρ_w Ratio

For optimum interaction impedance,

$d/\rho_w = 12$; $\ln(d/\rho_w) = 2.48$

Wire radius, ρ_w, and wire diameter, d_w

$\rho_w = d_i/10 = .2506X10^{-3}$ met = .009867"

$d_w = 2\rho_w = .5012X10^{-3}$ met = .019734"

Beam Radius

$b = .7725X10^{-3}$ met = .0304"

Beam Current

$$I_o = 48.937X10^{-3} \text{ amps}$$

The following additional parameters are calculated

Twist Propagation Constant, β_T

$$\beta_T = \frac{2\pi}{p} = \frac{2\pi}{5.3314X10^{-3}} = 1178.5 \text{ rad/met}$$

Pitch Angle, ψ

$$\cot \psi = \beta_T a = (1178.5)\ (3.0073X10^{-3}/2)$$

$$= 1.772$$

$$\psi = 29.436^o$$

$$\sin \psi = .4915$$

Free space propagation constant, β_f

$$\beta_o = \frac{\beta_f}{\sin \psi} = 127.84 \text{ rad/met}$$

Circuit propagation constant, β

$$\beta = \beta_o + \beta_T = 1306.34 \text{ rad/met}$$

Beam Velocity, v_o

$$v_o = \frac{\omega+\omega_c}{\beta} = \frac{(18.85 + 13.01)10^9}{1306.34} = 2.439X10^7 \text{ met/sec}$$

Beam Voltage, V_o

$$V_o = \frac{v_o^2}{2\eta} = \frac{(2.439)^2X10^{14}}{2X1.759X10^{11}} = 1691 \text{ volts}$$

Growth Constant, α (Equat. 6.3)

$$\alpha = \frac{1}{d}\left(\frac{377}{8\pi}\frac{\omega}{\omega_c}\frac{I_o}{V_o \ln(d/\rho_w)}\right)^{\frac{1}{2}}$$

$$= 5.296 \text{ nep/met}$$

Interaction Impedance, K_T (Equat. 5.18)

$$K_T = \frac{377}{4\pi\beta^2 d^2 \ln(d/\rho_w)}$$

$$= \frac{377}{4\pi(1306.34)^2\ (.0030073)^2\ (2.48)}$$

$$= .784 \text{ ohms}$$

Total number of turns of helix, n

$$n = \frac{L}{p} = \frac{13.668"}{.2099"} = 65$$

Small Signal Gain

The voltage gain G_V, is

$$G_V = \cosh \alpha L = \cosh (5.296X.3472)$$

$$= 3.22 = 10.17 \text{ dB}$$

Maximum Permissible Beam Deflection, a_{L1}, to Avoid Interception of Circuit

Using a filling factor, $K_f = 0.8$,

$$2(a_{L1} + b) = 0.8\ d_i$$

$$a_{L1} = 0.4\ d_i - b$$

$$= (0.4X2.506-.7725)X10^{-3}$$

$$= .22994X10^{-3} \text{ met} = .009053"$$

Maximum Electronic - Cyclotron Efficiency, $\eta_{ec\ max}$, and Maximum Electronic Efficiency, $\eta_{e\ max}$

With no overvoltaging of the beam,

$$\eta_{ec\ max} = 4\,\frac{\alpha}{\beta}$$

$$= \frac{4(5.296)}{1306.34} = .01622$$

$$\eta_{e\ max} = \frac{\omega}{\omega+\omega_c}\,\eta_{ec\ max}$$

$$= \frac{1}{1.69}\,(.01622) = .00960$$

Maximum Power, P_e, that can be extracted from beam by the circuit before complete desynchronization

With no overvoltaging,

$$P_e = \eta_{e\ max}\, I_o V_o$$

$$I_o V_o = (48.937 \times 10^{-3})\ (1691) = 82.75$$

$$P_e = (.00960)\ (82.75) = .794 \text{ watts}$$

This power can be doubled by overvoltaging the beam.

Overvoltaging to double the maximum power extracted from the beam

When the circuit and cyclotron wave start in synchronism, the effective voltage of the beam is

$$V_{eff} = V_o - V_{red}$$

where V_o = injection voltage

V_{red} = reduction in voltage of the beam caused by extraction of power by the circuit and cyclotron motion of the electrons

For the total length of the circuit,

$$V_{red} = \frac{P_e}{I_o} \frac{\omega+\omega_c}{\omega}$$

where P_e = maximum power extracted by the circuit

$$V_{red} = \frac{.794}{48.937X10^{-3}} \quad X1.69 = 27.4 \text{ volts}$$

If the circuit voltage is increased by $\Delta V = V_{red}$, twice the power can be extracted before complete desynchronization.

The circuit voltage then is

$$V_i = V_o + \Delta V = 1691 + 27 = 1718 \text{ volts}$$

The power extracted by the circuit then is

$$P_e' = 2P_e = 1.59 \text{ watts}$$

Maximum Bean Deflection, a_{L2}, for complete desynchronization with no overvoltaging

$$P_e = \frac{1}{2} \omega I_o B_o a_{L2}^2$$

$$a_{L2}^2 = \frac{2P_e}{\omega I_o B_o} = \frac{2X.794}{18.85X10^9X48.937X10^{-3}X739X10^{-4}}$$

$$a_{L2} = .1526X10^{-3} \text{ met}$$

With overvoltaging, the maximum beam deflection, a'_{L2}, is

$$a'_{L2} = \sqrt{2}\, a_{L2} = .2158X10^{-3} \text{ met}$$

$a'_{L2} < a_{L1}$, so that no interception of the beam on the circuit occurs.

Brillouin Focusing Field

$$B_B = \frac{8.32 I_o^{\frac{1}{2}}}{V_o^{\frac{1}{4}} b}$$

where B_B = Brillouin Field, gauss

I_o = Beam Current, amps

V_o = Beam Voltage, volts

b = beam radius, meters

$$B_B = \frac{8.32(48.937X10^{-3})^{\frac{1}{2}}}{(1691)^{\frac{1}{4}}\ (.7725X10^{-3})} = 371.54 \text{ gauss}$$

$$\frac{B_o}{B_B} = \frac{739}{371.5} = 1.99 \approx 2$$

Depressed Collector Efficiency, η_{opt}

Similar to the calculation for the 2 kW tube,

$$\eta_{opt} = \frac{1}{1+K_n \frac{\omega_c}{\omega} + \left(\frac{\omega+\omega_c}{\omega}\right)\left(\frac{\omega_R}{\omega_c}\right)\left(\frac{2b}{a_L}\right)}$$

With no overvoltaging

$$a_L = a_{L2} = .1526X10^{-3} \text{ met}$$

$$\frac{2b}{a_{L2}} = \frac{2(.7725)}{.1526} = 10.12$$

$$\frac{\omega_c}{\omega} = .69 \qquad \frac{\omega+\omega_c}{\omega} = 1.69$$

$$\frac{\omega_R}{\omega_c} = \frac{1}{16} \text{ (for } B_o = 2B_B)$$

$$\eta_{opt} = \frac{1}{1 + .69K_n + 1.069} = \frac{1}{2.069 + .69K_n}$$

With overvoltaging

$$\frac{2b}{a'_{L2}} = \frac{2(.7725)}{.2158} = 7.159$$

$$\eta_{opt} = \frac{1}{1.756 + .69K_n}$$

Values of η_{opt} for various values of K_n are given in Table 6-4 in the next paragraph.

Depressed Collector Voltage, V_{cn}

$V_{cn}I_o$ = total power supplied

$$\eta_{opt}K_n = \frac{P_e}{\text{Total power supplied}}$$

where P_e = power extracted by the circuit from the beam

$$\eta_{opt}K_n = \frac{P_e}{V_{cn}I_o}$$

Thus,

$$V_{cn} = \frac{P_e}{I_o\eta_{opt}K_n}$$

With no overvoltaging

$$V_{cn} = \frac{.794}{48.937X10^{-3}\ \eta_{opt}K_n} = \frac{16.22}{\eta_{opt}K_n}$$

With overvoltaging

$$V_{cn} = \frac{2X.794}{48.937X10^{-3}\eta_{opt}K_n} = \frac{32.45}{\eta_{opt}K_n}$$

Values of V_{cn} for various values of K_n are given in Table 6-4 below.

Table 6-4

	No overvoltaging		Overvoltaging	
K_n	$\eta_{opt}K_n$	V_{cn}, volts	$\eta_{opt}K_n$	V_{cn}, volts
1	.3624	44:8	.4088	79.4
.5	.4143	39.2	.4760	66.2
.1	.4677	34.7	.5479	59.2
0	.4833	33.6	.5695	57.0

The depressed collector efficiency for the one-watt tube is less than that for the 10 W tube because the final beam deflection is smaller (a smaller amount of power is extracted from the beam by the circuit). The maximum beam deflection for the 10 W tube can be greater because synchronism is maintained. The one-watt tube was not designed for very high efficiency, but was intended to verify equation (5.18) for the interaction impedance. The one-watt tube was also intended as a beam tester for the 10 W tube with the beam current, beam voltage, and beam diameter of both tubes being approximately equal.

For the one-watt tube, it is important that the beam be well focused so as to minimize beam interception on the circuit. Any small amount of interception will lower the overall efficiency because the power intercepted on the circuit is at circuit voltage and is comparable to the power extracted from the beam. As an example, for the one-watt tube with overvoltaging, let $K_n = 0.1$, Then

$$\eta_{opt} = 54.8\%$$

Collector voltage, $V_{cn} = 59.2$ V

Circuit voltage, $V_{ckt} = 1718$ V

If the beam interception is 2% (transmission = 98%), the current intercepted on the circuit is

$$I_{int} = .02X48.937X10^{-3} = .979X10^{-3} \text{ amps}$$

The current, I_c, to the collector is

$$I_c = (.98)\ (48.937X10^{-3}) = 47.96X10^{-3} \text{ amps}$$

The overall efficiency, η_{ov}, is

$$\eta_{ov} = \frac{P_e}{\text{Power supplied}}$$

$$= \frac{1.59}{I_c V_{cn} + I_{int} V_{ckt}}$$

$$+ \frac{1.59}{(47.96X59.2 + .979X1718)10^{-3}} = 35.2\%$$

Thus the efficiency is lowered to 35.2% from 54.8% by the interception.

This effect is not as great with the 10 W tube because the intercepted power is a smaller percentage of the extracted power. As an example, for the 10 W tube, let $K_\eta = 0.1$. Then

$$\eta_{opt} = 73\%$$

Collector voltage, $V_{cn} = 280$ V

Circuit voltage, $V_{ckt} = 1726$ V

$$I_{int} = .02I_o = .797X10^{-3} \text{ A}$$

$$I_c = .98I_o = 47.96X10^{-3} \text{ A}$$

$$\eta_{ov} = \frac{10}{(47.96X280 + .979X1726)10^{-3}}$$

$$= 66.1\%$$

Thus, the efficiency is lowered from 73% to 66.1% by the interception. Maintaining synchronism permits the extraction of more power from the beam, so that the intercepted power becomes smaller compared to the extracted power. The efficiency is then not lowered as much as with the one-watt tube. The focusing is not as critical with the 10-watt tube.

Figure 6-7 shows the essential features of the one-watt tube. Figure 6-4 shows the details of the bifilar helix support for the one-watt tube. Details of the electron gun for the one-watt tube are shown in Figure 6-5. The focusing solenoid for the one-watt tube is shown in Figure 6-6A, and the longitudinal magnetic field distribution is shown in Figure 6-6B.

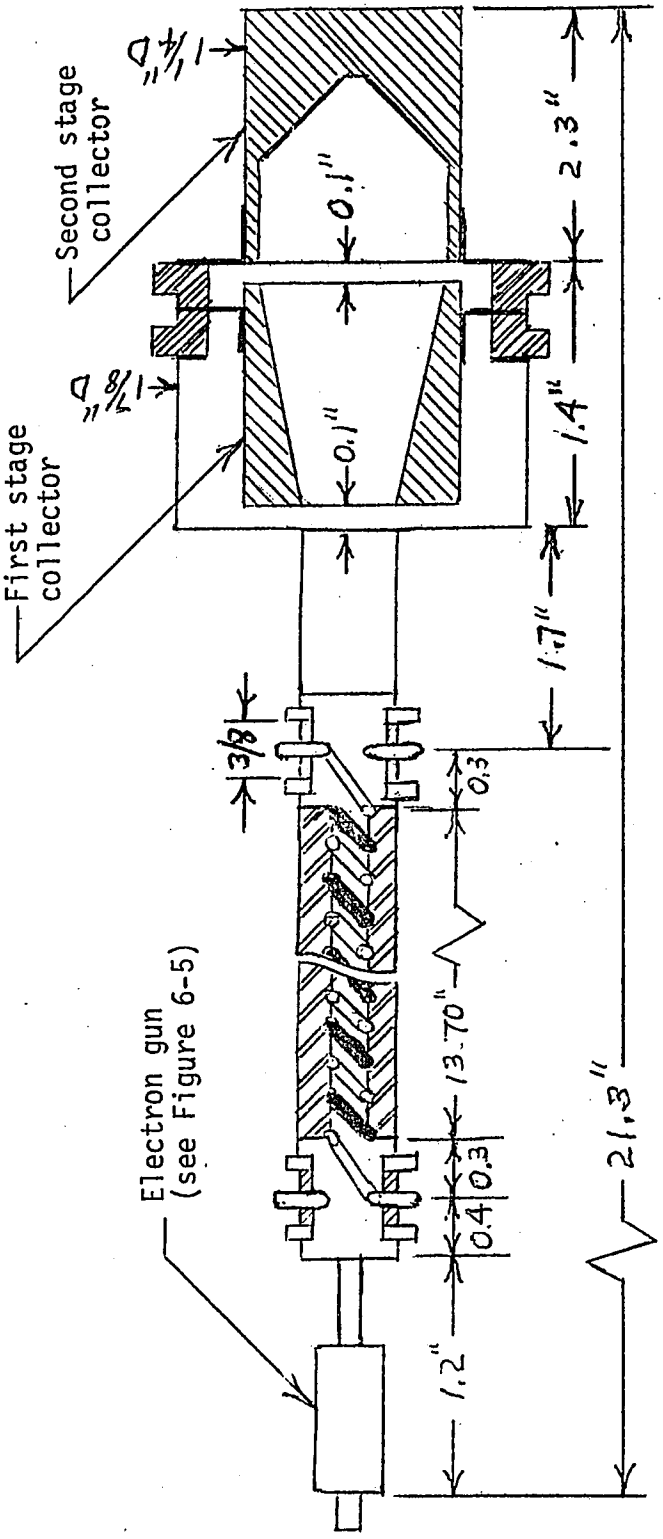

Figure 6-7 Sketch of experimental one-watt cyclotron-wave amplifier

CHAPTER VII

EXPERIMENTAL RESULTS

7.1 Test Procedure

The schematic for the d.c. connections is shown in Figure 7.1. The tests were performed under pulsed beam conditions. This was a safety precaution to avoid any possible destruction of the tube if too much beam current intercepted any of the electrodes. The magnitude of the pulsed beam current was controlled by a variable positive voltage pulse applied between modulating anode (grid) and cathode. The circuit-cathode and collector-cathode voltages were not pulsed. The pulsed currents were measured with current probes which surround the wire carrying the current and generate a pulse voltage proportional to the current pulse which is measured on an oscilloscope. Monitor Tee's at the inputs to the helices isolate the d.c. from r.f. input. "Inside" blocks (capacitors) isolate the d.c. potential of the helices from the r.f. output.

The same combinations of 50-ohm angles, extension connectors, and adapters were used to connect the #1 and #2 ports of the 180° hybrid to the two input cables connected to the tube input terminals. This was done to make the transmission lines feeding the tube exactly the same length so as to maintain the 180° phase between the two inputs to the tube. The same type of connections were made to the output cables.

A simplified schematic of the r.f. circuitry is shown in Figure 7-2. A 180° hybrid is used to apply equal amplitude signals to helices

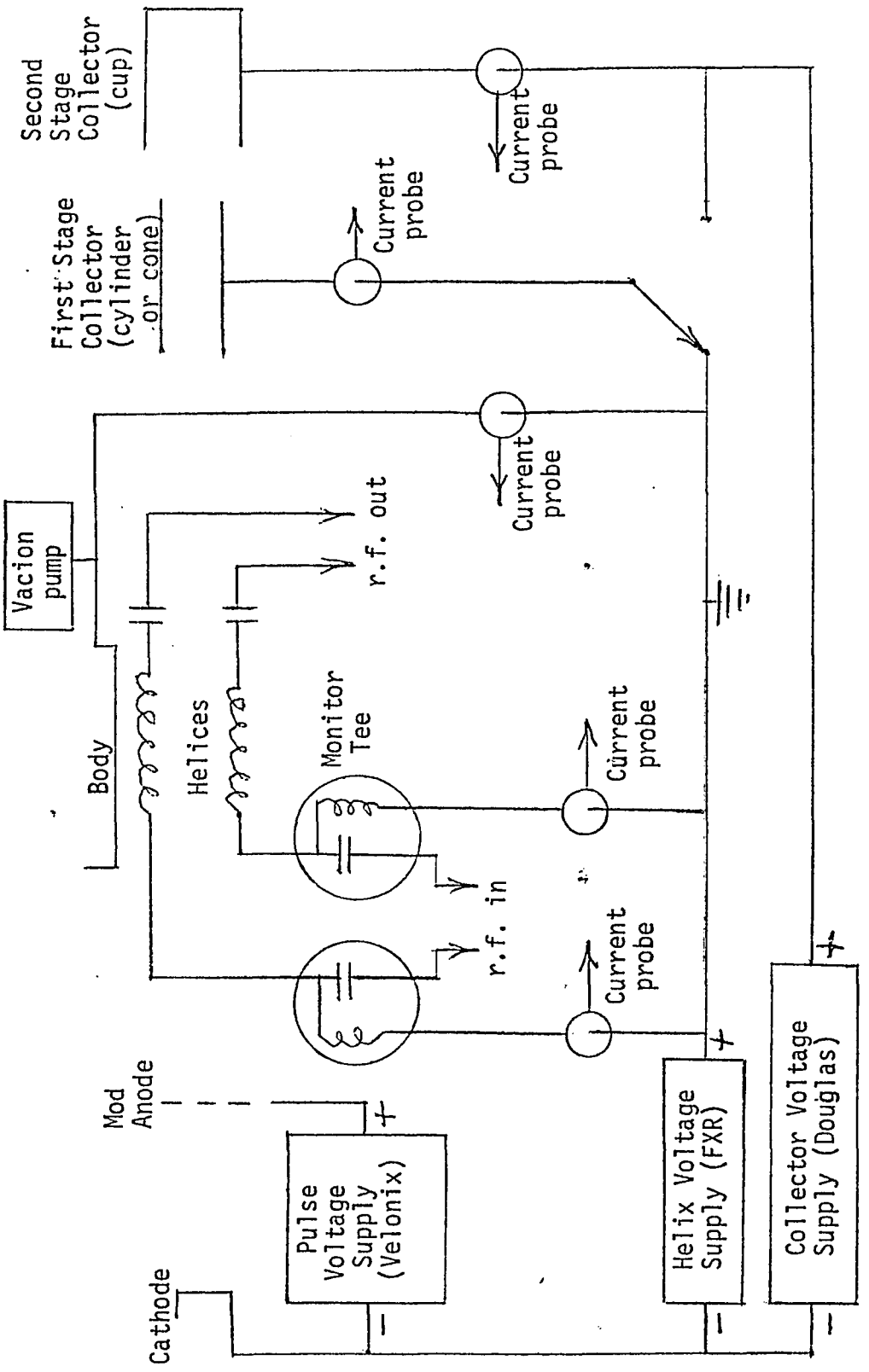

Figure 7-1 Schematic of d.c. Circuitry

#1 and #2 which are phased 180° apart (+ - feed). A property of the 180° hybrid is that when an r.f. signal is applied to the Δ-port, the equal amplitude signals out of ports #1 and #2 are 180° out of phase; when a signal is applied to the Σ-port, the equal amplitude output signals are in phase. In the reverse direction, the outputs of the Δ- and Σ-port are proportional to the difference and sum, respectively, of the inputs to ports #1 and #2.

Direction couplers are used to measure incident power from the signal generator into the Δ-port ($P_{inc\Delta}$), power out of the Δ-port ($P_{ref\Delta}$), power out of the Σ-port (P_{Σ}), power into 50-ohm loads #1 and #2 (P_{1out} and P_{2out}). $P_{inc\Delta}$ is measured by a milliwattmeter, since it is a CW signal. The other powers, which are pulsed, are measured by means of diode detectors fed to an oscilloscope.

The diode detectors are calibrated by substituting a CW signal for the pulsed signal, adjusting the CW signal level to produce the same voltage deflection on an oscilloscope as that produced by the pulsed signal, and then noting the reading of the CW signal on a milliwattmeter which is substituted for the diode. The CW and pulsed signals are fed to each diode through a buffer 50-ohm attenuator as shown in Figure 7-2.

The outputs from the terminals of the helices are fed through small 50-ohm cables routed out from the focusing solenoid at the electron gun end. These cables are unequal in length for the 10-watt tube, which causes a phase shift between the outputs of helices #1 and #2. To eliminate possible matching and attenuation problems, a 180° hybrid

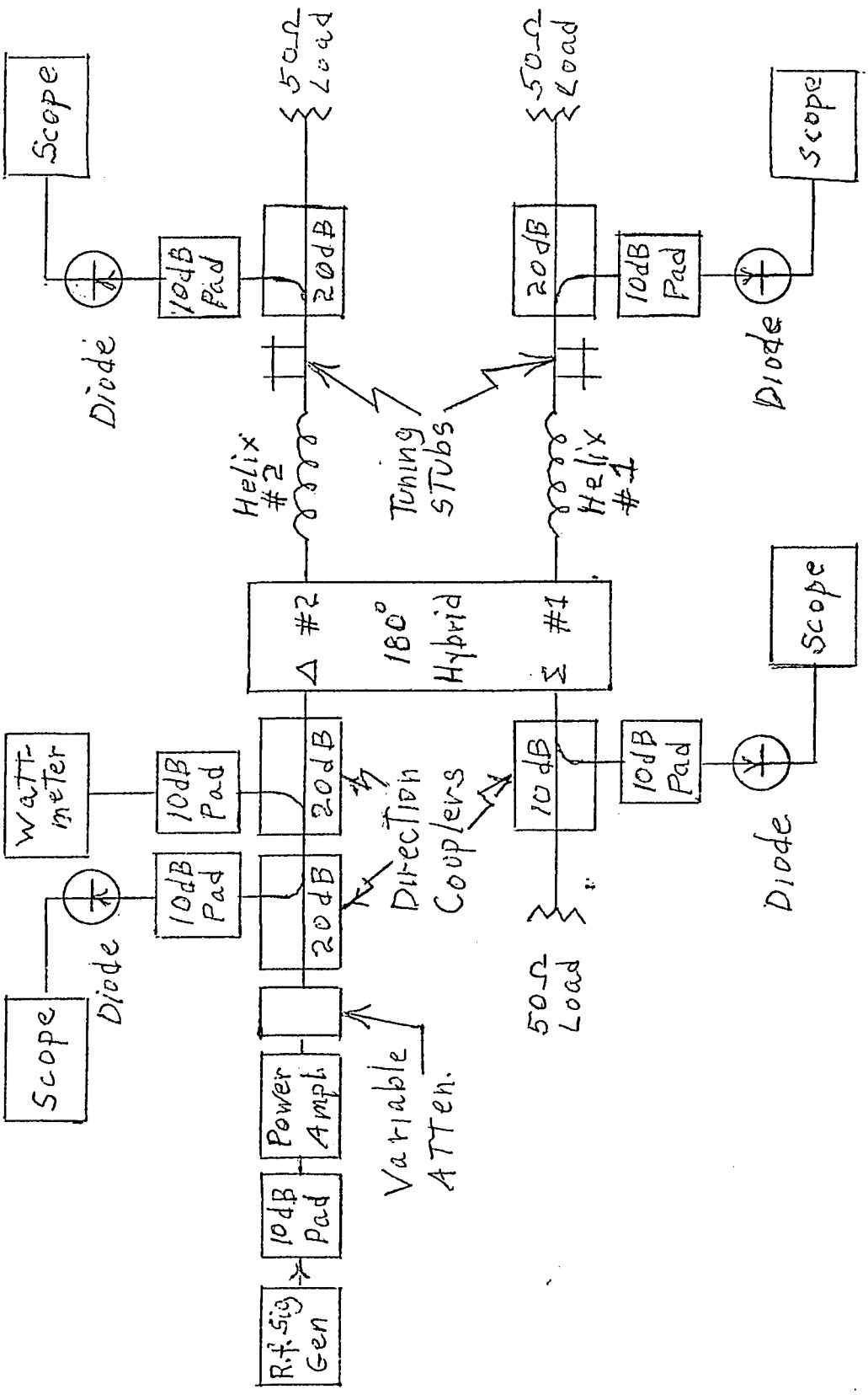

Figure 7-2 Schematic of r.f. Circuitry

combiner was not used at the output. Instead, the power output from each helix was measured individually, and then summed.

Double-stub tuners were used to maximize the output of each helix to a 50-ohm load.

The following were calibrated: direction couplers (coupling and insertion loss in both directions); attenuators; attenuation of input and output r.f. cables from the four terminals of the tube; insertion loss of the 180° hybrid. In measuring insertion loss of the hybrid, it was found that reflection losses (in a 50-ohm system) were small and could be neglected. The losses in the stub tuners were negligible. The cable insertion loss in dB/inch was found by measuring a 24" length.

Cable Loss

0.0625 dB/inch

Input cables to helix #1 and helix #2

(.0625)(5.25") = 0.33 dB

Output cable from helix #2

(.0625)(24") = 1.5 dB

Output cable from helix #2

(.0625)(25") = 1.56 dB

180° hybrid insertion loss

0.74 dB

A list of some of the important test equipment is given in Table 7-1.

From a knowledge of the attenuation through the 180° hybrid and the attenuation of the cables to the tube terminals, the following can be calculated: the total incident power at the tube input terminals, the total reflected power at the tube input terminals, and the total power out of the tube output terminals.

Figure 7-3 indicates the definition of symbols used for power at the 180° hybrid input terminals and power into the tube input terminals.

Figure 7-4 indicates the definition of symbols for total power at the tube terminals.

7.2 Tests of One-Watt Tube

7.2.1 R.F. Measurements. The operating conditions for the one-watt tube are given below.

Signal Frequency	3.09 GHz	Grid Pulse Voltage	1450V
Grid Current	0	Helix #1 and #2 Voltage	1725V
Helix #1 Current	0.4 ma	Cone Voltage	1560V
Helix #2 Current	0.4 ma	Collector Cup Voltage	1685V
Collector Cone Current	0	(All voltages with respect to cathode)	
Collector Cup Current	48 ma		
Body Current	0.3 ma		

Focusing Solenoid Currents

Main (Center Coil)	12.5A (737 gauss)
Gun	10.5A
Collector	10.7A

Table 7-1

List of Important Test Equipment

R. F. Signal Generator - Hewlett-Packard 8690A Sweep Oscillator

R. F. Power Amplifier - Varian Traveling-Wave Tube Amplifier, VZS 6950G1, 2-4 GHz, 10W

Pulse Voltage Generator - Velonix (with 1:1 output isolation transformer), Model 35D, 2000V, 10A

Beam Voltage Supply - FXR Universal Microwave Power Supply, Model Z817B

Collector Voltage Supply - Douglas 5 kV, 100 ma

Main Solenoid Supply - NJE Corp., Model EA-160-50, 0-160V, 0-50A

Collector Solenoid Supply - SFD Power Supply, 250V, 30A

Gun Solenoid Supply - Electronic Measurements, Regatran, 40V, 36A

Fluxmeter - Bell Model 640 Incremental Gaussmeter

Oscilloscope - Tektronix 5330 Oscilloscope with Type H Plug-in unit

Spectrum Analyzer - Tektronix Model 491

Power Meter - General Microwave, Model 454A, Thermoelectric Power Meter

Power Meter - Hewlett-Packard Model 431B Power Meter

Hybrid - Radiation Systems 180^{o} Hybrid, Model 2654-01, 1 to 10 GHz, Isolation 25 dB

Frequency Meter - General Microwave Corp., Model N604, 1.9-4 GHz

Variable Attenuator - Alfred Electronics, Model E103, 2-4 GHz

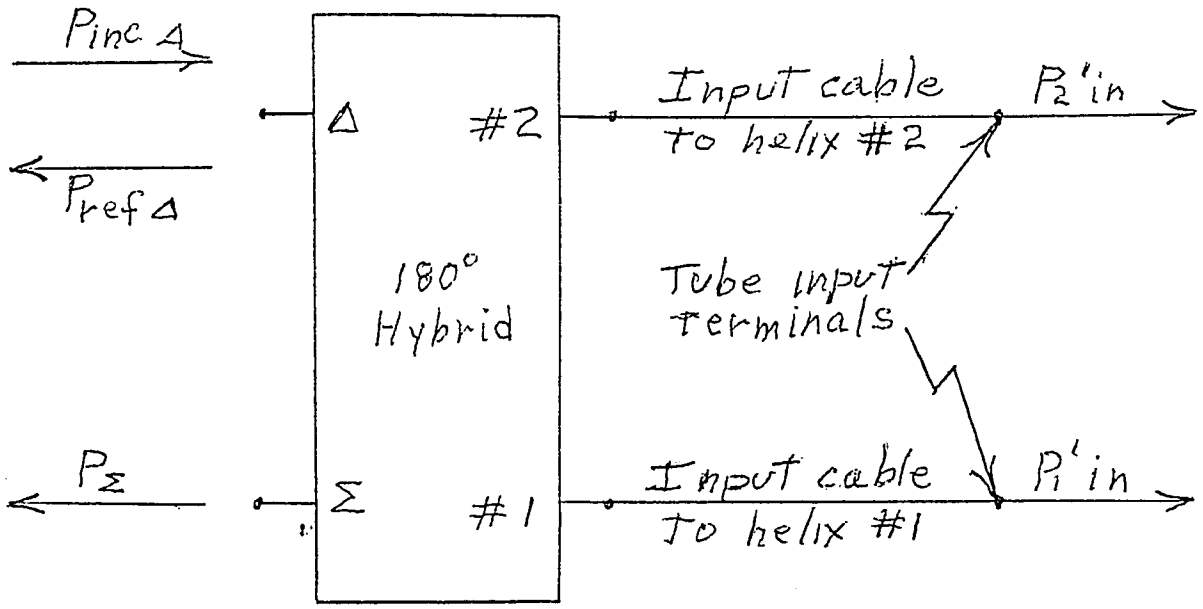

Figure 7-3 Definition of power symbols, at the input terminals of the 180° hybrid and at the input terminals of the tube.

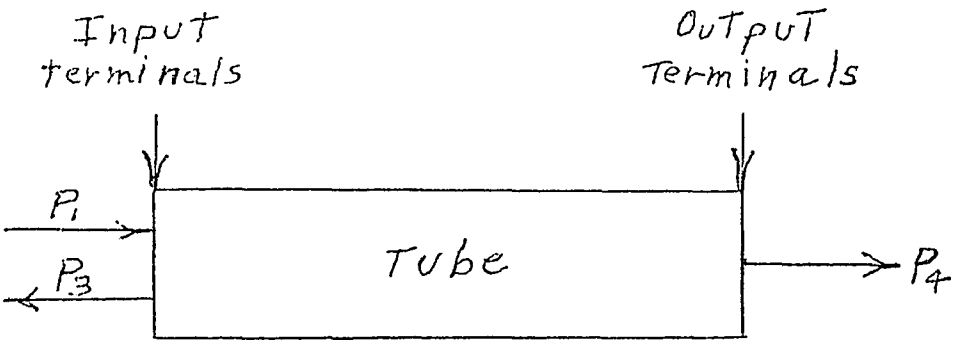

P_1 = sum of incident powers into input terminals of tube
= $P_1' + P_2'$ (Figure 7-3) = $P_{inc\Delta}$ (Figure 7-3) reduced by the attenuation of the 180° hybrid and one of the equal length cables to the input terminals of the tube.

P_3 = $P_{ref\Delta} + P_\Sigma$ (Figure 7-3) increased by the attenuation of one of the equal length input cables and the hybrid.

P_4 = sum of output powers from output cables #1 and #2, each power increased by the respective cable loss.

Figure 7-4 Definition of power symbols at the tube terminals

Grid Pulse

15 μsec, 8.6 Hz, Duty Cycle .00129

It was found that the r.f. matches at the tube terminals were fairly good for the one-watt tube. This permits calculation of electronic gain. The effect of mismatches at the input and output terminals of the tube are analyzed in Appendix B. Referring to Figure B-1 in Appendix B,

$P_3 \simeq 0$, $P_5 \simeq 0$, $\rho_2 \simeq 0$ and $\rho_4 \simeq 0$.

From equations (B.1), (B.2), (B.5), (B.6)

(7.1) $$P_{2G} = \frac{P_{2G}'}{L_1} = \frac{P_{1G}}{L_1}$$

(7.2) $$P_{2O} = \frac{P_{2O}'}{L_1} = \frac{P_{1O}}{L_1}$$

Using (7.1) and (7.2) in equat. (B.9)

(7.3) $$\frac{P_{4G}}{P_{4O}} = \frac{G\, P_{1G}}{P_{1O}}$$

Using the same incident power with beam on and beam off, $P_{1G} = P_{1O}$, so that (7.3) becomes

(7.4) $$\boxed{G = \frac{P_{4G}}{P_{4O}}}$$

Equat. (7.4) states that the electronic power gain of the one-watt tube is the ratio of the output with beam on to that with beam off, keeping the input power the same. The actual power gain is less

than the electronic gain and is equal to $(\frac{GP_2}{\alpha}) \div P_2 = \frac{G}{\alpha}$ as can be seen from Figure B-1.

Figure 7-5 gives the results of the gain test. The total output power at the tube terminals (in dBm) with beam on is plotted as a function of total output power (in dBm) with beam off. The 10 dB and 5 dB gain lines are shown dotted.

An oscillation at 2.29 GHz was noted on a spectrum analyzer when the output signal level was below 15 dBm (32 mw). The oscillation was suppressed by output signal levels greater than 15 dBm. Calculations indicate the oscillation at 2.29 GHz to be a backward wave one. The gain curve at the lower signal levels was extrapolated from the higher signal levels and falls on the 10 dB gain line. Thus, the small signal gain is 10 dB. The tube saturates at one-watt output. Approximately 3 dB tube insertion loss was measured with beam off.

The gain parameter, α, and the interaction impedance, K_T, can be calculated from the small signal voltage gain, G_V.

Measured α

$G_V = \cosh \alpha L$

where L = length of circuit in meters

$\sqrt{10} = \cosh \alpha L$

$\alpha L = 1.82 \quad L = 0.347$ met.

$\alpha = \frac{1.82}{.347} = 5.24$ nep/met.

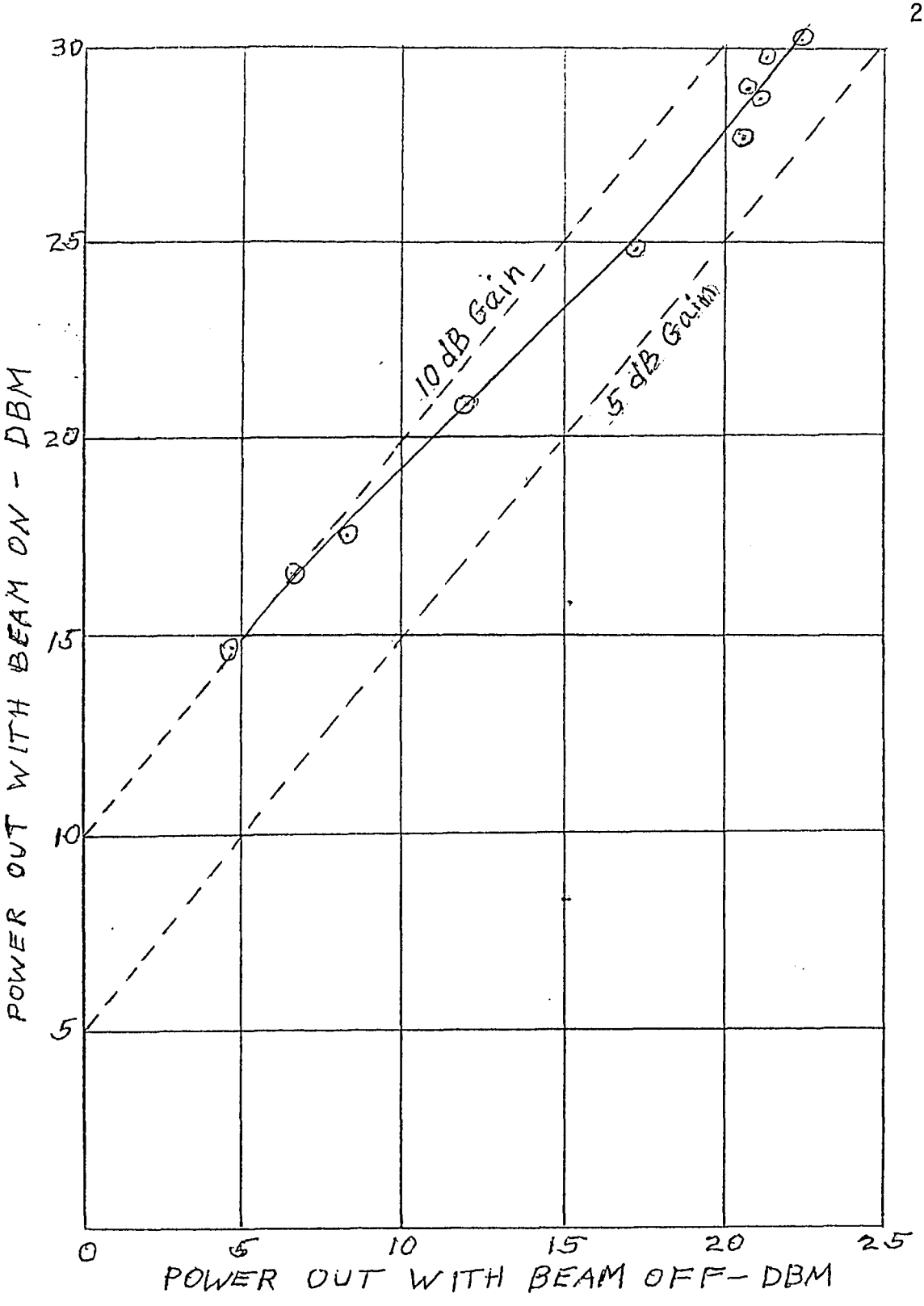

Figure 7-5 Electronic gain of one-watt tube

Measured Interaction Impedance, K_T

$$\alpha = \beta\left(\frac{1}{2}\frac{\omega}{\omega_c}\frac{I_o}{V_o}K_T\right)^{\frac{1}{2}}$$

$$\text{or } K_T = \frac{2\alpha^2}{\beta^2}\frac{\omega_c}{\omega}\frac{V_o}{I_o}$$

$\alpha = 5.24$ nep/met

$\omega = 3.09 \times 10^9 \times 2\pi = 19.40 \times 10^9$ rad/sec

$f_c = 2.8\, B_{gauss} \times 10^9 = 2.8 \times 737 \times 10^9$

$= 2.06 \times 10^9$ Hz

$\omega_c = 2\pi f_c = 12.92 \times 10^9$ rad/sec

$$\beta = \frac{\omega + \omega_c}{v_o}$$

$v_o = 5.93 \times 10^5 \sqrt{V_o} = 5.93 \times 10^5 \sqrt{1725}$

$$\beta = \frac{19.40 + 12.92}{2.46 \times 10^7} = 1312 \text{ rad/sec}$$

$V_o = 1725$ V

$I_o = 48 \times 10^{-3}$ A

Using these values,

$K_T = .763$ ohms measured

Theoretical Interaction Impedance, K_T

$$K_T = \frac{377}{4\beta^2 \pi d^2 \ln d/\rho}$$

where d = mean diameter of helix

ρ = radius of helix wire

$d = 3.0073 \times 10^{-3}$ met

$d/\rho = 12$; $\ln 12 = 2.48$

$\beta = 1312$ rad/sec (measured)

Using these values,

$$\boxed{K_T = .776 \text{ ohms}} \quad \text{theoretical}$$

These measured and theoretical interaction impedances are in good agreement. The accuracy of the measured value depends on the accuracy of the extrapolated small signal gain. The small signal gain must be used because the circuit and beam waves are still in synchronism for small signals.

7.2.2 Collector Depression. Ninety percent depression of the potential of the collector cup (with cone connected to circuit) could be accomplished with just enough r.f. signal on the beam to suppress oscillations. (The collector was depressed to 10% of beam voltage.) Further depression was limited by space charge buildup at the entrance to the cup. Slightly more depression was accomplished by depressing the cup and cone tied together. The space charge effect was reduced in the redesigned collector for the 10-watt tube, as indicated in Section 6.3.1.

The maximum depressed collector efficiency that could be obtained with saturated power output was

$$\eta_{dep} = \frac{P_e}{0.1V_oI_o} = \frac{1}{(0.1)(1725)(.048)} = 12\%$$

where P_e = r.f. power extracted from beam.

It should be noted that the one-watt tube was not designed for high efficiency, but was intended as a beam tester and to verify the theoretical formula for interaction impedance.

7.3 Tests of Ten-Watt Tube

Measurements were made with beam currents of 32 ma and 42 ma. Because of mismatches at the terminals of the tube, oscillations were encountered at 3.618 GHz. It was found that the oscillations could be locked out by driving the tube hard enough with a signal at 3.612 GHz.

Reversing the magnetic focusing field eliminated the oscillations. This indicates that the feedback causing oscillations was due to transverse wave interactions. Space charge wave interactions would not be affected by the direction of the magnetic field, whereas transverse-wave interactions would be affected because of the reversal of polarization. Transverse beam and circuit waves can interact only if they have the same polarization.

The equations derived in Appendix B permit calculation of the power extracted from the beam, in spite of the mismatches. A plot of

the magnetic focusing field is given in Figure 7-6. This plot can be used to obtain the magnetic field in the circuit region and at the collector for calculating theoretical depressed collector efficiency.

7.3.1 Measurements with Beam Current, I_b = 32 ma. The measurement results are given in Table 7-2. Calculations, in accordance with Appendix B, are given below. Note that subscript "G" means beam on (gain exists), and subscript "O" means beam off. The symbols are defined in Appendix B and Figure 7-4. Values in Table 7-2 are used.

Power Extracted from Beam, P_e

Power lost in tube with beam off

$$P_{LO} = P_{10} - P_{30} - P_{40}$$

$$P_{LO} = 3.955 - 1.662 - .993$$

$$= 1.300 \text{ W}$$

Power lost in tube with beam on

$$P_{LG} = P_{LO} \times \frac{P_{4G}}{P_{40}}$$

$$= \frac{1.3 \times 4.782}{.993} = 6.26 \text{ W}$$

Power extracted from beam

$$P_e = P_{3G} + P_{4G} + P_{LG} - P_{1G}$$

$$= 5.345 + 4.782 + 6.26 - 3.955$$

$$= 12.43 \text{ W}$$

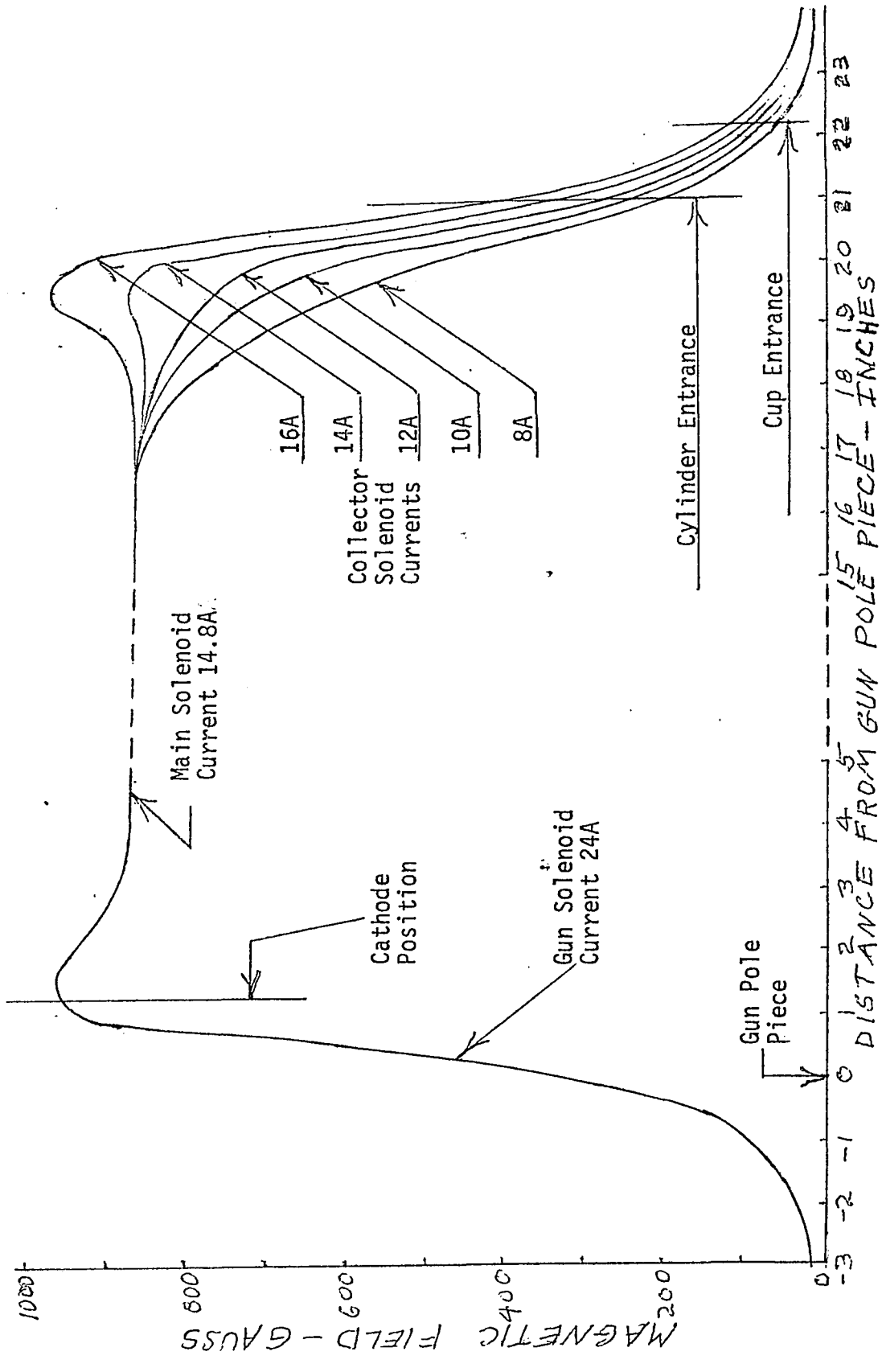

Figure 7-6 Magnetic field distribution for 10-watt tube

Table 7-2

Measurement Results for 10-Watt

Tube with Beam Current, I_b = 32 ma

Freq GHz	Beam on or off	Power Referred to Tube Terminals Symbol	Watts
3.612	on	$P_1 = P_{inc\Delta}$	3.955
		$P_{ref\Delta}$	2.008
		P_Σ	3.337
		$P_3 = P_{ref\Delta} + P_\Sigma$	5.345
		P_{1out}	.718
		P_{2out}	4.064
		$P_4 = P_{1out} + P_{2out}$	4.782
3.612	off	$P_1 = P_{inc\Delta}$	3.955
		$P_{ref\Delta}$	.248
		P_Σ	1.414
		$P_3 = P_{ref\Delta} + P_\Sigma$	1.662
		P_{1out}	.436
		P_{2out}	.756
		$P_4 = P_{1out} + P_{2out}$	.993

Oscillation Frequency	3.618 GHz (Locked out by signal)
Beam Current	32 ma
Pulse Control Voltage	400 V
Circuit-Cathode Voltage	1725 V
Solenoid Focusing Currents	
Main	14.8 A
Gun End	24 A
Collector End	7.8 A
Filament Voltage	6.4 V
Filament Current	5.3 A

Grid Pulse - 15 μsec, 8.6 Hz, Duty Cycle .000129

Depressed Collector Measurements (I_b = 32 ma)

The collector cylinder was connected to ground (the potential of the circuit) and the collector cup was voltage depressed with respect to the circuit. The maximum allowable depression voltage was defined as the voltage at which the collector cup current, with beam on, decreased from 32 ma to 31.5 ma while the r.f. input signal was 3.955 W (as in Table 7-2). The following were the results.

Voltage of cup with respect to ground	-1150 V
Cup current, I_{cup}	31.5 ma
Circuit-Cathode Voltage (Beam Voltage), V_b	1725 V
Pulse Control Voltage	400 V
Solenoid Focusing Currents	
Collector	8 A
Main	14.8 A
Gun	24 A
Frequency of Signal	3.612 GHz

Measured Depressed Collector Efficiency (I_b 32 ma)

The depressed collector efficiency (neglecting the power intercepted at 1725 V and the loss in the tube) is defined as

$$\eta_{dep} = \frac{P_e}{P_c}$$

where P_e = power extracted from beam

P_c = power supplied by collector

Power supplied by the collector is

$$P_c = (V_{ck})(I_{cup})$$

where V_{ck} = collector - cathode voltage

$$V_{ck} = V_b + V_{cup \text{ wrt gnd}}$$

$$= 1725 - 1150 = 575V$$

$$P_c = (575)(.0315) = 18.11 \text{ W}$$

$$\eta_{dep} = P_e/P_c = 12.43/18.11$$

$$\boxed{\eta_{dep} = 68.6\%} \text{ (measured)}$$

Theoretical Depressed Collector Efficiency (neglecting r.f. circuit loss)

The theoretical depressed collector efficiency is given by equation (4.241) and is

$$\eta_{opt} = \frac{1}{1+K_n \frac{\omega_c}{\omega} + (\frac{\omega+\omega_c}{\omega})(\frac{\omega_R}{\omega_c})(\frac{2b}{a_L})} \tag{7.6}$$

The parameters in (7.6) are given below.

Let $B_o = nB_B$, where B_o, the magnetic focusing field in the circuit region, is "n" multiples of the Brillouin focusing field. Then,

$$\omega_c = n\omega_{CB} \tag{7.7}$$

The Brillouin field is given by

$$\omega_{CB}^2 = 2\omega_p^2$$

$$\text{or } \omega_{CB} = \sqrt{2}\,\omega_p \tag{7.8}$$

Substituting (7.8) into (7.7)

$$\omega_p^2 = \frac{\omega_c^2}{2n^2} \tag{7.9}$$

Now,

$$\omega_R = \frac{\omega_p^2}{2\omega_c} \tag{7.10}$$

Using (7.9) in (7.10)

$$\boxed{\frac{\omega_R}{\omega_c} = \frac{1}{4n^2}} \quad \text{with } n = B_o/B_B \tag{7.11}$$

The Brillouin field can be calculated from

$$B_B = \frac{8.32 I_o^{\frac{1}{2}}}{V_o^{\frac{1}{4}} b}$$

In this case,

$$I_o = .032A$$

$$V_o = 1725V$$

$$b = .7725 \times 10^{-3} \text{ met.}$$

$$B_B = \frac{8.32(.032)^{\frac{1}{2}}}{(1725)^{\frac{1}{4}}(.7725 \times 10^{-3})}$$

$$= 299 \text{ Gauss}$$

B_o = 870 Gauss (From Figure 7-6, for main solenoid current = 14.8A)

$n = B_o/B_B = 870/299 = 2.910$

$$\frac{\omega_R}{\omega_c} = \frac{1}{4(2.91)^2} = .0295$$

B_{coll} = 70 Gauss (From Figure 7-6, for collector solenoid current = 8A)

$K_n = B_{coll}/B_o = 70/870 = .0805$

$f_c(mHz) = 2.8B_o$; $f_c = 2.436 \times 10^9$ Hz

$\omega_c = 2\pi f_c = 15.306 \times 10^9$ rad/sec.

$\omega = 2\pi f = 2\pi \times 3.612 \times 10^9 = 22.695 \times 10^9$

$\omega_c/\omega = .6744$

Calculation for final beam deflection, a_L

$$P_e = \frac{1}{2}\omega I_o B_o a_L^2$$

$$\text{or } a_L^2 = \frac{2P_e}{\omega I_o B_o}$$

$$= \frac{2X12.43}{22.695X10^9X.032X087Q}$$

$$= 3.935X10^{-7}$$

$$a_L = .6273X10^{-3} \text{ met}$$

$$2b/a_L = \frac{2X.7725X10^{-3}}{.6273X10^{-3}} = 2.463$$

Using these values in equation (7.6)

$$\eta_{opt} = \frac{1}{1 + (.0805)(.6744) + (1.6744)(.0295)(2.463)}$$

$\boxed{\eta_{opt} = 85.0\%}$ (theoretical)

7.3.2 Measurements with Beam Current, I_b = 42 ma. The measurement results are given in Table 7-3. Calculations, in accordance with Appendix B, are given below.

Power Extracted from Beam, P_e

Power lost in tube with beam off

$$P_{LO} = P_{10} - P_{30} - P_{40}$$

$$P_{LO} = 3.955 - 1.507 - 1.154$$

$$= 1.294 \text{ W}$$

Power lost in tube with beam on

$$P_{LG} = P_{LO} \times \frac{P_{4G}}{P_{40}}$$

$$= 1.294 \times \frac{8.579}{1.154} = 9.62 \text{ W}$$

Power extracted from beam

$$P_e = P_{3G} + P_{4G} + P_{LG} - P_{1G}$$

$$= 2.122 + 8.579 + 9.62 - 3.955$$

$$= 16.366 \text{ W}$$

Depressed Collector Measurements (I_b = 42 ma)

In this case, because better depression could be attained, the collector cup and cylinder were tied together and voltage was depressed with respect to the circuit. The maximum allowable depression voltage was defined as the voltage at which the total collector current, with beam on, decreased from 42 ma to 41.5 ma while the r.f. signal was

Table 7-3

Measurement Results for 10-Watt

Tube with Beam Current, I_b = 42 ma

Freq GHz	Beam on or off	Power Referred to Tube Terminals	
		Symbol	Watts
3.612	on	$P_1 = P_{inc\Delta}$	3.955
		$P_{ref\Delta}$	.306
		P_Σ	1.816
		$P_3 = P_{ref\Delta} + P_\Sigma$	2.122
		P_1 out	2.100
		P_2 out	6.479
		$P_4 = P_1$ out + P_2 out	8.579
3.612	off	$P_1 = P_{inc\Delta}$	3.955
		$P_{ref\Delta}$	.239
		P_Σ	1.268
		$P_3 = P_{ref\Delta} + P_\Sigma$	1.507
		P_1 out	.467
		P_2 out	.687
		$P_4 = P_1$ out + P_2 out	1.154

Oscillation Frequency	3.619 GHz (Locked out by signal)
Beam Current	42 ma
Pulse Control Voltage	750 V
Circuit-Cathode Voltage	1740 V
Solenoid Focusing Currents	
Main	14.8 A
Gun End	24 A
Collector End	16 A
Filament Voltage	6.4 V
Filament Current	5.2 A

Grid Pulse - 15 μsec, 8.6 Hz, Duty Cycle .000129

3.955W (as in Table 7-3). The following were the results.

Voltage of Cup and Cylinder Wrt ground	-1050V
Collector current, I_{coll}	41.5 ma
Circuit-cathode voltage (beam voltage), V_b	1740V
Pulse control voltage	750V
Solenoid focusing currents	
Collector	16A
Main	14.8A
Gun	24A
Frequency of signal	3.612 GHz

Measured Depressed Collector Efficiency (I_b = 42 ma)

The depressed collector efficiency (neglecting the power intercepted at 1740V and loss in the tube) is again defined as

$$\eta_{dep} = \frac{P_e}{P_c}$$

Power supplied by collector is

$$P_c = (V_{ck})(I_{coll})$$

$$V_{ck} = V_b + V_{coll} \text{ wrt gnd}$$

$$= 1740 - 1050 = 690V$$

$$P_c = (690)(.0415) = 28.64W$$

$$\eta_{dep} = \frac{16.366}{26.64}$$

$$\boxed{\eta_{dep} = 57.1\%} \quad \text{(measured)}$$

Theoretical Depressed Collector Efficiency (neglecting r.f. circuit loss)

The theoretical depressed collector efficiency is again given by equation (7.6) and the equations following (7.6).

Brillouin field,

$$B_B = \frac{8.32 I_o^{\frac{1}{2}}}{V_o^{\frac{1}{4}} b}$$

$$= \frac{(8.32)(.042)^{\frac{1}{2}}}{(1740)^{\frac{1}{4}} (.7725 \times 10^{-3})}$$

$$= 341.8 \text{ Gauss}$$

$B_o = 870$ Gauss (From Figure 7-6, for main solenoid current = 14.8A)

$n = B_o/B_B = 870/341.8 = 2.545$

$$\frac{\omega_R}{\omega_c} = \frac{1}{4n^2} = \frac{1}{4(2.545)^2} = 0.386$$

$B_{coll} = 400$ Gauss (From Figure 7-6 for collector solenoid current = 16A)

$K_n = B_{coll}/B_o = 400/870 = .460$

$f_c = 2.8\ B_o = 2.8 \times 870 \text{ MHz} = 2.436 \times 10^9 \text{ Hz}$

$\omega_c = 2\pi f_c = 15.306 \times 10^9 \text{ rad/sec}$

$\omega = 2\pi f = 2\pi \times 3.612 \times 10^9 = 22.695 \times 10^9 \text{ rad/sec}$

$\omega_c/\omega = .6744$

Calculation for final beam deflection, a_L,

$$a_L^2 = \frac{2P_e}{\omega I_o B_o} = \frac{2 \times 16.366}{22.695 \times 10^9 \times .042 \times .0870}$$

$$= 3.947 \times 10^{-7}$$

$$a_L = .6283 \times 10^{-3} \text{ met.}$$

$$\frac{2b}{a_L} = \frac{2 \times .7725 \times 10^{-3}}{.6283 \times 10\text{-}3} = 2.459$$

Using these values in equation (7.6),

$$\eta_{opt} = \frac{1}{1 + (.460)(.6744) + (1.6744)(.0386)(2.459)}$$

$$\boxed{\eta_{opt} = 68.1\%} \quad \text{(theoretical)}$$

A summary of the results of the tests on the 10 W tube is given in Table 7-4.

Table 7-4

Summary of Results with Ten-Watt Tube

Freq. MHz	Beam Current, I_b ma	Beam Voltage, V_b Volts	Collector Voltage, V_{ck} Volts	Measured Depressed Collector Efficiency %	Theoretical Depressed Collector Efficiency %
3,612	32	1725	575	68.6	85.0
3,612	42	1740	690	57.1	68.1

Voltages are with respect to cathode

CHAPTER VIII

CONCLUSIONS AND SUGGESTIONS FOR FUTURE WORK

8.1 Conclusions

A theory and design procedure for slow cyclotron wave amplifiers has been developed. A one-watt, 3 GHz tube and a ten-watt, 3 GHz tube, which were scaled from a two-kilowatt, 5 GHz design, utilizing a bifilar helix circuit, were constructed and tested. The purpose of the one-watt tube was not to demonstrate high efficiency, but to verify the theoretical interaction impedance and for use as a beam tester. The one-watt tube had a circuit with constant diameter and pitch, while the ten-watt tube had a circuit with tapered diameter and pitch to maintain synchronism between circuit and slow cyclotron waves. The r.f. terminals of the one-watt tube were fairly well matched to 50-ohm cables, but those of the 10-watt tube were badly mismatched inside the tube. Because of feedback inside the tubes due to mismatches in the tubes, oscillations were generated by transverse-wave interactions. It was possible to lock out the oscillations with high drive power.

Gain of the one-watt tube at low r.f. drive levels could not be measured directly because of the oscillations. However, because the mismatches were not large, small signal gain could be obtained by extrapolating results with measurements at large signals at which the oscillations could be suppressed. The small signal gain thus obtained (10 dB) verified the theoretical calculation for interaction impedance given by equation (5.18).

At the operating frequency of 3.09 GHz, the one-watt tube saturated at one watt output because of the desynchronization effect. At signal output levels above 32 mW, an oscillation at 2.29 GHz was suppressed. Calculations indicated this oscillation was a backward wave one.

For the 10-watt tube, it was not possible to measure directly the power extracted from the beam by the circuit because of the bad mismatches in this tube, even though oscillations were suppressed by a large drive power. However, formulas were developed to enable calculation of the power extracted from the beam, in spite of the mismatches. The gain could not be calculated because not enough information could be obtained from measurements outside the tube. The collector voltage was depressed until beam current interception on the circuit and body was detectable. The depressed collector efficiency, η_{dep}, was then defined as the ratio of the r.f. power extracted from the beam to the d.c. power supplied by the depressed collector.

Depressed collector efficiencies were measured with beam currents of 32 ma and 42 ma at a signal frequency of 3.612 GHz. The signal suppressed the oscillation frequency of 3.619 GHz. Because of the proximity of the oscillation and signal frequencies, the oscillation was probably a forward wave one, with feedback due to reflection of the circuit wave. Because of the tapered circuit pitch, desynchronization of the backward circuit wave mode would tend to suppress backward wave oscillations.

The theoretical depressed collector efficiency, given by equation (4.241) was then calculated, utilizing measured values for the parameters. With beam current of 32 ma, the power extracted from the beam was 12.4 watts, the measured depressed collector efficiency was 68.6%, and the theoretical depressed collector efficiency was 85.0%. With beam current of 42 ma, the power extracted from the beam was 16.4 watts, the measured depressed collector efficiency was 57.1%, and the theoretical depressed collector efficiency was 68.1%.

In general, the theory appears to be verified, although errors may have been introduced by the mismatches. The test results indicate the possibility of attaining high efficiency, of the order of 70%, in a cyclotron wave amplifier with kilowatts output at 5 GHz. Because of the low transverse interaction impedance of known circuits, such as twisted transmission lines and twisted finned waveguides, it is estimated that the attainable gain is of the order of 1 dB/inch.

8.2 Suggestions for Future Work

Before constructing tubes at kilowatt output levels, cyclotron wave amplifiers at watts output levels should be constructed with good matches to enable more accurate verification of the theory.

The 180^{o} hybrids at the input and output tube terminals should be designed for direct connections to the terminals with minimum transmission line lengths. This would eliminate undesired imbalance in amplitude and phase of the signals on each half of the transverse circuit.

Attenuation should be deposited on the helix support rods, similar to that used in ordinary space-charge wave traveling-wave tubes, to assist in suppressing oscillations.

After the theory is verified more accurately, an increase in instantaneous bandwidth of operation can be investigated. By designing the slow cyclotron beam wave line on the ω-β plot to coincide with the circuit-wave line ($n = +1$ component), synchronism over large frequency bandwidths should be attainable.

The methode of maintaining synchronism by tapering the magnetic field, as discussed in section (4.5.5), should be investigated. The phase velocity of the slow cyclotron wave is given by $v_p = (\omega + \omega_c)/\mu_0$, where μ_0 is the velocity of the electrons. μ_0 decreases as energy is extracted from the beam. v_p can be maintained constant by decreasing ω_c (the magnetic field) with increasing distance along the tube when μ_0 decreases. This provides the advantage of a method of maintaining synchronism by an adjustment of a parameter outside the tube.

References

1. R. J. Briggs, S. F. Paik, A. H. Gottfried, "Transverse-Wave Tubes as High-Efficiency Microwave Amplifiers," IEEE Trans. on Electron Devices, Vol ED-18, No. 8, August 1971, pp. 511-520.

2. R. G. Hutter, Beam and Wave Electronics in Microwave Tubes, D. Van Nostrand Co., N.Y., N.Y., 1960.

3. E. C. Jordan, Electromagnetic Waves and Radiating Systems, Prentice-Hall, N.Y., N.Y., 1950.

4. W. H. Louselle, Coupled Mode and Parametric Electronics, John Wiley and Sons, N.Y., N.Y., 1960

5. J. R. Pierce, Traveling-Wave Tubes, D. Van Nostrand Co., N.Y., N.Y., 1950.

6. S. Sensiper, "Electromagnetic Wave Propagation on Helical Structures," (A Review and Survey of Recent Progress), Proc IRE, 43, Feb 1955, pp. 149-161, and references contained therein.

7. A. E. Siegman, "Waves on a Filamentary Beam in a Transverse-Field Slow-Wave Structure," J. Appl Phys, 31, Jan 1960, pp. 17-26.

8. P. K. Tien, "Bifilar Helix for Backward-Wave Oscillators," Proc IRE, 42 No. 7, July 1954, pp. 1137-1143.

9. P. K. Tien, "Traveling-Wave Tube Helix Impedance," Proc IRE, 41, Nov 1953, pp. 1617-1623.

10. D. A. Watkins, Topics in Electromagnetic Theory, John Wiley and Sons, N.Y., N.Y., 1958.

11. J. R. Pierce, Theory and Design of Electron Beams, D. Van Nostrand Co., N.Y., N.Y., 1949.

APPENDIX A

FIELD ANALYSIS FOR POWER IN SPACE HARMONICS AND FOR INTERACTION IMPEDANCE[10]

To compute power carried by the space harmonic components of the forward traveling wave on a helix, Tien[10] has used an infinitesimally thin tape helix approximation for the actual helix. The pitch angle, ψ, and the pitch, p, are the same as for the actual helix. The radius, a, and the width of the tape, δ, are equal respectively to the mean radius and wire diameter of the actual helix. Cylindrical coordinates r, ϕ, z are used in the analysis. The interaction impedance is computed without the presence of the beam. The transverse interaction impedance, K_T, for the n = +1 space harmonic component of the forward traveling mode which interacts with the slow cyclotron beam wave is defined by

$$K_T = \frac{\{E_{r1}^{i}(0)\}^2}{2\beta_1^2 \sum_{n=-\infty}^{\infty} P_n} \tag{A1}$$

where

$E_{r1}^{i}(0)$ is the amplitude of the transverse radial field of the n = +1 space harmonic component at r = 0 where the beam would be located. (The superscript "i" indicates inside the helix.)

β_1 = propagation constant for n = +1

P_n = average power carried by the n'th space harmonic component

For the bifilar helix with balanced (+-) feed, the "n" are positive and negative odd integers. The transverse fields for "n" even are equal to zero.

The fields of the n'th space harmonic as functions of the coordinates have been derived in Chapter III and are given by equations (3.48) through (3.60), with the subscript n added to the field quantities on the left side of the equations and to β and γ_r wherever they appear. The superscripts "0" and "i" indicate fields outside and inside the helices, respectively. $k = \omega/c = \omega\sqrt{\mu\varepsilon}$ is the free space propagation constant. β_n is the propagation constant of the n'th harmonic and is given by equation (3.82), i.e.,

$$\beta_n = \beta_0 + \frac{n2\pi}{p} \tag{A2}$$

where p = longitudinal pitch of the helix

β_0, the group velocity, is given by equation (3.122) and is

$$\beta_0 = \pm \frac{k}{\sin \psi} \tag{A3}$$

where ψ = pitch angle of the helix

The radial propagation constant for the n'th space harmonic is given by equation (3.60) and is

$$\gamma_{rn} = (\beta_n^2 - k^2)^{\frac{1}{2}} \tag{A4}$$

The A_n's and B_n's of equations (3.48) through (3.59) are constants associated with the solutions for the fields and are determined by the

boundary conditions and current distribution assumed over the helical tapes.

The current in the bifilar tapes is assumed to be parallel to the tapes, uniformly distributed across the width of a tape. The current perpendicular to the tapes is equal to zero. Figures 3-7a and 3-7b in Chapter III show this distribution. The current in the tapes can be expanded into Fourier components. For the bifilar helix with balanced (+-) feed, the current density for the n'th harmonic is given by equation (3.108) and is

$$(A5) \qquad j_{\parallel n} = \frac{2J\delta}{p} \frac{\sin(\frac{n\pi\delta}{p})}{\frac{n\pi\delta}{p}} = C \frac{\sin(\frac{n\pi\delta}{p})}{\frac{n\pi\delta}{p}} \qquad n \text{ only odd}$$

where $C = \frac{2J\delta}{p}$ = a constant

J = current density in tape in amps/meter width

δ = width of tape, met.

p = pitch of tape, met.

The subscript "$\parallel$" means parallel to the tape.

The ϕ- and z- components of the current density for the n'th harmonic are

$$(A6) \qquad j_{\phi n} = j_{\parallel n} \cos \psi$$

$$(A7) \qquad j_{zn} = j_{\parallel n} \sin \psi$$

where ψ = pitch angle of the helix

The boundary conditions at the helix, where $r = a$, are given by equations (3.83), (3.84) and (3.85) and are

(A8) $$E_{\phi n}^{i} = E_{\phi n}^{o}$$

(A9) $$E_{zn}^{i} = E_{zn}^{o}$$

(A10) $$j_{\phi n} = H_{zn}^{i} - H_{zn}^{o}$$

(A11) $$j_{zn} = H_{\phi n}^{o} - H_{\phi n}^{i}$$

Utilizing equations (3.48), (3.49), (3.51), (3.53), (3.54), (3.55), (3.57), (A6), (A7) in the boundary conditions (A8) through (A11) results in

(A12) $$\boxed{A_n^i = \frac{j_{\parallel n}\, \gamma_{rn}^2\, a \cos\psi}{j\omega\varepsilon} \left\{ \frac{n\beta_n}{\gamma_{rn}^2\, a} - \tan\psi \right\} K_n(\gamma_{rn} a)}$$

(A13) $$\boxed{B_n^i = -j_{\parallel n}\, \gamma_{rn} a\, (\cos\psi)\, K_n'(\gamma_{rn} a)}$$

(A14) $$\boxed{A_n^o = A_n^i \frac{I_n(\gamma_{rn} a)}{K_n(\gamma_{rn} a)}}$$

(A15) $$\boxed{B_n^o = B_n^i \frac{I_n'(\gamma_{rn} a)}{K_n'(\gamma_{rn} a)}}$$

where the derivative of the Bessel functions are with respect to the arguments, and $j_{\parallel n}$ is given by equation (A5).

β_n and γ_{rn} are evaluated from equations (A2), (A3) and (A4).

In (A12) through (A15), the following identity was used.

(A16) $$I_n(\eta_n)\, K_n'(\eta_n) - I_n'(\eta_n) K_n(\eta_n) = -\frac{1}{\eta_n}$$

(A17) where $\eta_n = \gamma_{rn} a$

Tien also uses the following to obtain power.

(A18) $$M_n = \frac{\{\eta_n^2 - n\beta_n\, a \cot\psi\}\, I_n(\eta_n) K_n(\eta_n)}{\eta_n^2\, (ka)^2}$$

where $k = \omega/c$ = free space propagation constant

(A19) $$Q_n = \frac{1}{\eta_n} I_n(\eta_n) K_n'(\eta_n) \cot\psi$$

(A20) $$S_n = \frac{1}{\eta_n} I_n'(\eta_n) K_n(\eta_n) \cot\psi$$

From equations (A12) through (A20) and the field expressions (3.50) to (3.53) and (3.56) to (3.59), the power associated with the n'th component of the fields can be computed using Poynting's theorem.

(A21) $$P_n = P_n^i + P_n^o$$

(A22) $$P_n^i = \mathrm{Re}\left\{\frac{1}{2} \int_o^{2\pi} d\theta \int_o^a (E_{rn}^i \tilde{H}_{\theta n}^i - E_{\theta n}^i \tilde{H}_{rn}^i) r d\theta\right\}$$

(A23) $$P_n^o = \mathrm{Re}\left\{\frac{1}{2} \int_o^{2\pi} d\theta \int_o^{\infty} (E_{rn}^o \tilde{H}_{\theta n}^o - E_{\theta n}^o \tilde{H}_{rn}^o) r d\theta\right\}$$

where ~ denotes the conjugate value and "Re" means the real component.

For $n \neq 0$ we have:

(A24) $$P_n^i = \pi a^2 \omega\mu a \sin^2\psi \, T_n^i$$

(A25) $$T_n^i = \left|j_{\parallel n}\right|^2 \{\beta_n a \, (k^2a^2M_n^2 + Q_n^2) \cdot \left[\eta_n \frac{I_n'(\eta_n)}{I_n(\eta_n)} + \frac{\eta_n^2}{2} \frac{I_n'^2(\eta_n)}{I_n^2(\eta_n)} - \frac{1}{2}(\eta_n^2 + n^2)\right] - nM_nQ_n \, (\beta_n^2a^2 + k^2a^2)\}$$

(A26) $$P_n^o = \pi a^2 \omega\mu a \sin^2\psi \, T_n^o$$

(A27) $$T_n^o = \left|j_{\parallel n}\right|^2 \{\beta_n a \, (k^2a^2M_n^2 + S_n^2) \cdot \left[-\eta_n \frac{K_n'(\eta_n)}{K_n(\eta_n)} - \frac{\eta_n^2}{2} \frac{K_n'^2(\eta_n)}{K_n^2(\eta_n)} + \frac{1}{2}(\eta_n^2 + n^2)\right] + nM_nS_n \, (\beta_n^2a^2 + k^2a^2)\}$$

To evalute E_{rn}^i inside the helix, equation (3.50) together with equations (A12) and (A13) are used. Thus,

(A28) $$E_{rn}^i = j_{\parallel n} \frac{\beta_n}{\omega\varepsilon} \gamma_{rn} a(\cos\psi) \left\{\frac{n\beta_n}{\gamma_{rn}^2 a} - \tan\psi\right\} K_n(\gamma_{rn}a) I_n'(\gamma_{rn}r) + j_{\parallel n}(\cos\psi) \; a\omega\mu \left\{\frac{I_{n-1}(\gamma_{rn}r) - I_{n+1}(\gamma_{rn}r)}{2}\right\} K_n'(\gamma_{rn}a)$$

Use can be made of the following identities.

(A29) $$I_n'(x) = \frac{I_{n-1}(x) + I_{n+1}(x)}{2}$$

(A30) $$I_n'(x) = \frac{n}{x} I_n(x) + I_{n+1}(x)$$

(A31) $$K_n'(x) = -\left(\frac{K_{n-1}(x) + K_{n+1}(x)}{2}\right)$$

(A32) $$K_n'(x) = \frac{n}{x} K_n(x) - K_{n+1}(x)$$

(A33) $$I_{n+1}(x) = I_{n-1}(x) - \frac{2n}{x} I_n(x)$$

(A34) $$K_{n+1}(x) = K_{n-1}(x) + \frac{2n}{x} K_n(x)$$

(A35) $$I_{-n}(x) = I_n(x)$$

(A36) $$K_{-n}(x) = K_n(x)$$

At r = 0

For n ≠ 0

(A37) $$I_n(0) = 0$$

For n = 0

(A38) $$I_0(0) = 1$$

Using (A29), (A37) and (A38) in (A28), it is found that

$$E^i_{rn}(0) \neq 0 \text{ only for } n = \pm 1$$

Using (A28), (A29), (A31), (A36), (A37) and (A38),

For n = 1 and r = 0

(A39)
$$E^i_{r1}(0) = \frac{j_{\parallel 1}}{2}\frac{\beta_1}{\omega\varepsilon}\gamma_{r1}aK_1(\gamma_{r1}a)(\cos\psi)\left(\frac{\beta_1}{\gamma_{r1}a} - \tan\psi\right) - \frac{j_{\parallel 1}}{4}\omega\mu a(\cos\psi)\{K_2(\gamma_{r1}a) + K_o(\gamma_{r1}a)\}$$

For n = -1 and r = 0

(A40)
$$E^i_{r(-1)}(0) = \frac{j_{\parallel(-1)}}{2}\frac{\beta_{-1}}{\omega\varepsilon}\gamma_{r(-1)}aK_1(\gamma_{r(-1)}a)(\cos\psi)\left(\frac{-\beta_{-1}}{\gamma_{r\,2}(-1)a} - \tan\psi\right) + \frac{j_{\parallel(-1)}}{4}\omega\mu a(\cos\psi)\{K_2(\gamma_{r(-1)}a) + K_o(\gamma_{r(-1)}a)\}$$

where $j_{\parallel 1}$ and $j_{\parallel(-1)}$ are evaluated from (A5)

To evaluate the transverse interaction impedance, K_T, given by (A1),

$E^i_{r1}(0)$ is given by (A39)

$$\Sigma P_n = \Sigma(P_n{}^i + P_n{}^o)$$

where $P_n{}^i$ and $P_n{}^o$ are given by (A24) and (A26), respectively.

The factor, C, in equation (A5) appears in both the numerator and denominator of (A1) and cancels out. Thus, we can let C = 1 without affecting the calculation for K_T from (A1).

K_T was calculated from (A1) for the bifilar helix of the one-watt tube that has been constructed. A computer was utilized to obtain the power carried by all odd space harmonic components up to n = $\pm$23. It was found that the interaction impedance utilizing Tien's analysis was 1.109 ohms, while that given by equation (5.18) utilizing the transmission line analysis was 0.776 ohms. With Tien's analysis, the n = +1 component carries 35.7% of the power, and the n = -1 component carries 41.8%. The remainder of the power is carried by the other components.

With C = 1 in equation (A5), the following values were obtained:

$$E_{r1}^{i}(0) = 55.24 \qquad E_{r}^{i}{}_{(-1)}(0) = 70.02$$

$$P_1^{i} = 1.638 \times 10^{-4} \qquad P_{(-1)}^{i} = 2.012 \times 10^{-4}$$

$$P_1^{o} = 1.215 \times 10^{-4} \qquad P_{(-1)}^{o} = 1.327 \times 10^{-4}$$

$$P_1 = P_1^{i} + P_1^{o} \qquad P_{(-1)} = P_{(-1)} = P_{(-1)}^{i} + P_{(-1)}^{o}$$

$$= 2.85 \times 10^{-4} \qquad = 3.34 \times 10^{-4}$$

$$\Sigma P_n^{i} = 4.606 \times 10^{-4}$$

$$\Sigma P_n^{o} = 3.382 \times 10^{-4}$$

$$\Sigma(P_n^{i} + P_n^{o}) = 7.988 \times 10^{-4}$$

APPENDIX B

EFFECT OF MISMATCHED INPUT AND OUTPUT TUBE TERMINALS

Figure B-1 shows the total powers in waves traveling to the right and to the left inside and outside the tube. Total power in a wave is the sum of the powers involved with each helix. The total power across each boundary between regions is continuous. In the following analysis, subscript "G" indicates "beam on," subscript "0" indicates "beam off."

With beam on

At boundary 1-2

$$P_{1G} - P_{3G} = P_{2G}' - \frac{P_{5G}}{L_1} \tag{B1}$$

At boundary 2-3

$$\frac{P_{2G}'}{L_1} - P_{5G} = P_{2G}\left(1 - \frac{G\rho_2^2}{\alpha^2}\right) \tag{B2}$$

At boundary 3-4

$$P_{4G}'\left(1 - \frac{\rho_4^2}{L_2^2}\right) = \frac{GP_{2G}}{\alpha}\left(1-\rho_2^2\right) \tag{B3}$$

At boundary 4-5

$$P_{4G} = \frac{P_{4G}'}{L_2}\left(1-\rho_4^2\right) \tag{B4}$$

With beam off (G = 1)

At boundary 1-2

$$P_{10} - P_{30} = P_{20}' - \frac{P_{50}}{L_1} \tag{B5}$$

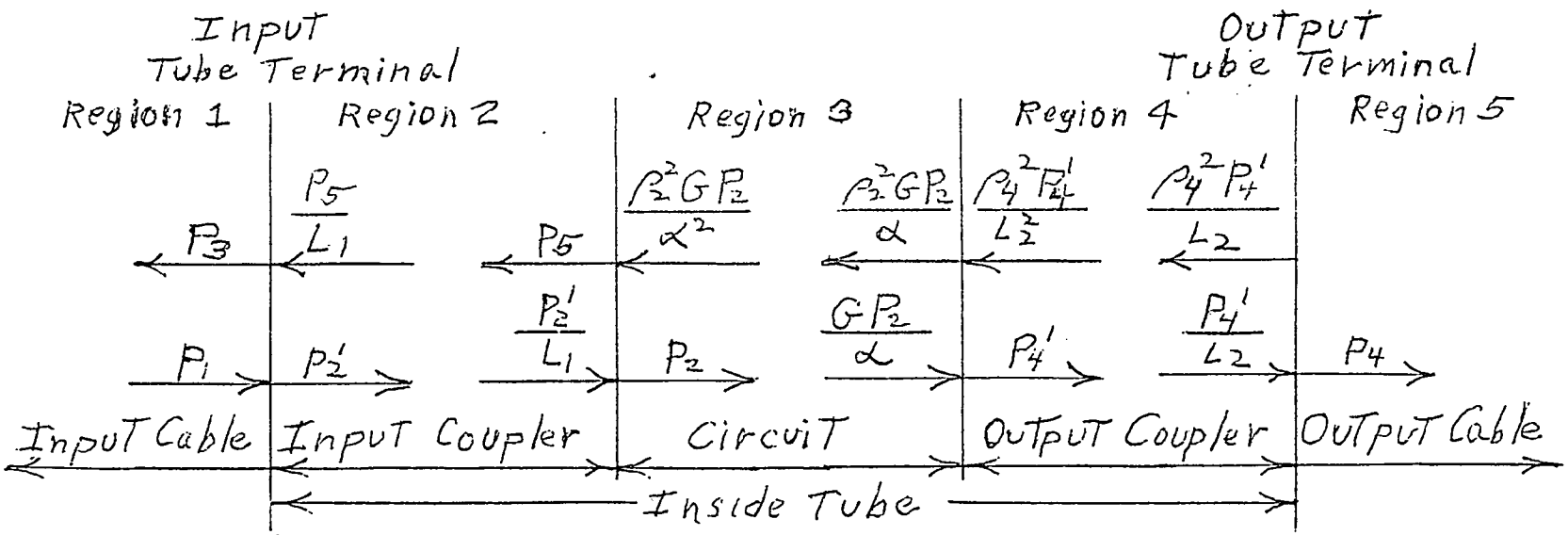

$P_{1,2,3,4,5}$ and $P_{2',4}$ = power in waves

ρ_2, ρ_4 = absolute values of voltage reflection coefficients at region boundaries 3-4, and 4-5, respectively

L_1, α, L_2 = one-way r.f. power attenuation in regions 2,3, and 4, respectively, expressed as ratios greater than 1. These attenuations are the result of losses in the regions

G = power gain in region 3, going to the right (in the direction of electron beam travel)

P_1, P_3 and P_4 are observables outside the tube. There is no left traveling wave in region 5 because P_4 enters a matched load.

Figure B-1 Power in waves traveling to right and left, inside and outside tube

At boundary 2-3

$$\frac{P_{20}'}{L_1} - P_{50} = P_{20}\left(1 - \frac{\rho_2^2}{\alpha^2}\right) \tag{B6}$$

At boundary 3-4

$$P_{40}'\left(1 - \frac{\rho_4^2}{L_2^2}\right) = \frac{P_{20}}{\alpha}\left(1 - \rho_2^2\right) \tag{B7}$$

At boundary 4-5

$$P_{40} = \frac{P_{40}'}{L_2}\left(1 - \rho_4^2\right) \tag{B8}$$

From equations (B3), (B4), (B7), (B8)

$$\frac{P_{4G}}{P_{40}} = \frac{GP_{2G}}{P_{20}} \tag{B9}$$

Total r.f. power lost in tube, P_L

The power lost in each region is the sum of the powers lost in the right and left traveling waves in the region.

With beam on

$$P_{LG} = P_{2G}'\left(1 - \frac{1}{L_1}\right) + P_{5G}\left(1 - \frac{1}{L_1}\right) + GP_{2G}\left(1 - \frac{1}{\alpha}\right) + \frac{GP_{2G}\rho_2^2}{\alpha}\left(1 - \frac{1}{\alpha}\right) + P_{4G}'\left(1 - \frac{1}{L_2}\right) + \frac{P_{4G}'\rho_4^2}{L_2}\left(1 - \frac{1}{L_2}\right) \tag{B10}$$

(In region 3, the power lost by the right traveling wave is $(GP_{2G} - GP_{2G}/\alpha)$, where GP_{2G} is the power in the right traveling wave at at boundary 3-4 if there were no loss in region 3 ($\alpha = 1$).

If the loss in the input coupler (region 2) is small, then $L_1 \approx 1$ (this is a good approximation since the coupling region is very short in length). This is equivalent to assuming the loss in the input coupler is small compared to that in the rest of the tube.

Then, using equation (B3), (B10) becomes

(B11)
$$P_{LG} = GP_{2G}\left\{\left(1-\frac{1}{\alpha}\right)\left(1+\frac{\rho_2^2}{\alpha}\right) + \frac{(L_2-1)(L_2+\rho_4^2)(1-\rho_2^2)}{\alpha(L_2^2-\rho_4^2)}\right\}$$

With the beam off, G = 1 and P_{2G} becomes P_{20} in (B11) and P_{LG} becomes P_{LO}. Thus,

(B12)
$$\frac{P_{LG}}{P_{LO}} = \frac{GP_{2G}}{P_{20}}$$

Comparing (B12) with (B9)

(B13)
$$\boxed{P_{LG} = P_{LO}\left(\frac{P_{4G}}{P_{40}}\right)}$$

Now, r.f. power into the circuit = (power out of the circuit) + (power lost in the tube).

Thus, with beam off,

$$P_{10} = P_{30} + P_{40} + P_{LO}$$

(B14) or, $\boxed{P_{10} = P_{10} - P_{30} - P_{40}}$

With beam on,

$$P_{1G} + P_e = P_{3G} + P_{4G} + P_{LG}$$

(B15) or $\boxed{P_e = P_{3G} + P_{4G} = P_{LG} - P_{1G}}$

where P_e = r.f. power extracted from the beam.

P_e can be computed by utilizing equations (B14) and (B13) in (B15). (P_{1G}, P_{3G}, P_{4G}, P_{10}, P_{30}, and P_{40} are measurable.)